GEOCHEMISTRY OF THE SABIE RIVER BASALT FORMATION IN THE CENTRAL LEBOMBO, KAROO IGNEOUS PROVINCE

by

Russell James Sweeney

VOLUME II

Appendices

Thesis submitted in fulfilment of the requirements
for the degree of
Doctor of Philosophy

Department of Geochemistry
University of Cape Town

April, 1988

VOLUME II : Table of Contents

APPENDIX A. ANALYTICAL TECHNIQUES 1
1.1 Whole Rock XRF Analysis 1
1.1.1 Major Elements 1
1.1.2 Trace Elements 1
1.2 XRF Slab Analysis 4
1.2.1 The Technique 4
1.2.2 Calibration 9
1.2.3 Accuracy 11
1.3 Radiogenic Isotope Analysis 20
1.3.1 Procedure for Sr and Sm-Nd Sample Preparation 20
1.3.1.1 Sample dissolution 20
1.3.1.2 Column separations 20
1.3.1.3 Filament preparation 21
1.3.2 Pb-Pb Sample Preparation 21
1.3.2.1 Column separation 22
1.3.2.2 Filament preparation 22
1.3.3 Data Accumulation and Reduction 22
1.3.4 Replication 26
1.4 Stable Isotopes 26
1.5 Electron Microprobe Analysis 29
1.5.1 Routine Analysis 29
1.5.2 Analysis of V in Opaque Oxides 30

APPENDIX B. PETROGRAPHIC DESCRIPTIONS 34

APPENDIX C. ANALYTICAL DATA 52

APPENDIX D. SAMPLE LOCALITIES 78

APPENDIX E. PARTITION COEFFICIENT COMPILATION 93

Tables

Pg

A1. Major element oxide analysis by XRF. 2
A2. Trace element analysis by XRF and SSMS. 3
A3. Comparison between XRF, SSMS and ID trace element data. 5
A4. Comparison of Nd data obtained by XRF and ID. 5
A5. Replication of XRF data 6
A6. Slab analysis measuring parameters. 7
A7. Standard slabs. 7
A8. Duplicate slab analyses. 15
A9. Radiogenic isotope standards data. 24
A10. Isotope equations. 27
A11. Isotope data replication (on separate dissolutions). 28
A12. Electron microprobe analysis. 31

C1. Central Lebombo whole rock data 56
C2. REE data (SSMS). 72
C2a. Trace element data (SSMS) 73
C3. Soil analyses by XRF. 74
C4. Central Lebombo isotopic data. 75

Figures

		Pg
A1.	Wavelengths of selected analyte lines and major element absorption edges	10
A2.	Fe and the Fe absorption edge	10
A3.	Absorption coefficient calibration curves	12
A4.	Major element calibration curves (corrected for absorption)	14
A5.	Major element calibration curves (uncorrected for absorption)	16
A6.	Comparison between quantitative and semi-quantitative data	18
A7.	Pb-isotope measurements on NBS 981	25
A8.	Electron microprobe scan over Ti Kb and V Ka peaks	33
D1.	Central Lebombo sample locality maps	78
D2.	Stratigraphic location of central Lebombo samples	90
D3.	Detailed stratigraphy of the upper portion of the Sabie River section (dots = LFE group; triangles = N group; squares = HFE group)	92

APPENDIX A. ANALYTICAL TECHNIQUES

1.1 WHOLE ROCK XRF ANALYSIS

X-ray fluorescence (XRF) spectroscopic techniques currently in use in the Department of Geochemistry (University of Cape Town) were used for the analysis of major and trace elements on whole rock samples and have been described by Willis *et al.* (1971, 1972), le Roex *et al.* (1981) and Duncan *et al.* (1984a). These are summarized below and the data is reported in Appendix C.

Whole rock samples in excess of 1 kg were reduced to less than 300# size by splitting, crushing (Mn-steel jaws) and grinding in a carbon-steel swing-mill. Weathered surfaces were removed before crushing and an attempt was made to exclude amygdaloidal material.

1.1.1 Major Elements

Major elements (except Na) were determined on duplicate glass discs using the fusion method of Norrish and Hutton (1969): sample powder (.28 g ashed at 1000°C) fused with Johnson Matthey Spectroflux 105 (1.5 g of 47% $Li_2B_4O_7$ + 37% Li_2CO_3 + 16% La_2O_3) and a small amount of $NaNO_3$ (.02 g). Na was determined on pressed powder briquettes. Interelement effects except for Na were corrected by iteration using the factors given in Norrish and Hutton (1969). Estimates of precision and accuracy are given in Table A1. Volatile constituents were estimated by drying for consecutive periods in excess of 12 hours at 110°C (H_2O^-) and ashing at 1000°C (loss on ignition, LOI). Data are reported in Appendix C with total Fe as Fe_2O_3 (as analysed).

1.1.2 Trace Elements

Trace elements determined by XRF in powder briquettes are listed in Table A2. Analytical techniques used (e.g. spectral line, matrix corrections, interferences) are described by Duncan *et al.* (1984a). Typical analytical counting errors and estimated lower limits of detection

Table A1. Major element oxide analysis by XRF (from table A1b, Bristow, 1980; table II, Duncan *et al.*, 1984a).

oxide	% concentration	precision	"accuracy"	lld
SiO_2	50.0	.140	.264	.04
TiO_2	1.0	.008	.008	.005
Al_2O_3	15.0	.080	.079	.02
Fe_2O_3	9.0	.038	.064	.014
MnO	.15	.008	.003	.008
MgO	8.0	.148	.086	.07
CaO	12.0	.028	.030	.008
Na_2O	2.5	.032	.067	.08
K_2O	.20	.002	.022	.002
P_2O_5	.20	.012	.018	.011

Precision is expressed as an absolute error in % oxide (2 s.d. counting error) on the given concentration. "Accuracy" is the average absolute difference between the recommended values for standards on the calibration line and their calculated values. The lld is the lower limit of detection at the 99% confidence level. All values as % oxide.

Table A2. Trace element analysis by XRF and spark-source mass spectrography: typical lower limits of detection and precisions.

element	XRF concentration range (ppm)	XRF lld (ppm)	XRF 2 s.d. errors	SSMS concentration range (ppm)	SSMS 2 s.d. errors
Nb	3 - 50	2.0	1.3 - 1.5		
Zr	70 - 550	1.8	1.4 - 2.0	500	80
Y	20 - 80	2.2	1.4 - 1.8	48	8
Rb*	2 - 100	2.7	1.1 - 1.5		
		.6	.4 - .6		
U	<lld	3.5	2.0	.18 - .85	.04 - .08
Sr*	130 - 1300	1.7	1.6 - 3.0		
		.6	.7 - 2.0		
Th*	lld - 12	4.5	2.6	.5 - 4.0	.12 - .4
		1.5	1.0		
Pb*	lld - 20	6.0	3.0	1 - 6	.2 - 1.6
		1.6	1.1		
Zn	80 - 180	1.9	1.4 - 1.8		
Cu	30 - 450	2.3	1.5 - 2.6		
Ni	lld - 280	2.5	1.5 - 2.4		
Ba	50 - 2000	6.0	3 - 7	100 - 800	20 - 160
Sc	15 - 45	2.0	1.6		
Co	20 - 60	3.3	2.0 - 2.5		
Cr	lld - 480	2.4	1.6 - 3.2		
V	100 - 400	4.0	2.0 - 2.5		
Mo	lld - 11	1.8	1.2		
Cs	<6.0	4.0	2.0	.2	.04
La	lld - 70	3.4	2.0 - 2.7	10 - 52	2 - 7.5
Ce	lld - 150	7.0	4.0 - 5.0	20 - 120	4 - 40
Pr	3 - 14			3 - 16	.7 - 2.8
Nd	lld - 110	4.0	2.5 - 3.0	14 - 60	2 - 20
Sm				4 - 13	.5 - .7
Eu				1.4 - 3.6	.2 - .25
Gd				4 - 10	.4 - 1
Tb				.7 - 1.4	.1 - .2
Dy				4.3 - 8.0	.3 - 1
Ho				1.0	.1
Er				3.0	.3
Yb				2.0	.2

Precision is expressed as an absolute error (2 s.d. counting error) for the given concentration range. The lower limit of detection (lld) is given at the 99% confidence level for XRF data only.

* For these elements the lower values represent precisions and lld's obtained for longer counting times conducted on central Lebombo samples selected for Sr-isotope analysis (n=34). This is particularly important for abundances close to the detection limit which is the case for most of the Th and Pb data.

are given in Table A2.

A more comprehensive suite of REE analyses were obtained for 6 samples (2 from each basalt type) by S. R. Taylor at the Australian National University. The spark-source mass spectrographic technique used has been described by Taylor (1965, 1971), Taylor and Gorton (1977) and Duncan *et al.* (1984a). Data obtained by XRF and spark-source mass spectrography are compared in Table A3 and determinations using the two techniques are generally within the quoted 2 s.d. errors (Table A2). A comparison of Nd data obtained by XRF and isotope dilution is made in Table A4; generally the XRF values are consistently 10-15% higher than the isotope dilution values.

Within sample homogeneity was tested by the analysis of two aliquots of a sample (RSV21) separated after the jaw-crushing stage and processed separately (Table A5). Only CaO, Zr, Sr, Ba and V are outside the range expected at the 95% confidence level (i.e. 2 s.d.) and then the differences are not substantially in excess of 2 standard deviations.

1.2 XRF SLAB ANALYSIS

Use of the slab analysis technique ensured that at least a semi-quantitative analysis was obtained for every sample and enabled the careful selection of material for more accurate quantitative determinations. The data is reported Appendix C (microfiche).

1.2.1 The Technique

Circular slabs 30 mm in diameter and 5-10 mm thick were cut from slices of rock using a diamond-tipped core bit mounted on a drill press. One side of the slab was then ground and polished to a mirror finish using medium and then fine-grained carborundum powder and cleaned in an ultrasonic bath. The slabs were placed in a XRF spectrometer and analysed for Si, Ti, Fe, Ca, K, Rb, Sr and Zr. The measuring parameters used for this analysis are summarized in Table A6. A W tube ensured the maximum excitation for the spectrum of analyte elements and background corrections involved the measurement of two adjacent backgrounds in the case of trace elements and one

Table A3. Comparison of data obtained by XRF, spark source mass spectrography and isotope dilution where avalailable (ppm).

	RSV31		RSS2		RSC35		RSC38	
	SSMS	XRF	SSMS	XRF	SSMS	XRF	SSMS	XRF
La	51.9	41	64.1	56	28.2	29	53.3	50
Ce	117	94	139	125	68.4	69	118	116
Nd	59.2	66	72.0	84	44.3	50	72.4	80
Th	3.94	6.0	5.42	8.5	3.06	4.4	5.45	6.7
Pb	6.2	8.2	8.1	10.6	4.1	5.0	8.2	7.4
Ba	775	799	800	830	315	431	560	695
Zr	375	362						
Nb	21	19						
Y	34	35						

	RSC32			RSS40		
	SSMS	XRF	ID	SSMS	XRF	ID
La	9.79	10	-	14.7	11	-
Ce	23.8	17	-	35.3	46	-
Nd	14.5	14	14.4	23.5	33	23.7
Sm	3.95	-	4.18	5.87	-	6.19
Th	.52	<1.4		1.74	2.2	
Pb	1.02	1.6		3.6	3.5	
Ba	105	98		175	178	

Table A4. Comparison of Nd determinations made using XRF and isotope dilution analytical techniques (ppm).

sample	XRF	ID
RSS138	78	65.8
RSS152	63	56.8
RSV18	58	53.2

sample	XRF	ID
RSS150	67	57.1
RSS160	51	43.6
RSS165	85	70.4
RSC70	81	68.3

sample	XRF	ID
RSS40	33	23.7
RSS162	26	22.0
RSV11	28	23.3
RSV16	28	23.6
RSC4	21	18.8
RSC22	21	16.8
RSC32	13.9	14.4

Table A5. Sample homogeneity test and the replication of XRF data

	RSV21 (1)	RSV21 (2)	actual difference	expected difference*
%				
SiO_2	53.19	53.06	.13	.52
TiO_2	2.72	2.72	0	.02
Al_2O_3	12.45	12.46	.01	.16
Fe_2O_3t	11.02	11.00	.02	.12
MnO	.15	.15	0	.01
MgO	5.17	5.12	.05	.18
CaO	7.07	7.21	.14	.06
Na_2O	2.48	2.52	.04	.13
K_2O	1.81	1.82	.01	.04
P_2O_5	.41	.41	0	.04
H2O-	.93	.90		
LOI	2.07	2.29		
TOTAL	99.48	99.65		
ppm				
Nb	16.6	14.3	2.3	2.8
Zr	330	320	10	4
Y	36	35	1	3
Sr	738	723	15	5
Rb	37	35	2	2.6
Ba	858	870	12	10
Sc	20	22	2	3.2
La	35	36	1	5
Ce	80	82	2	8
Nd	54	58	4	5.4
Zn	114	112	2	3.2
Cu	50	49	1	4
Ni	93	91	2	4
Co	46	45	1	4.5
Cr	85	87	2	4
V	229	234	5	4.5

* This is a maximum difference expected at the 95% confidence (2 s.d.) level (from Tables A1 and A2).

Table A6. Slab analysis measuring parameters

element (K_a)	approx. 2 angles	crystal	other
bgr Mo+	21.0		Philipps PW1400
->Zr	22.6	LIF200	spectrometer
bgr Y+	24.6		W tube
->Sr	26.2	LIF200	spinner on
bgr Sr+	25.8		two cycles measured
->Rb	26.6	LIF200	
bgr Pb+	29.3		
->Fe	85.8	LIF220	
bgr Fe+	90.5		
bgr Ti-	82.0		
->Ti	86.2	LIF200	
bgr Ca-	?		
->Ca	113.2	InSb	
->K	136.8	LIF200	
bgr K+	140.3		
bgr Si1	138.0		
->Si	144.6	InSb	

Table A7. Standard slab element abundances (from Bristow, 1980).

	CL110	CL111	CL113	CL120	CL132	CL143	CL351
%							
SiO_2	50.39	51.38	50.54	51.24	51.00	49.96	51.29
TiO_2	3.01	2.92	2.93	2.91	3.28	1.95	1.97
Fe_2O_3t	12.30	12.05	12.43	12.27	15.89	15.11	13.62
CaO	8.25	8.05	8.01	7.22	7.12	10.13	9.83
K_2O	2.57	2.08	1.82	2.81	1.63	.50	.48
ppm							
Rb	54	39	50	60	36	11	10.9
Sr	1093	768	900	1144	509	204	326
Zr	351	329	414	333	347	143	139
	CL356	CL360	KA121	CL209	KA13	KA42	L340
%							
SiO_2	49.14	47.30	66.75	68.45	67.01	65.36	70.35
TiO_2	2.35	2.65	.70	.53	.56	.80	.50
Fe_2O_3t	13.67	14.67	6.41	6.60	6.72	6.39	6.27
CaO	9.96	11.50	1.25	2.18	2.39	2.03	1.05
K_2O	.50	.39	5.18	4.19	5.15	4.98	4.10
ppm							
Rb	13	4	120	122	132	107	124
Sr	204	355	275	208	284	302	153
Zr	143	120	1095	1193	1230	1000	1163

in the case of each major element. Corrections were made for interelement interference between Rb and Sr, dead-time, instrumental drift and background effects.

A major part of any data reduction procedure in XRF spectrometry is correction for sample errors: principally absorption and particle effects. In the slab technique counting errors were insignificant (<0.1%) compared to these matrix effects. Particle effects were minimized by restricting the technique to relatively fine-grained (generally <1 mm and typically .5 mm grain size) samples which were presumed to be homogeneous on the scale of a slab. Sample homogeneity was improved by spinning the sample during analysis.

Corrections must be made for the absorption of secondary X-rays (generated by the element of interest) by the sample itself. If the matrix in each case (samples and standards) is the same, no problem would exist. However, sample matrices are typically variable with absorption varying as a function of major element content - principally Fe as the heaviest absorber. The most successful matrix correction technique (and that routinely used by the Geochemistry Department at UCT) is the use of mass absorption coefficients (μ). These may be estimated by calculation from whole rock major element data, direct measurement (on a thin sample) or using the intensity of the Compton scatter peak. Major element data were unavailable and direct measurement was impractical in the case of slabs, and therefore the Compton scatter method was used.

Compton scattered radiation is caused by the incoherent scatter of primary X-rays (from the tube) by the sample, i.e. part of the energy of the incoming tube radiation is lost to an electron (expelled) in an outer shell of an element. Such scattered radiation is therefore at a lower energy than the tube radiation and produces Compton peaks on the long wavelength side of tube peaks. The intensity (I_c) of this peak is related to the average atomic number (major element content) of a sample: e.g. the higher the average atomic number the lower the Compton peak intensity and the higher the absorbance of a sample. The linearity of the relationship I_c *vs* μ was established by Reynolds (1963, 1967). The Compton peak method is limited to the X-ray tubes available: a Mo tube was used for the determinations and hereafter I_c refers to the intensity of the Mo K_a Compton peak.

A significant limitation of the technique is that it is restricted to wavelengths shorter than the first major element absorption edge: the Fe K-absorption edge in silicates (Fig. A1). The situation in samples of variable Fe content is illustrated in Fig. A2: the change in μ across the Fe K-absorption edge will be most significant in high Fe samples. Thus the Mo Compton μ correction may be applied directly for elements shorter than the Fe K-absorption edge (Rb, Sr and Zr in this instance) but not in the case of the major elements.

Nesbitt *et al.* (1976) established that a high degree of linear correlation existed for $1/(\mu_{long}.I_c)$ *vs* I_{Fe}, where μ_{long} is the μ of a wavelength longer than the Fe K-absorption edge (i.e. at the Fe K_a analyte line) but shorter than the next major element absorption edge (Ti K-absorption edge in this instance, Mn is excluded as it is generally present only in low abundances). There is also a linear relationship between I_c and $1/\mu_c$ (μ_c is the μ determined by measuring the Mo Compton peak intensity), thus μ_c/μ_{long} and I_{Fe} will also be related by some linear function. Initially $\mu_{long} = \mu_{Fe}$ which permits absorption corrections to be made for Fe K_a analyte intensity. This technique of absorption edge "jumping" is extrapolated to longer wavelengths assuming similar linearity between μ_{Fe}/μ_{Ti} *vs* I_{Ti}; μ_{Ti}/μ_{Ce} *vs* I_{Ce}; μ_{Ce}/μ_K *vs* I_K; μ_K/μ_{Si} *vs* I_{Si}; or generally μ_{short}/μ_{long} *vs* I_{long}.

1.2.2 Calibration

The results of standard calibrations for one slab analysis run (February, 1986) are used as an example of the calibrations achieved. The slab standards used comprised Jozini Rhyolites and Sabie River Basalts and are given in Table A7. Quantitative chemical determinations by conventional XRF techniques for these samples are from Duncan *et al.* (1984a) and μ values for these slabs were calculated from the major element oxide data. The μ's at major element wavelengths and Mo Compton μ's (measured on slab standards) remain constant and it is only the measured intensities of each element which may fluctuate from run to run. Calibration curves of μ_{short}/μ_{long} *vs* I_{long} (dead time and background corrected) are given in Fig. A3 and demonstrate linear relationships. Thus measurement of

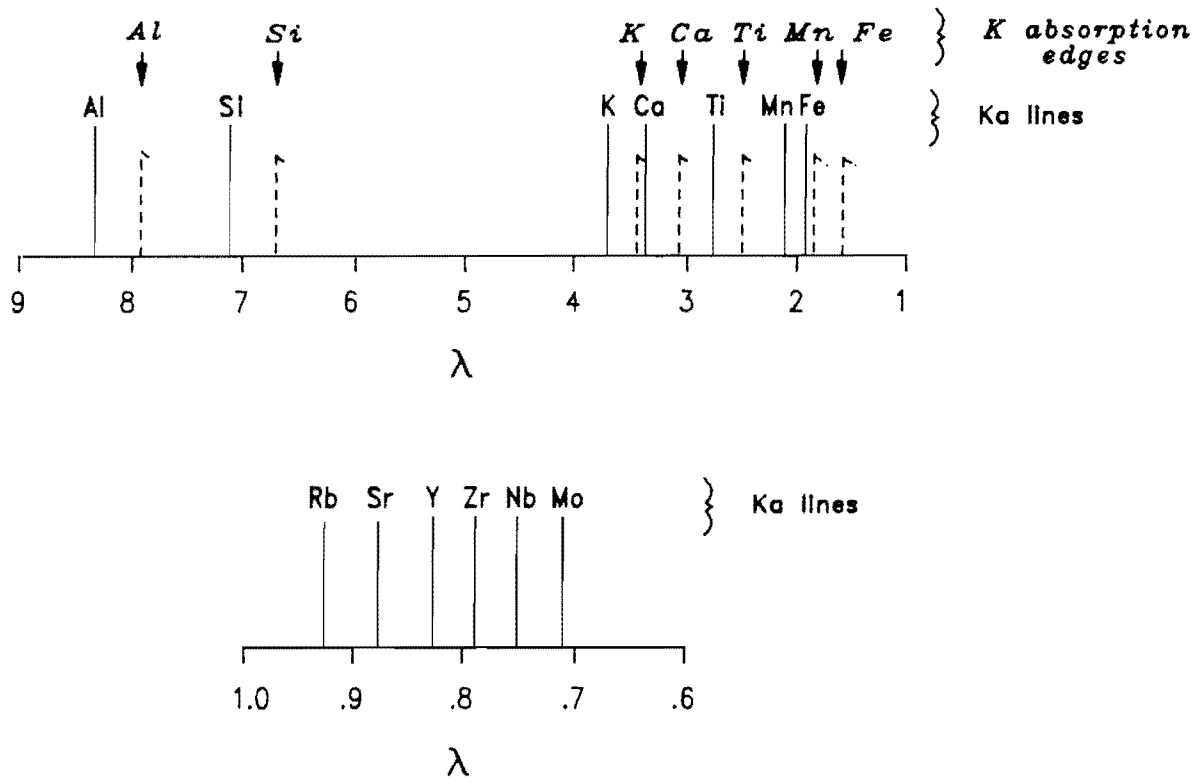

Figure A1. Wavelengths of Ka analyte lines and absorption edges in A units.

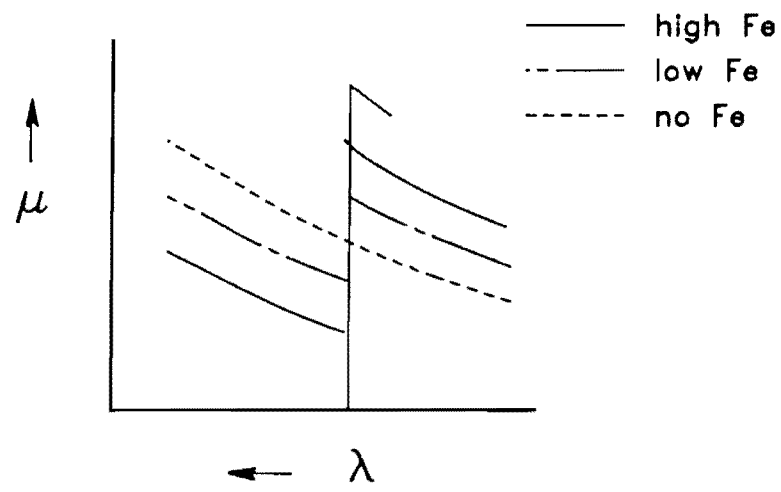

Figure A2. Effect of Fe on u on opposite sides of the Fe absorption edge.

Mo Compton μ's of the unknowns enables μ's to be estimated at the major element wavelengths of interest and concentration calibration curves for the major element intensities (absorption corrected) to be set up (Fig. A4). These major element calibration curves indicate that Fe_2O_3t (Fe reported as total Fe_2O_3) and SiO_2 may be expected to be the most imprecisely determined elements.

Linearity is maintained for Fe_2O_3t, TiO_2 and K_2O but not CaO and SiO_2 calibrations when intensities are uncorrected for absorption effects (Fig. A5). Thus the Si and Ca K_a radiation is differentially absorbed depending on the composition of the sample. The Ca K_a peak is positioned just on the short wavelength side of the K K-absorption edge (Fig. A1, a .04 A difference). This causes the absorption of Ca K_a radiation to be extremely sensitive to K abundance, thereby causing a slightly greater absorbance in the high-K basalts (also slightly lower in CaO content) relative to the low-K basalts (Fig. A5e).

The greater absorbance of Si K_a radiation in the basalt samples relative to the rhyolites is due to their "heavier" matrix (mainly Fe). Why Si and not K, Ti and Fe K_a radiation should be affected is perhaps a function of the much longer wavelength of Si K_a radiation and therefore greater susceptibility to absorption.

1.2.3 Accuracy

The most precise estimate of accuracy may be made by comparing the set of quantitative determinations with the slab data obtained for each sample. The deviation of data from a 45° line is the best estimate of accuracy of the slab technique (Fig. A6). Thus the errors suggested for the HFSE (Ti, Zr) indicate that the slab technique is capable of resolving differences between the "normal" (N) and "enriched" (LFE and HFE) groups. The error in Fe_2O_3t ($\pm$ 1.5%), however, makes the technique less efficient in distinguishing between the low-Fe and high-Fe "enriched" suites. Duplicate slabs were cut for selected samples and the replication achieved (Table A8) is consistent with the errors (given in Fig. A6) on median values.

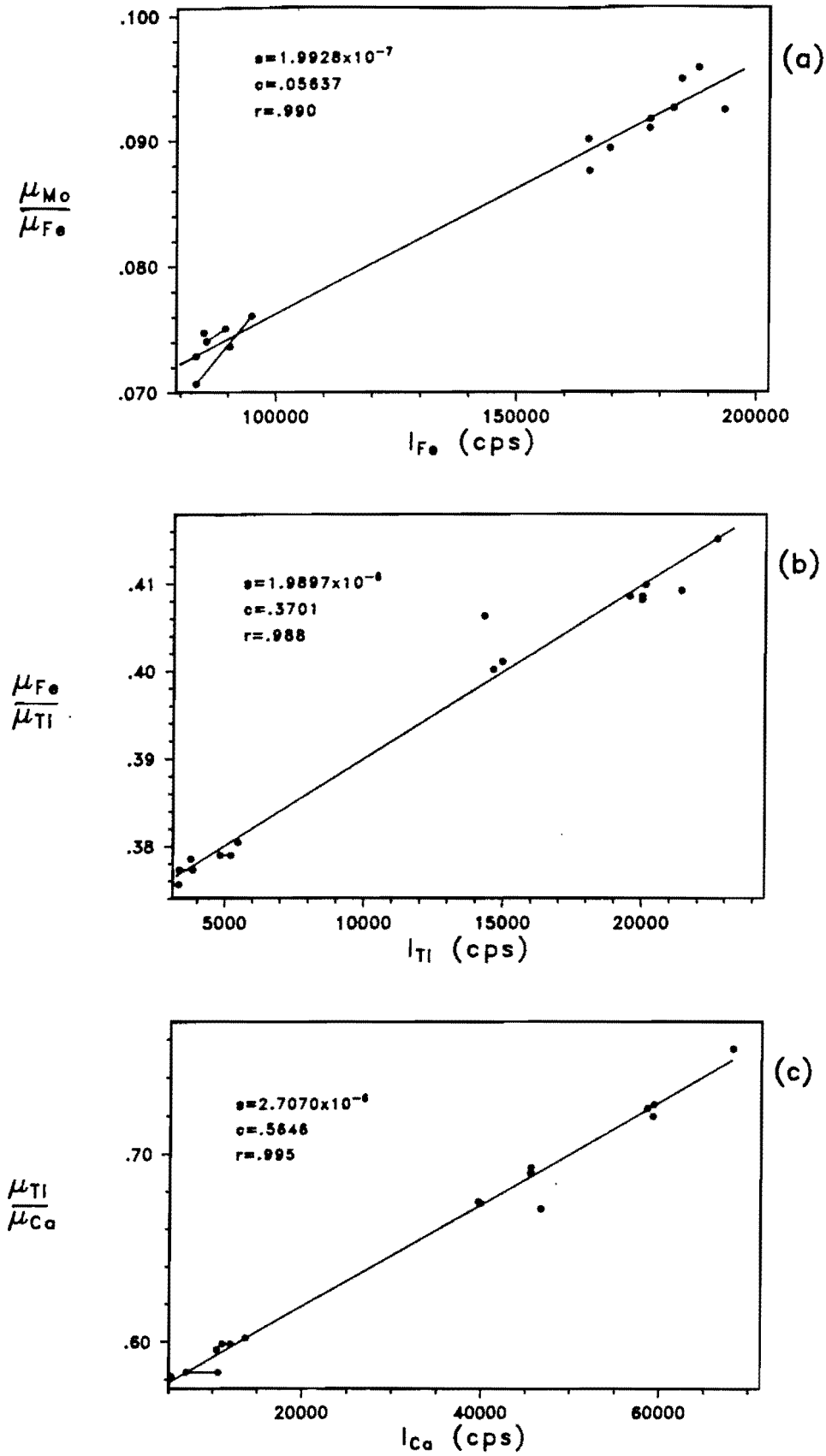

Figure A3. Calibration curves for the determination of unknown μ's at major element wavelengths from the intensity of the K_a line for the element of interest (February, 1986, slab run).

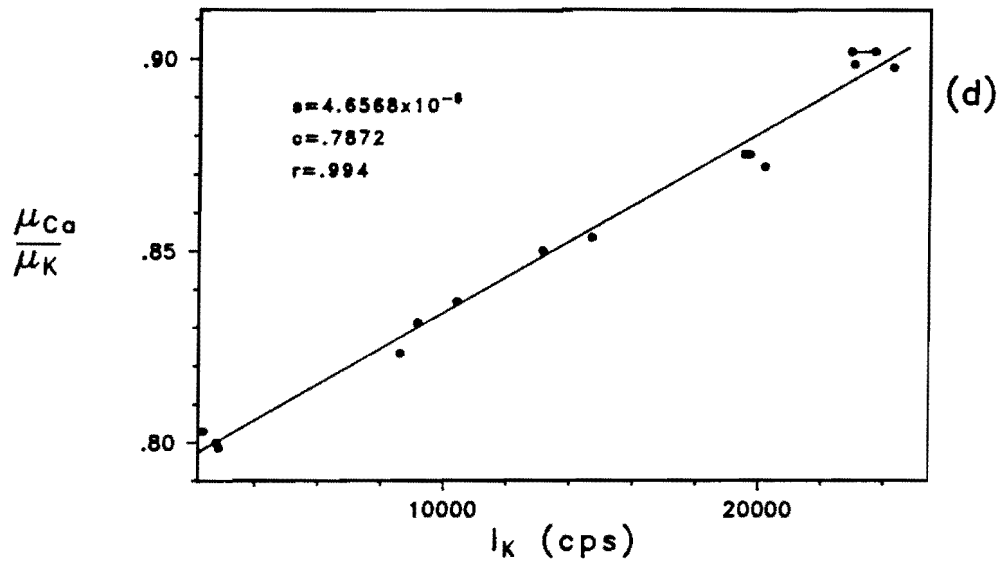
.90
.85
.80
$\frac{\mu_{Ca}}{\mu_K}$
a=4.6568x10^{-6}
c=.7872
r=.994
10000
20000
I_K (cps)
(d)

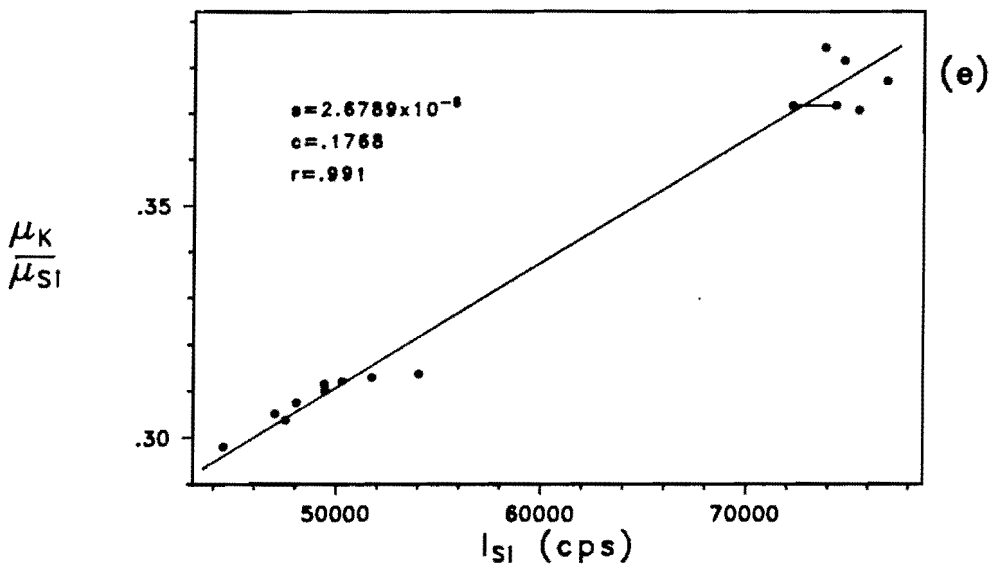
.35
.30
$\frac{\mu_K}{\mu_{Si}}$
a=2.6789x10^{-6}
c=.1768
r=.991
50000
60000
70000
I_{Si} (cps)
(e)

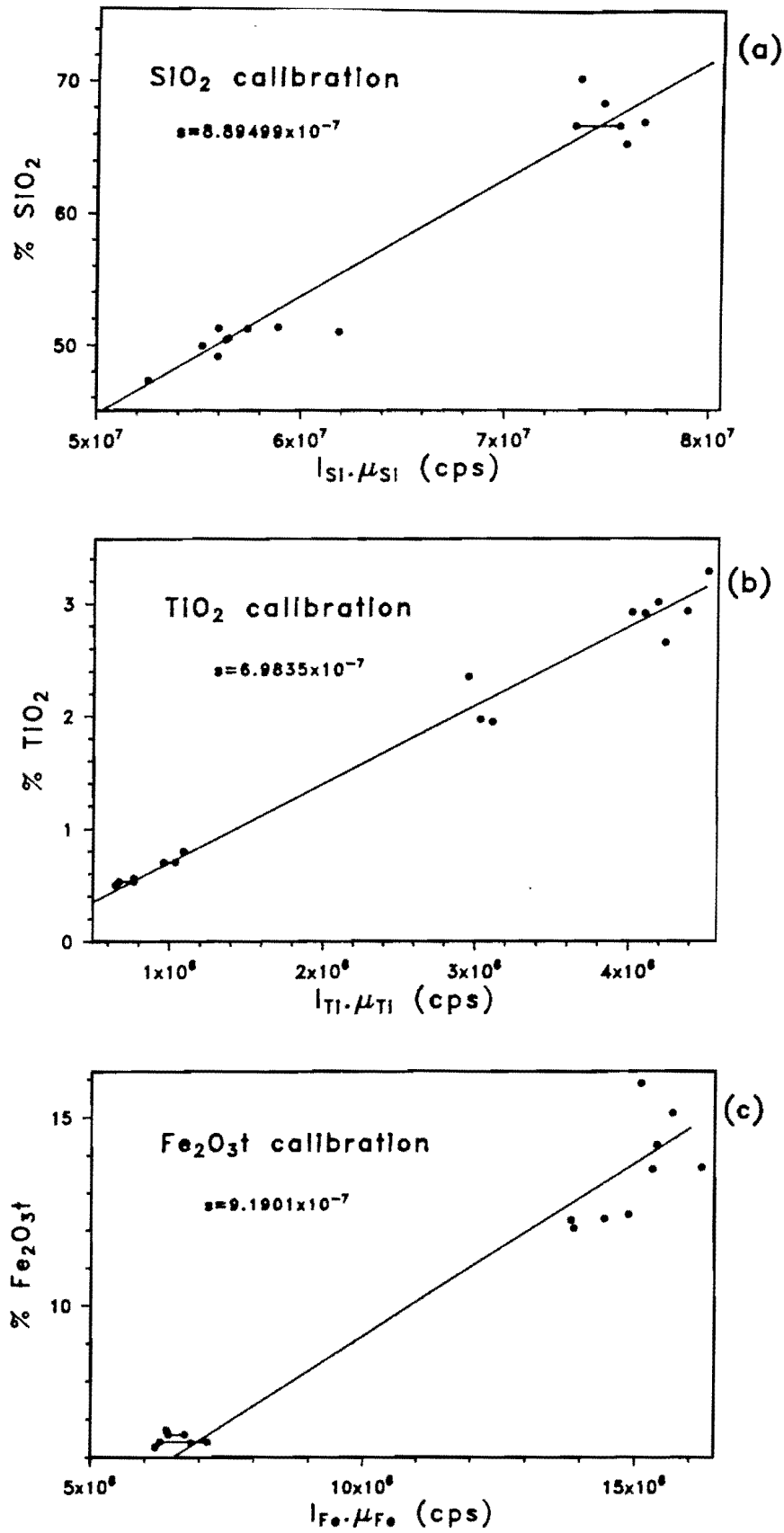

Figure A4. Calibration curves for determining major element concentrations using intensities corrected for absorption (February, 1986, slab run).

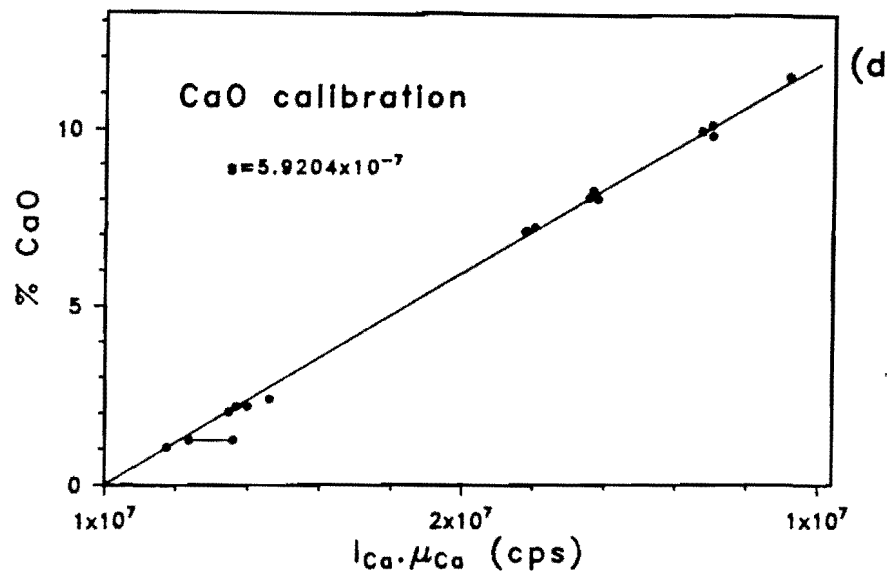

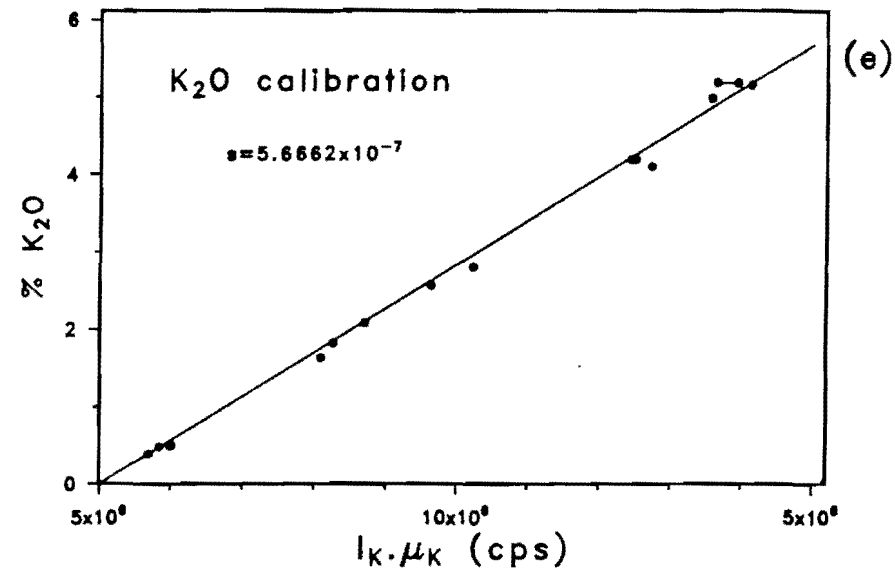

Table A8. Duplicate slab analyses

	RSS49		RSC11		RSC18		RSS183	
	A	B	A	B	A	B	A	B
%								
SiO_2	53.22	52.63	50.55	48.11	47.58	45.44	50.75	50.26
TiO_2	2.04	1.77	3.98	3.21	3.72	3.40	2.76	2.70
Fe_2O_3t	13.02	11.12	13.11	12.70	15.56	15.61	14.72	14.55
CaO	8.25	8.02	10.06	10.37	7.53	6.95	9.67	9.57
K_2O	1.57	1.64	2.16	2.05	1.15	.89	.81	.78
ppm								
Rb	33	35	35	32	19.8	15.5	18.5	17.3
Sr	415	452	868	836	334	293	243	243
Zr	168	147	337	335	295	282	216	207
	plag-phyric basalt?		massive basalt		amygdaloidal basalt		basaltic	

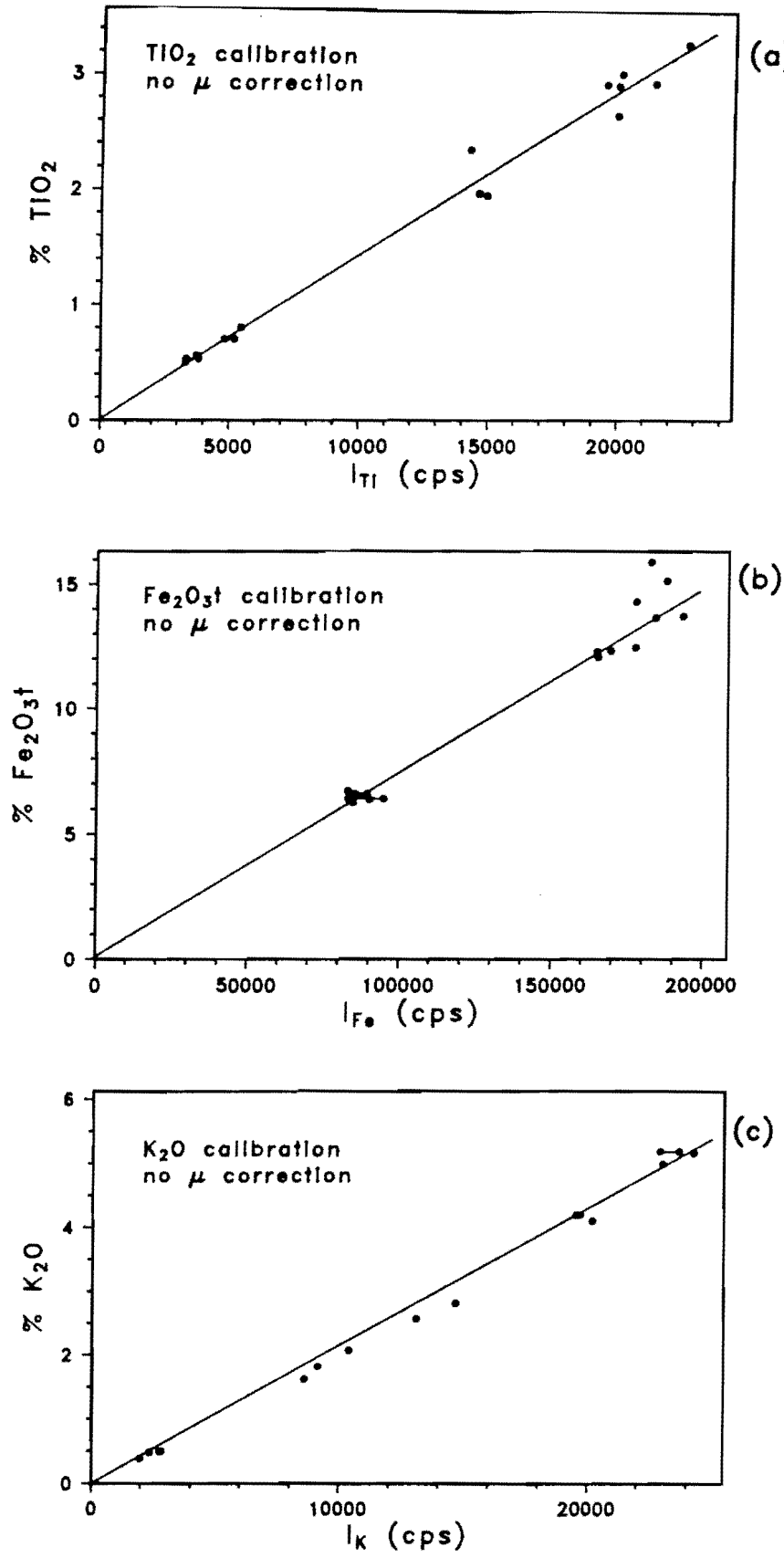

Figure A5. Calibration curves for determining major element concentrations from intensities uncorrected for absorption. Dashed lines on (d) and (e) are an estimate of the calibration without differential absorption effects

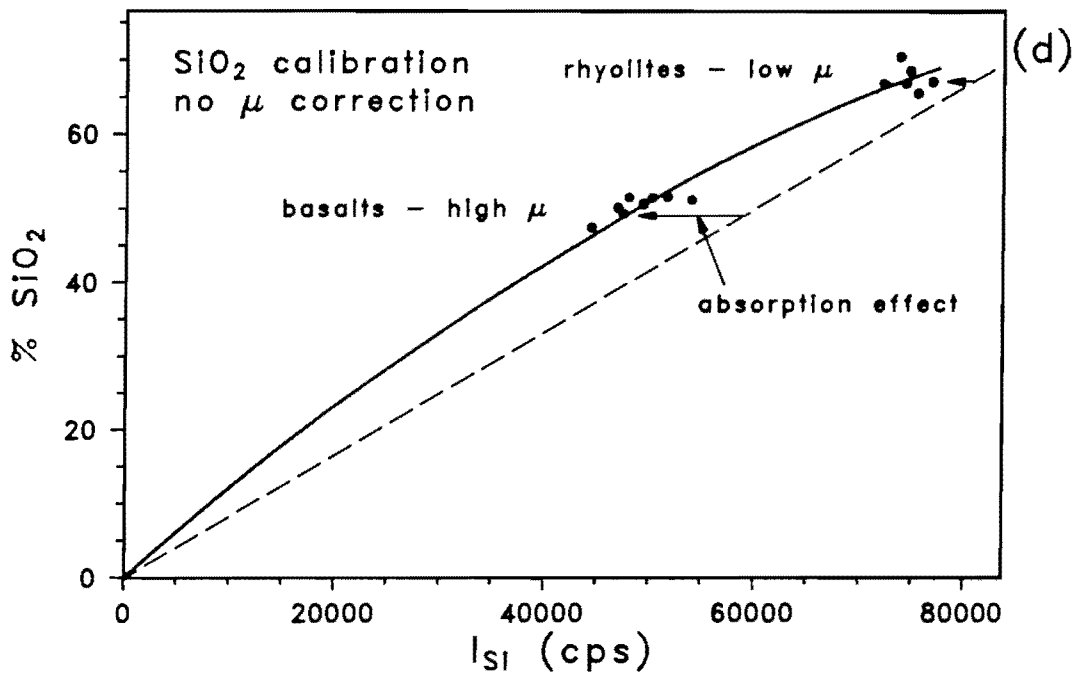
SiO2 calibration
no μ correction
rhyolites – low μ
basalts – high μ
absorption effect
(d)
% SiO2
0
20
40
60
0
20000
40000
60000
80000
ISI (cps)

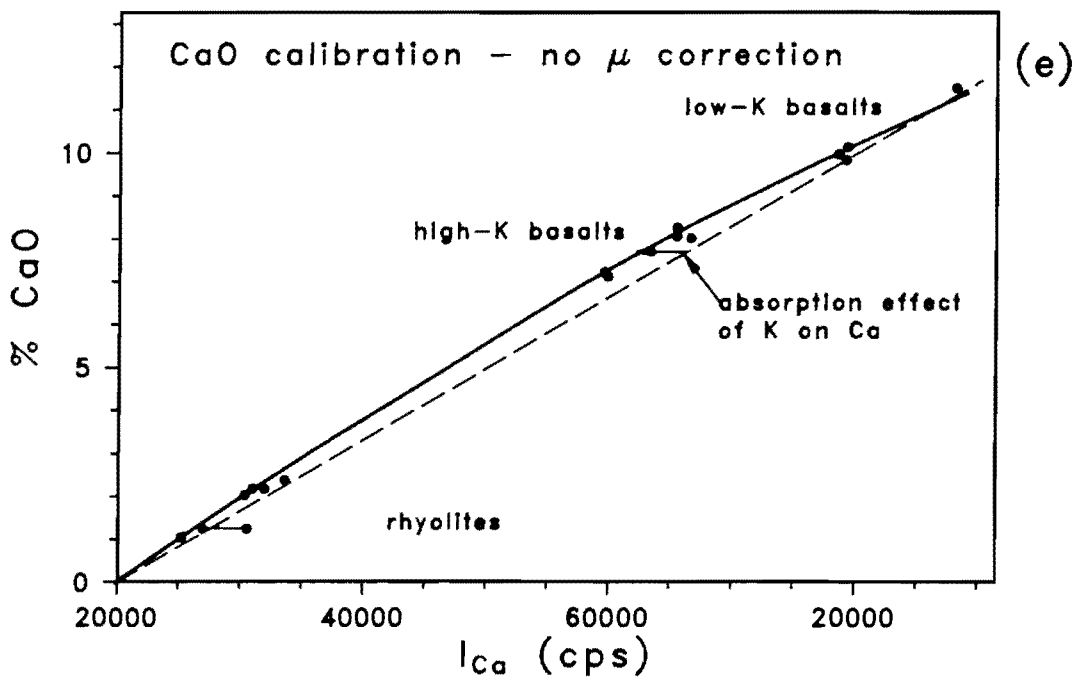
CaO calibration – no μ correction
low–K basalts
high–K basalts
absorption effect
of K on Ca
rhyolites
(e)
% CaO
0
5
10
20000
40000
60000
20000
ICa (cps)

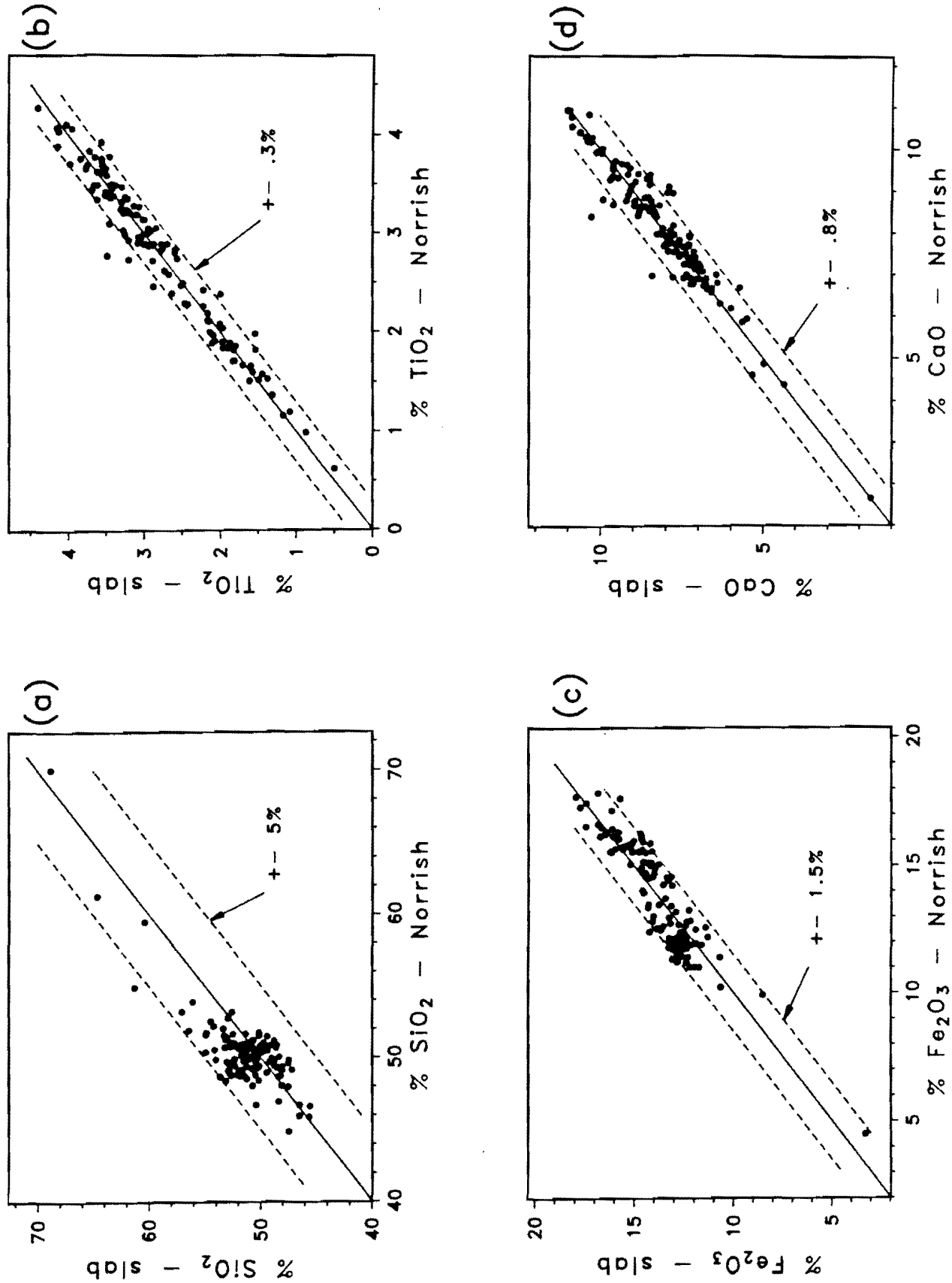

Figure A6. Comparison of quantitative data with data obtained on slabs and an estimation of the accuracy of the slab data for the elements determined (n=125).

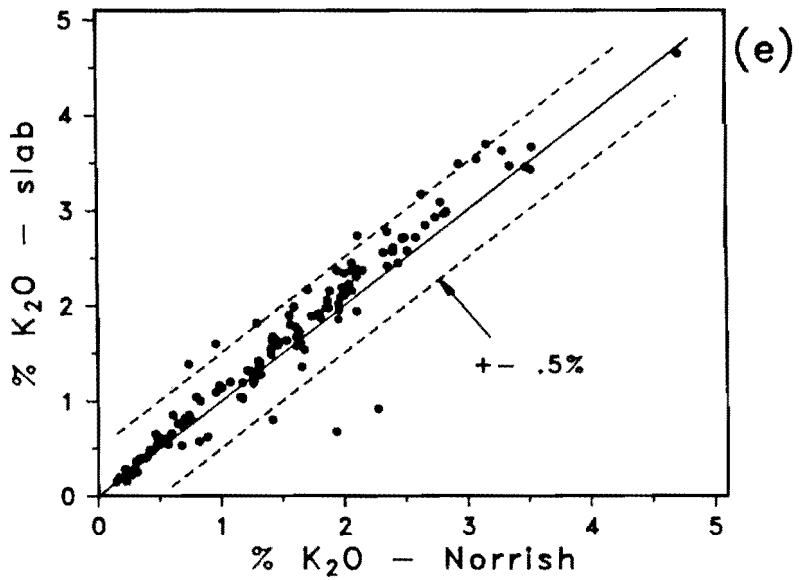
(e)
% K_2O – slab
% K_2O – Norrish
+– .5%
0
1
2
3
4
5

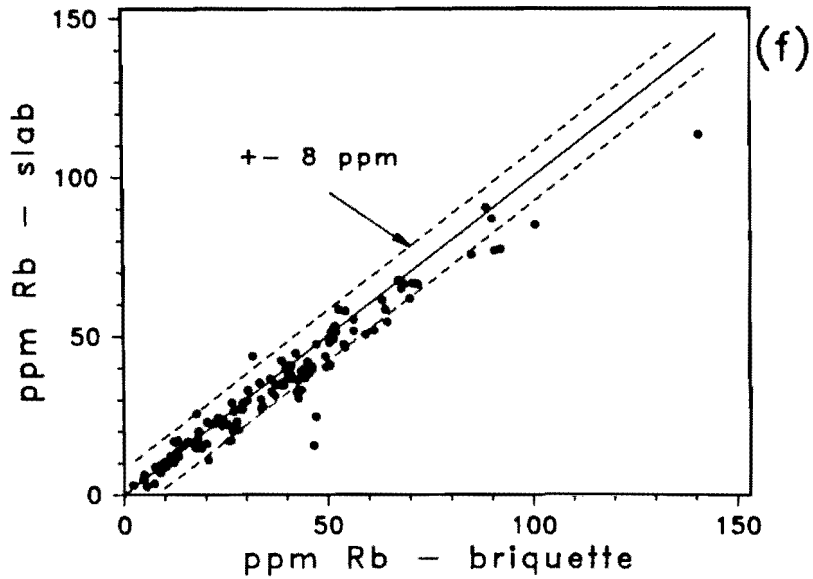
(f)
ppm Rb – slab
ppm Rb – briquette
+– 8 ppm
0
50
100
150

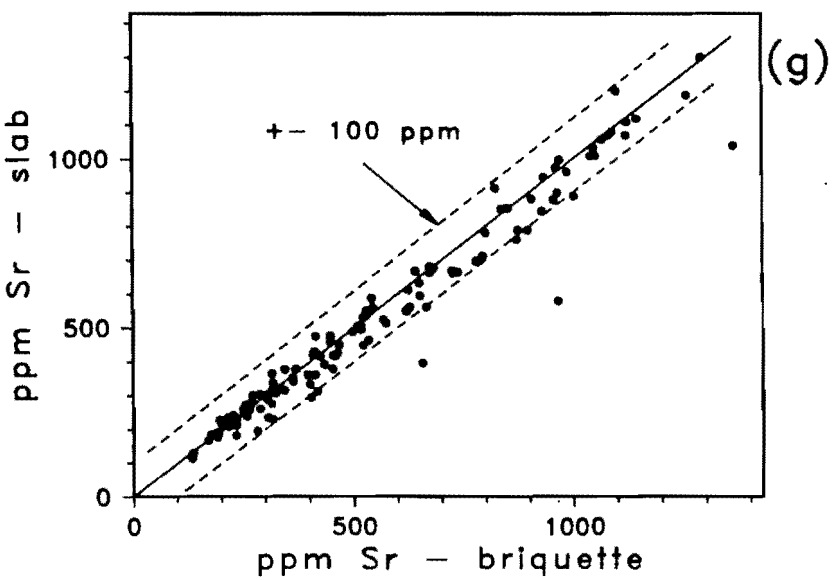
(g)
ppm Sr – slab
ppm Sr – briquette
+– 100 ppm
0
500
1000

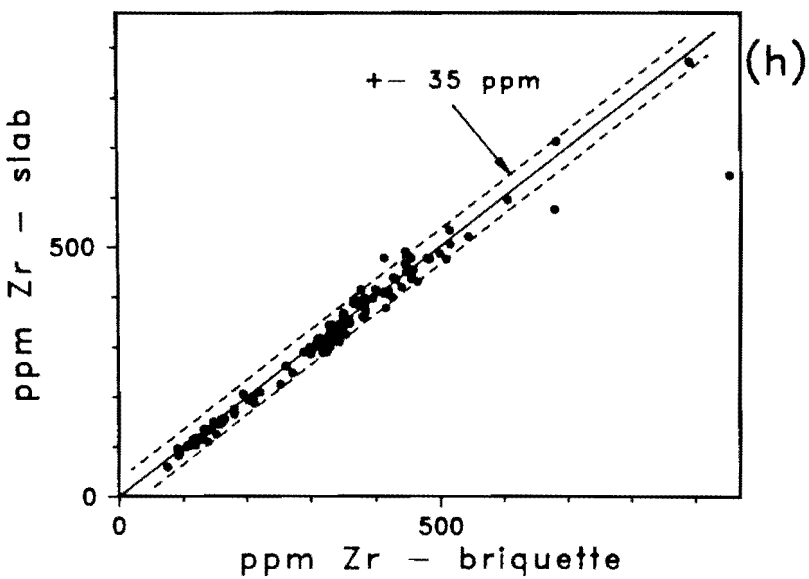
(h)
ppm Zr – slab
ppm Zr – briquette
+– 35 ppm
0
500

1.3 RADIOGENIC ISOTOPE ANALYSIS

The procedures described are those currently in use at the National Physical Research Laboratory (NPRL) of the Council for Scientific and Industrial Research (CSIR) in Pretoria. These are given in detail by Harmer *et al.* (1986) and are summarized below. All determinations were conducted on the whole-rock powders analysed by XRF techniques. Data are reported in Appendix C.

1.3.1 Procedure for Sr and Sm-Nd Sample Preparation

Reagents are labelled with an "x" for each distillation and a "r" for each pass through an ion exchange resin.

1.3.1.1 Sample dissolution

Samples may be spiked with an internal standard for concentration measurements or unspiked for isotopic composition determinations ("natural"). Only natural determinations of $^{87}Sr/^{86}Sr$ were made as the Rb and Sr concentrations were known from XRF data. In the case of Sm and Nd both concentration and natural determinations were made on separate dissolutions of a sample. About 200 μg of sample powder was used for each dissolution. In the case of spiked samples the amount of sample and mixed ^{149}Sm-^{150}Nd spike added was precisely known, generally within $\pm$ .02μg.

Samples were dissolved in a mixture of 15M HNO_3^{xx} (1-2 ml) and HF^{xx} in a sealed vessel left on a hot-plate overnight. Evaporation and addition of HNO_3 was repeated until the volume of fluoride precipitate was reduced. The sample was converted to a chloride by the repeated (twice) addition of 6M HCl^{xx} and complete drying down. About 5 ml 6M HCl was added to the precipitate and left to reflux in a sealed vessel overnight to ensure complete conversion. This solution was dried down and covered ready for columns.

1.3.1.2 Column separations

Two sets of columns were used:

(1) 6 ml of Bio-Rad AG50W-X12, 200-400# cation resin packed in a 10 mm internal diameter quartz-glass column was used to separate the Sr and

bulk REE fractions;

(2) 2.5 ml of Teflon/HDEHP (KEL-F) reverse-phase ion exchange resin packed in a 8 mm internal diameter quartz-glass column was used to separate pure Nd and Sm fractions from the bulk REE fraction collected off the cation columns.

The sample was dissolved in 1-2 ml of 2.5M HCl[xx] of which 1 ml was loaded directly onto the resin bed of the cation resin columns previously equilibrated with this molarity HCl. The Sr and REE fractions were then separated according to the column log and dried down. The Sr fraction was converted to a nitrate and dried down ready for loading onto filaments. The REE fraction was dissolved in 100μl of .2M HCl[xx] and loaded onto the KEL-F resin equilibrated with HCl of the same molarity. Nd and Sm (in the case of spiked samples) were then separated according to the column log. The collected Nd fraction was passed through the columns again to ensure clean separation of Nd from Sm as ^{144}Sm interferes on ^{144}Nd in the analysis.

1.3.1.3 Filament preparation

Single filament beads were strung with Ta ribbon for Sr and Sm. Triple filament beads were strung with Ta (sides) and Re (centre) ribbon for the analysis of Nd. Once strung, beads were placed in a Decon solution in an ultrasonic bath for 10 minutes, washed and boiled in H_2O[xx] for a further 10 minutes and left to dry in a convection oven overnight. Single filaments were outgassed for 10 minutes at 4 amps and triples at 5 amps under a vacuum better than $4x10^{-6}$ torr. Filaments were left for two days before loading to help prevent sample spreading.

Ta filaments were prepared for loading Sr fractions with 1 drop of 1M H_3PO_4 dried down to a thin film (at 1 amp. under a lamp). The Sr fraction was then loaded as a nitrate and current increased to fume off the H_3PO_4. Nd and Sm fractions were loaded directly onto Ta filaments (single for Sm, two sides of triple for Nd) as nitrates.

1.3.2 Pb-Pb Sample Preparation

Natural Pb-isotope ratios were determined on unspiked samples. The sample dissolution procedure is identical to that set out for the Sr method

until the drying down stage where the sample was converted from a chloride to a nitrate using 15M HNO_3.

1.3.2.1 Column separation

Samples were passed through two column separations which eliminates the necessity of purifying the Pb by electrodeposition. Approximately 30 μl (2-3 drops) of AG1X8 anion exchange resin was loaded into 4 mm internal diameter quartz glass columns. Resin was discarded and columns cleaned after each passage. Loaded resin was washed and pre-conditioned with 1 ml .5M HBr^{rr}. Sample was dissolved in 1 ml .5M HBr and loaded onto the column. Sample was washed onto the resin with 2x1 ml washes of .5m HBr^{rr}, collected with 1 ml H_2O^{xrx} and dried down. The Pb fraction from the second column separation is collected in a beaker containing a drop of .2M H_3PO_4 which once dried down assists in location of the sample when loading onto filaments.

1.3.2.2 Filament Preparation

Single beads were strung with Re for Pb, cleaned using the method described previously and outgassed for 10 minutes at 5 amps. Filaments were primed with silica gel and 1M H_3PO_4, both evaporated to a thin film. The Pb sample was dissolved in 1 drop of 1M HNO_3^{xx}, loaded onto the filament and dried down to a thin film. An attempt was made to load consistent amounts of Pb (*ca* 500 ng) for standards and samples based on estimates of the whole rock Pb content (the more precise XRF determinations of Pb were not available at this stage).

1.3.3 Data Accumulation and Reduction

In naturally occurring Pb-isotopes, only ^{204}Pb does not have a radiogenic contribution and therefore no Pb-isotope ratio is constant in nature. Therefore the fractionation correction applied to the Pb-isotope data is empirical: based on the fractionation observed in analysis of standards. All Pb-isotope analyses were conducted manually (on the MM30) using an optical pyrometer to monitor filament temperature (maintained between 1160-1200°C) in an attempt to ensure relatively constant fractionation effects. Two Pb standards (NBS981) were included with each

barrel of 8 samples. Accepted and measured ratios for NBS981 are summarised in Table A9.

The lower abundance of ^{204}Pb results in the measurement of any ratio involving this isotope being potentially susceptible to '^{204}Pb-error'. A way of differentiating ^{204}Pb-error from mass fractionation effects is to plot $^{207}Pb/^{204}Pb$ *vs* $^{207}Pb/^{204}Pb$ for the NBS981 results (Fig. A7). Mass fractionation should result in the standards plotting along a locus of points were the gradient is 1.5, while ^{204}Pb-error will effect both ratios simultaneously and produce data which falls along a line of gradient 1 (Fig. A7). Although errors do not allow perfect resolution, all the standards do plot within-error of the fractionation line but not all are within-error of the ^{204}Pb-error line (Fig. A7). Thus it appears mass fractionation is the dominant effect.

Measured ratios were corrected to an average calculated for the NBS981 determinations using the relation assuming linear fractionation:

$$Rc = Rm * [1 + a * (D_{Rm-Rc}]$$

where $a = [(Rn/Rm) - 1]/(D_{Rn-Rm})$

Rn = natural 'known' ratio (constant in nature)

Rm = measured ratio of isotopes of interest (unknown)

Rc = fractionation corrected ratio

D = mass difference

$^{87}Sr/^{86}Sr$ ratios were corrected also assuming linear fractionation and calculating a value for 'a' by normalization to $^{88}Sr/^{86}Sr$ (Rn above = 8.375, and is constant in nature) continually within each run. Similarly $^{143}Nd/^{144}Nd$ was corrected for isotopic fractionation using a constant $^{146}Nd/^{144}Nd$ ratio of .7219.

To minimize interlaboratory differences all $^{87}Sr/^{86}Sr$ data are normalized to a ratio of the accepted value of NBS987 (.710240) over an average of 5 measured determinations (.710300) of the standard (Table A9). $^{143}Nd/^{144}Nd$ and Sm and Nd (ppm) determinations are reported relative to averages obtained for BCR-1 when compared to accepted values (Table A9).

The interference of ^{144}Sm on ^{144}Nd was monitored by measuring ^{147}Sm average net peak which was always close to or below detection limit.

Table A9. Isotope standards data. Bracketted numbers represent the measurements used relative to total measurements. Errors are 2 s.d. on bracketed replications.

Lead - NBS 981

207/206	206/204	207/204	208/204
0.914046 ±164 (85/100)	16.91707 ±504 (91/100)	15.46100 ±479 (84/100)	36.60479 ±523 (93/100)
0.913910 ±335 (91/100)	16.90622 ±725 (87/100)	15.45495 ±826 (88/100)	36.58910 ±2444 (90/100)
0.914005 ±241 (88/100)	16.92189 ±429 (84/100)	15.46805 ±552 (87/100)	36.61073 ±1600 (86/100)
0.913764 ±335 (73/90)	16.92454 ±876 (78/90)	15.46887 ±999 (79/90)	36.62206 ±2759 (77/90)
0.914267 ±422 (100/110)	16.92152 ±814 (95/110)	15.47209 ±1006 (92/110)	36.63215 ±2847 (94/110)
0.913721 ±465 (76/90)	16.91640 ±1180 (84/90)	15.46768 ±1458 (80/90)	36.63270 ±3814 (80/90)
0.913989 ±255 (95/110)	16.92847 ±748 (99/110)	15.46843 ±818 (100/110)	36.62251 ±1990 (98/110)
mean $\overline{0.913957}$	a=.000747		
NBS accepted: 0.91464	16.9374	15.4916	36.7219

Strontium

NBS 987		BCR-1	
87/86	(no. determinations)	87/86	
0.710302 ±10	(126/150)	0.705013 ±13	(134/150)
0.710291 ±14	(131/150)	0.705021 ±16	(138/150)
0.710307 ±14	(133/150)		
0.710318 ±16	(109/130)		
0.710284 ±30	(104/120)		
mean $\overline{0.710300}$		mean $\overline{0.705017}$	
NBS accepted: 0.710240		NBS accepted: 0.704950	

Neodymium - BCR-1

	$^{143}Nd/^{144}Nd$	Sm (ppm)	Nd (ppm)
1986:	0.512664 ±38 (59/70)	6.64	28.9
		6.80	29.5
1987:	0.512695 ±10 (127/140)		29.0
		mean $\overline{6.72}$	$\overline{29.1}$
NBS accepted:		NBS accepted:	
	0.512664	6.58	28.7

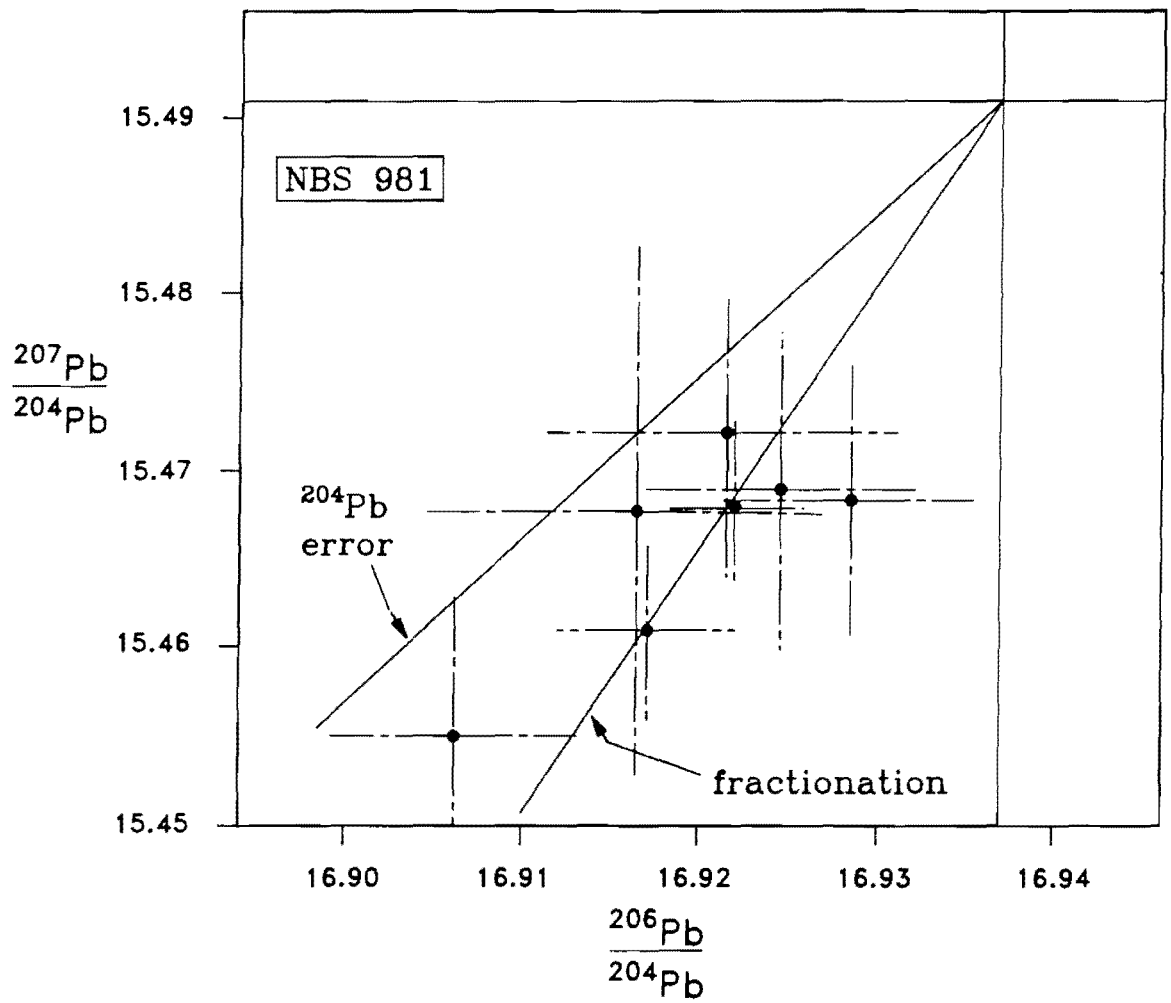

Figure A7. The deviation expected from accepted values for NBS 981 standards due to ^{204}Pb measurement error and mass fractionation with data for NBS 981 run in this study.

Thus the REE column procedure used ensured near complete separation of Nd from Sm.

Data reduction for isotope dilution (Sm and Nd) used the method of Boelrijk (1968) as applied at the NPRL. Equations and constants used for the calculation of $^{87}Sr/^{87}Sr$ and $^{143}Nd/^{144}Nd$ initial ratios, ϵ-values and Nd-isotope model ages are given in Table A10.

1.3.4 Replication

The values obtained for standards and accepted values for these standards are given in Table A9. The replication of standards is good; within counting statistics of a mean value in all instances (Sr, Nd and Pb, Table A9). This is the case for duplicate and replicate analyses of unknowns for their Sr- and Nd-isotope content, even when compared to results previously by J. W. Bristow at the Bernard Price Institute (Table A11). Unfortunately the only Pb duplicates obtained were done so because of the poor nature of the initial determination so the results for Pb-istopes in Table A11 are not strictly representative of reproducibility.

1.4 STABLE ISOTOPES

The $\delta^{18}O$ contents of 11 samples were determined by Dr H. S. Smith and Dr C. Harris of the Department of Geochemistry, University of Cape Town, using methods described in Smith (1988).

The standard $\delta^{18}O$ notation used for the data reported in Appendix C is defined:

$$\delta^{18}O = [(R_x - R_{std})/R_{std})] * 1000$$

where $R = {}^{18}O/{}^{16}O$, x is the sample and V-SMOW is the standard.
The isotope fractionation factor between two substances A and B is defined as:

$$a_{A-B} = R_A/R_B = (1000 + \delta^{18}O_A)/(1000 + \delta^{18}O_B)$$

which is related to the equilibrium constant K:

$$a_{A-B} = K^{1/n}$$

Table A10. Equations and constants for the calculation of initial ratios, ϵ-values and Nd-isotope model ages.

Bulk Earth Values

Sr	Nd
$(^{87}Sr/^{86}Sr)_p = 0.70470$	$(^{143}Nd/^{144}Nd)_p = 0.512638$
$^{87}Rb/^{86}Sr = 0.0857$	$^{147}Sm/^{144}Nd = 0.1966/7$

For t = 4.57 Ga:

$(^{87}Sr/^{86}Sr)_i = 0.69898$	$(^{143}Nd/^{144}Nd)_i = 0.506670$

For t = 190 Ma:

$^{87}Sr/^{86}Sr = 0.70447$	$^{143}Nd/^{144}Nd = 0.512394$

(p=present, i=initial)

Equations

Sr

$$(^{87}Sr/^{86}Sr)_p = (^{87}Sr/^{86}Sr)_i + {}^{87}Rb/^{86}Sr * (e^{\lambda t} - 1)$$

$$^{87}Rb/^{86}Sr = Rb/Sr_{ppm} * (2.692948 + 0.2803040 * {}^{87/86}Sr)$$

Decay constant (λ) = 1.42×10^{-11} yr.$^{-1}$

$$\epsilon_{Sr} = [((^{87/86}Sr)_i \text{ at } T)/(^{87/86}Sr)_{BE} \text{ at } T) - 1] * 10^4$$

Nd

$$(^{143}Nd/^{144}Nd)_p = (^{143}Nd/^{144}Nd)_i + {}^{147}Sm/^{144}Nd * (e^{\lambda t} - 1)$$

$$^{147}Sm/^{144}Nd = Sm/Nd_{ppm} * (0.531497 + 0.142521 * {}^{143/144}Nd)$$

Decay constant (λ) = 0.654×10^{-11} yr^{-1}

$$\epsilon_{Nd} = [((^{143/144}Nd)_i \text{ at } T/(^{143/144}Nd)_{BE} \text{ at } T) - 1] * 10^4$$

model ages:

$$T_{CHUR} = \frac{1}{\lambda} * \ln \left[\frac{((^{143}Nd/^{144}Nd)_p - 0.512638)}{((^{147}Sm/^{144}Nd)_{meas} - 0.1966)} + 1 \right]$$

Table A11. Isotope data replication - done on separate dissolutions of the indicated samples. Errors are 2 s.d. on replicates.

Strontium - all measured $^{87}Sr/^{86}Sr$ ratios unless otherwise indicated

	RSV31	RSS2	RSS165	RSC22
1.	0.705292 ±11	0.706693 ±12	0.705381 ±24	0.705601 ±12
2.	0.705347 ±14	0.706685 ±15	0.705428 ±10	0.705608 ±11
3.	0.705339 ±13			

	KA24	KP121
1.	0.705290 ±40*	0.705770 ±40*
2.	0.705313 ±14+	0.705755 ±12+

Samarium and Neodymium (as measured, in ppm)

	RSS162		RSV16		RSC4	
	Sm	Nd	Sm	Nd	Sm	Nd
1.	4.10	22.4	5.98	23.8	4.86	18.8
2.	5.94	22.2	5.91	24.1	5.07	19.4

* from Erlank *et al.* (1984) - obtained at BPI by Bristow
\+ after normalization to an NBS 987 value of 0.71024

Lead - all measured - no fractionation correction

Note: second determination in each instance was repeated because of the poor nature of the initial determination so these comparisons are not strictly representative of reproducibility.

	207/206	206/204	207/204	208/204
RSV31				
1.	0.885743 ±283 (62/70)	17.42896 ±692 (63/70)	15.44451 ±667 (64/70)	37.55895 ±1642 (61/70)
2.	0.889663 ±157 (26/30)	17.37527 ±3758 (26/30)	15.50852 ±3203 (26/30)	37.69415 ±7942 (26/30)
RSS40				
1.	0.908782 ±142 (51/60)	16.86281 ±342 (51/60)	15.32367 ±454 (53/60)	37.85762 ±923 (51/60)
2	0.908514 ±248 (26/30)	16.89843 ±3545 (26/30)	15.36066 ±3191 (26/30)	37.92539 ±8071 (26/30)
RSV16				
1.	0.891838 ±116 (51/60)	17.31988 ±517 (53/60)	15.45031 ±471 (54/60)	37.86726 ±1401 (55/60)
2	0.892019 ±1049 (44/50)	17.28251 ±2035 (42/50)	15.40710 ±2837 (44/50)	37.77457 ±7193 (39/50)

where n is the number of atoms exchanged and is usually 1.
The difference in $\delta^{18}O$ values is termed the Δ-value and is identical to the ‰ fractionation ($10^3\ln(a_{A-B})$) within the limits of analytical error:
$\Delta_{A-B} = \delta^{18}O_A - d^{18}O_B \simeq 10^3\ln(a_{A-B})$
These relations are summarized and explained in greater detail in O'Neil (1986).

1.5 ELECTRON MICROPROBE ANALYSIS

Electron microprobe analysis of olivine, pyroxene, feldspar, glass and opaque oxides were undertaken using a Cameca-Camebax electron microprobe. This data is given in Appendix C (microfiche). Samples were prepared as polished carbon-coated thin sections.

1.5.1 Routine Analysis

The following instrumental conditions were observed:

beam current:	40 nA
accellerating voltage:	15 kV
analyte line:	K_a
analysing crystals:	TLAP for Na, Mg, Si and Al
	LiF(200) for Fe, Mg, Ni and Zn
	PET for Ca, K, Ti, Cr and P
detectors:	flow counters with Ar/CO_2 gas mixture
beam:	2 - 4 μm for olivines, clinopyroxenes and oxides
	8 - 12 μm for feldspars and glass.

Standards used:

	olivine	pyroxene	feldspars	oxides	glass
Si	M-OL	DIOP	NUNI	K-P	DIOP
Ti	RUT	RUT	-	RUT	RUT
Al	K-P	K-P	NUNI	CHRO	K-P
Fe	M-OL	K-P	K-H	ILMT	K-P
Mn	RHOD	RHOD	-	RHOD	RHOD
Mg	M-OL	DIOP	K-H	CHRO	DIOP
Ca	K-P	DIOP	LACO	K-P	DIOP
Na	-	K-H	NUNI	-	K-H
K	-	K-H	OR-1	-	K-H
P	-	-	-	-	APAT
Ni	NISI	-	-	-	-
Cr	CHRO	CHRO	-	CHRO	-
Zn	-	-	-	GAHN	-

CHRO - chromite 52NL11
DIOP - diopside
GAHN - gahnite
ILMT - ilmenite
K-H - Kakanui hornblende
K-P - Kakanui pyrope
LACO - labradorite, Lake Co., Ore.
M-OL - Marjalahti olivine
NISI - synthetic Ni_2SiO_4
NUNI - Nunivak Is. plagioclase
OR-1 - orthoclase
RHOD - rhodonite
RUT - synthetic rutile

Raw counts were corrected for dead time and background, and nominal concentrations calculated using the standards. Nominal concentrations were corrected for interelement matrix affects using the method of Bence and Albee (1968) for sub-calcic clinopyroxenes (pigeonite) and the ZAF procedure used at UCT (modified after Henoc *et al.*, 1973) for all other minerals. Precisions and lower limits of detection for typical analyses are given in Table A12.

1.5.2 Analysis of V in Opaque Oxides

The analysis of V in opaque oxides was conducted using the LiF(200) crystal with a 10 second counting time on the K_α peak and 5 seconds on the

Table A12. Typical precisions (2 s.d.) and lower limits of detection (at the 99% confidence level) for electron microprobe data.

	CPX1 centre - RSS2			OXID7 - RSS162 (spinel)		
oxide %	concentration	precision	lld	concentration	precision	lld
SiO2	52.05	.27	.04	.08	.03	.04
TiO2	1.01	.05	.04	24.73	.20	.05
Al2O3	1.48	.05	.03	1.26	.05	.04
FeO	9.46	.26	.07	68.38	.64	.09
MnO	.18	.06	.07	.53	.08	.08
CgO	17.42	.15	.03	.17	.03	.03
CaO	17.92	.18	.03	<.03	.02	.03
Na2O	.20	.03	.02			
K2O	<.02	.02	.02			
Cr2O5	.25	.04	.05	.06	.03	.05
ZnO				.20	.14	.19
V2O5				.94	.12	.10

elements not determined are indicated by blanks

backgrounds. A problem with the measurement of the V K_a peak (= 2.505 A) is the interference of Ti K_b (= 2.514 A) (Fig. A8). The magnitude of this interference is estimated by measurement of intensity at the V K_a and Ti K_b positions in a synthetic glass standard doped with .449% V (.801% V_2O_5, glass w) and the synthetic rutile standard (TiO_2 = 100%) used for routine analysis. The net peaks (in counts/10s) determined for these and an unknown magnetite (mag 1 - RSC22) for a wavelength scan similar to that sketched in Fig. A8 are:

positions	Rutile	Glass W	Sample (magl-RSC22)
Ti K_b	608.1	3.15	147.2
V K_a	20.1	26.0	50.4

Thus for 100% TiO_2 (rutile) the 'Ti K_b/V K_a' ratio is 30.1 which implies that the intensity measured at V K_a when TiO_2 = 100% will be increased by 3.3% of the Ti K_b intensity. However, successive analyses of magnetite 1 (RSC22) indicated a TiO_2 content of 25%. In this instance the Ti K_b peak will only contribute 1.2 counts or .04% V_2O_5 to the V measurement (less than the detection limit, Table A12). Similarly for an ilmenite with 50% TiO_2 this contribution would still be small: *ca* .08%. This suggests that the contribution of Ti K_b to the V K_a peak is negligible and therefore no correction is made to the V_2O_5 abundances reported in Appendix C (microfiche). This conclusion was also reached by Snetsinger *et al.* (1968) in a comparison between wet chemical analyses of mineral separates and microprobe values. These authors suggested that in an ilmenite containing 32% Ti (53% TiO_2) and 1% V (1.78% V_2O_5) the V value would be approximately .06% (.11% V_2O_5) too high, similar to the estimates made here.

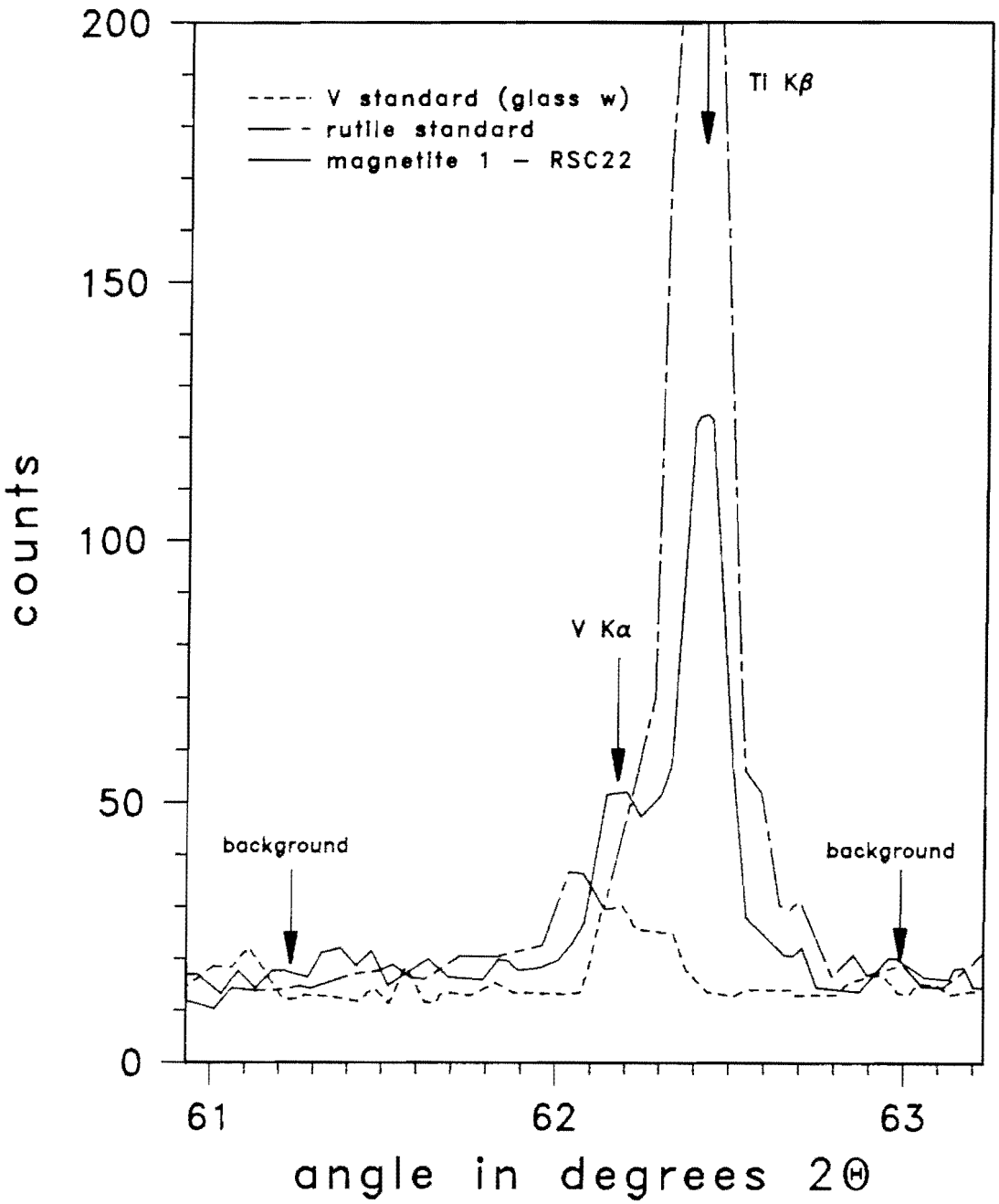

Figure A8. Step-scan (wavelength in degrees 2-theta) over Ti K_b and V K_a for a V standard, rutile standard and a sample. Counts are measured for 10 seconds every .05°.

APPENDIX B. PETROGRAPHIC DESCRIPTIONS

It is emphasized that the rock descriptions below are based wholly on evidence seen in the thin-section. Furthermore, the terms phyric and micro-phyric are taken to refer to a phenocryst population which is obvious and not obvious to the naked eye respectively. The textural terms used here are described in the main text (Chapter 4). Generally samples described as coarse-grained are >5 mm, medium-grained 2-5 mm and fine-grained <2 mm, in grain size. Unless otherwise stated all basalts are fine-grained.

The mineral modes given are all estimated volume %'s in the thin-section(s) studied. In addition **minor** and **accessory** mineral phases in a rock are those which occupy less than 5% and 1% respectively of the thin section studied. Without the use of reflected light, a degree of uncertainty exists in the identification of opaque phases. Where the opaque mineralogy has been positively identified by examination of a polished section the minerals are labelled specifically otherwise commentary is only made on their crystal shape. Typically, but not categorically, acicular minerals are usually ilmenites while equidimensional minerals are most probably magnetites. Descriptions of the opaque mineralogy use the oxidation-'exsolution' classification (C1-7, R1-7) of Haggerty (1976). This classification scheme has been summarised in Chapter 4.

The prefixes RSS, RSV, RSC and RSK refer to rocks sampled on the Sabie, Vurhami, Crocodile and Komati Rivers respectively. The designations LFE (low Fe enriched), HFE (high Fe enriched) and N (normal) correspond to the chemical subdivisions dealt with in this thesis.

RSS0 Dolerite: porphyritic
Intrudes basement gneiss (near Skukuza) - is of an uncertain age. Phenocrysts of plagioclase (partially sericitised) occur in a coarse-grained groundmass of augite and plagioclase. Accessory minerals include quartz and magnetite.

RSS2 Basalt: aphyric
LFE
Intersertal texture of plagioclase lathes and glomeroporphyritic clinopyroxene (augite) grains with interstitial brown glass. Minor ilmenite and accessory quartz and chlorite (alteration) are present. The ilmenite is present predominantly as acicular grains and infrequently as phenocrysts. Grains range from pristine (R1) to containing some Fe-rutile exsolution (R3). Estimated mineral modes are plagioclase (55%), clinopyroxene (38%), ilmenite (5%), glass (10%) and interstitial chlorite (2%).

RSS5 Basalt: aphyric
LFE
A hyaloophitic texture of plagioclase (37%) and clinopyroxene (20%) dispersed in a glassy (35%) matrix. Lathes of acicular oxide (8%) are particularly abundant. Accessory quartz and chlorite are interstitial.

RSS7 Dolerite: aphyric
HFE
A sub-ophitic texture of kaolinised plagioclase and altered clinopyroxene. Magnetite (C3) is the dominant opaque phase (*ca* 80%) with subordinate acicular ilmenite (R1). Composite intergrowths of these two minerals are rare.

RSS8 Basalt: slightly amygdaloidal
LFE
glomeroporphyritic clusters of clinopyroxene (35%) and small dispersed plagioclase lathes (20%) in a dark brown glass matrix (45%). Accessory phases include quartz and chlorite.

RSS12 Basalt: aphyric, amygdaloidal
LFE
An intersertal texture of altered plagioclase and clinopyroxene with minor acicular oxide, glass, chlorite and accessory quartz.

RSS13 Basalt: aphyric, amygdaloidal
LFE
Highly altered plagioclase (47%) with intergranular clinopyroxene (30%), minor acicular oxide (3%). amygdaloidal phases represent ~20% in the thin section studied.

RSS14 Basalt: aphyric
LFE
An intersertal texture of highly altered plagioclase and smaller clinopyroxenes with some brown glassy material. Minor ilmenite (R1) and interstitial chlorite are also present.

RSS19 Basalt: aphyric, sparsely amygdaloidal
LFE
Dispersed plagioclase and clinopyroxene, often glomeroporphyritic, microphenocrysts in a matrix of plagioclase, clinopyroxene and a dark brown glass. Acicular oxide and pseudomorphs after olivine (chlorite + opaque phase) are also present.

RSS20 Basalt: aphyric, amygdaloidal
LFE
Kaolinised plagioclase with glomeroporphyritic clinopyroxene and acicular oxide as a minor phase. A brown glassy material is also present with amygdaloidal phases being dominantly composed of chlorite.

RSS21 Basalt: aphyric
LFE
Kaolinised plagioclase with intergranular clinopyroxene and minor chlorite (interstitial), acicular opaques and glassy material.

RSS22 Basalt: aphyric
LFE
Kaolinised plagioclase with intergranular clinopyroxene and minor chlorite (interstitial), acicular opaques and glassy material.

RSS23 Dolerite: aphyric
LFE
Altered plagioclase and clinopyroxene, minor equant oxides and accessory quartz.

RSS26 Basalt: pyroxene-phyric
LFE
Large poikilitic clinopyroxene phenocrysts (~3 mm), with smaller clinopyroxenes and plagioclase lathes set in a dark brown glass (hyaloophitic texture). Interstitial chlorite and pseudomorphed olivine (chlorite + opaque oxide) are present as minor phases. Estimated mineral modes are plagioclase 30%, clinopyroxene 20%, glass 45%, interstitial chlorite 3% and pseudomorphed olivine 2%.

RSS27 Basalt: aphyric, amygdaloidal
LFE
Intersertal texture of clinopyroxene and kaolinised plagioclases with an acicular oxide occupying grain boundaries. Interstitial and amygdaloidal phases include chlorite, epidote and a serpentine-group mineral.

RSS28 Basalt: aphyric, sparsely amygdaloidal
LFE
Intersertal texture of plagioclase (60%), clinopyroxene (25%) and interstitial glassy material (10%). Chlorite fills in spaces (2%) and opaques are present as acicular needles (3%).

RSS29 Basalt: micro-pyroxene-phyric
LFE
glomeroporphyritic clinopyroxene microphenocrysts in a groundmass of intergranular plagioclase, clinopyroxene and interstitial glassy material.

RSS33 Basalt: feldspar-phyric
LFE
Plagioclase phenocrysts are present in a fine-grained groundmass of plagioclase, clinopyroxene and acicular and equant opaques. This groundmass becomes even finer-grained adjacent the phenocrysts.

RSS34 Basalt: feldspar-phyric
LFE
Feldspar (plagioclase/alkali feldspar?) phenocrysts in a very fine-grained granular mesh of clinopyroxene, plagioclase, and an opaque oxide phase. Minor and accessory phases include quartz, chlorite and apatite.

RSS35 Basalt: micro-feldspar-phyric
N
Rather coarse-grained with respect to plagioclase than feldspar-phyric. Clinopyroxene is present in the intergranular

spaces, equant and subordinate acicular oxides are present as minor phases and olivine (chlorite) and apatite are present as accessory phases.

RSS36 Basalt: feldspar-phyric
LFE
Large plagioclase phenocrysts in an intergranular textured groundmass of plagioclase, clinopyroxene and pseudomorphs after olivine (~6% by volume) with ilmenite in variable stages of oxidation (R1-R7) and accessory apatite (large needles).

RSS37 Basalt: feldspar-phyric
LFE
The thin section studied contains a bimodal grain size distribution. The fine-grained (0.1-0.5 mm) section contains phenocrysts of pseudomorphed olivine, glomeroporphyritic plagioclases and smaller clinopyroxenes. The intergranular groundmass contains plagioclase (65%), clinopyroxene (15%), pseudomorphs after olivine (10%), minor equant oxide (5%) and accessory apatite. The coarse-grained (up to 2 mm) section consists of poikiloophitic plagioclase and augite, minor acicular opaque oxides, accessory pseudomorphs after olivine and large apatite needles. The contact between the two portions appears as a comb-layered or crescumulate texture. The suggestion is that it is a segregation vein, i.e. as the basalt cooled it contracted, creating spaces and the last or residual melt moved into and crystallized in these spaces.

RSS40 Basalt: aphyric
N
Altered plagioclase (60%) and clinopyroxene (30%) in an intergranular relationship. Minor equant oxide (5%) and interstitial chlorite (5%) are present. Plagioclase is altered to kaolinite.

RSS41 Basalt: feldspar-phyric
LFE
Intergranular texture of plagioclase (60%), clinopyroxene (10%), an opaque-rich glassy material (30%) and large (*ca* 2 cm) plagioclase phenocrysts. All plagioclase has a dusting of kaolinite. Ilmenites are typically oxidised to predominantly pseudobrookite (R7).

RSS44a Basalt: aphyric
HFE
Plagioclase (60%), clinopyroxene (30%) and acicular opaques (10%) are arranged in a variolitic texture (a conical series of radiating fibres).

RSS44b Basalt: feldspar-phyric
HFE
Plagioclase phenocrysts, somewhat sericitised, in a variolitic groundmass of plagioclase, clinopyroxene and opaque oxides.

RSS45 Basalt: aphyric
LFE
Coarse-grained lava (0.5-1.0 mm) with plagioclase (60%) and intergranular clinopyroxenes (35%), large acicular and equant opaque

oxides (5%), interstitial chlorite, accessory apatite and pseudomorphs after olivine. Some kaolinite dusting on plagioclase.

RSS47 Basalt: micro-pyroxene-phyric
LFE
Microphenocrysts of glomeroporphyritic clinopyroxenes in an intergranular groundmass of plagioclase (50%), clinopyroxene (22%), glass (15%), acicular opaques (5%) and interstitial chlorite (2%). All phases are relatively unaltered.

RSS63 Basalt: feldspar-phyric, amygdaloidal
N
Feldspar phenocrysts (up to 0.5 cm) in a groundmass of plagioclase, glass, clinopyroxene, opaques and pseudomorphs after olivine. The phenocrysts are both plagioclase and alkali feldspar. These alkali feldspars are coarsely perthitic in character and contain no twin lamellae.

RSS65 Basalt: feldspar-phyric, amygdaloidal
N
Intersertal texture with plagioclase having a range of sizes, small clinopyroxenes and a glassy matrix containing opaque oxides. Chlorite is present interstitially and as an alteration product in this very altered rock.

RSS66 Basalt: amygdaloidal
N
Intergranular texture of exclusively plagioclase and an opaque-rich glass.

RSS67 Basalt: aphyric
HFE
Plagioclase lathes (74%) with intergranular clinopyroxene (20%) and equant opaques (3%). Chlorite (3%) is present as a minor alteration product. All plagioclase is slightly kaolinised.

RSS69 Basalt: very feldspar-phyric
N
Large very poikilitic, comparatively fresh plagioclase phenocrysts in a groundmass of interlocking plagioclase lathes, intergranular clinopyroxene, glass and opaque oxides.

RSS70 Basalt: micro-phyric, amygdaloidal
N
Small plagioclase and equant oxide phenocrysts in a glassy groundmass.

RSS73 Basalt: amygdaloidal
N
Intersertal texture of interlocking plagioclase lathes, intergranular clinopyroxene, opaque oxides (equant), glassy material and interstitial chlorite.

RSS74 Basalt: amygdaloidal
HFE
Interlocking plagioclase (50%) and intergranular clinopyroxene (10%)

in a matrix of dark brown glass (30%) containing acicular opaques (5%). Amygdaloidal phases (5%) include epidote and zeolite.

RSS75 Basalt: amygdaloidal
HFE
Intergranular texture of plagioclase (55%), clinopyroxene (12%), equant oxide (12%), pseudomorphed olivine (8%), and interstitial chlorite (11%) and quartz (2%).

RSS76 Basalt: amygdaloidal
HFE
This rock has a bimodal grain-size variation. In the fine-grained region sub-parallel plagioclase microphenocrysts are set in a glassy groundmass. The coarser-grained region is comprised of interlocking plagioclases and intergranular clinopyroxene, glassy material and opaques (equant).

RSS78 Basalt: aphyric
HFE
Interlocking kaolinised plagioclase lathes with clinopyroxene and glass arranged in an intersertal fashion.

RSS80 Basalt: aphyric
HFE
Interlocking plagioclase lathes with interstitial clinopyroxene, glass, equant opaques and pseudomorphs after olivine. Apatite is an accessory phase.

RSS81 Basalt: amygdaloidal
HFE
Intersertal texture of plagioclase, clinopyroxene, equant oxide and glass. Olivine (pseudomorphed) is an accessory phase. One orthopyroxene (hypersthene) is present in the thin-section.

RSS82 Basalt: aphyric
HFE
Interlocking kaolinised plagioclases (70%) with intergranular clinopyroxenes (16%) and pseudomorphed olivine (6%). Opaque-oxides are present (8%) as equant idiomorphic minerals. Rare microphenocrysts of clinopyroxene and plagioclase in an ophitic intergrowth are present. Apatite is present as an accessory phase.

RSS83 Dolerite: feldspar-phyric
N
Plagioclase phenocrysts in an ophitic textured groundmass of plagioclase and clinopyroxene. Equant opaques are present as a minor phase.

RSS84 Granophyre: micro-porphyritic
Hedenbergite and magnetite microphenocrysts in a spherulitic (glassy) groundmass.

RSS85 Basalt: amygdaloidal
N
A very altered rock consisting of crystallites in a brown oxidised

glass with occasional microphenocrysts of plagioclase. Amygdaloidal phases include quartz, chlorite, opaque-oxides and calcite.

RSS86 Granophyre: porphyritic
Glomeroporphyritic clusters of hedenbergite, plagioclase, opaque-oxides and K-feldspar in a matrix of predominantly K-feldspar with lesser quartz.

RSS87 Granophyre/dolerite mix: porphyritic
Partially resorbed glomeroporphyritic clusters of feldspar and hedenbergite in a microgranular groundmass of plagioclase, clinopyroxene and minor opaques. Apatite is present as an accessory phase. Melanocratic patches result from a greater concentration of opaque minerals and contain augite and plagioclase.

RSS89 Basalt: amygdaloidal
HFE
Intergranular texture of plagioclase (65%), clinopyroxene (15%), and equant oxide (20%). Calcite and quartz are present as amygdaloidal and interstitial phases.

RSS91 Basalt: slightly feldspar-phyric
N
Intersertal texture of very altered (kaolinised) plagioclase (59%) and intergranular clinopyroxene (6%) in a glassy matrix (20%). Chlorite (15%) is present interstitially.

RSS92 Dolerite: aphyric
HFE
Sub-ophitic texture of plagioclase (70%) and clinopyroxene (20%). Opaque-oxides (10%) have both a skeletal and prismatic habit. Apatite is an accessory phase. All minerals are relatively unaltered.

RSS93 Basalt: amygdaloidal
HFE
Interwoven plagioclase (60%) with intergranular clinopyroxene (12%) and equant oxide (8%). Amygdaloidal minerals (20%) include quartz and chlorite. Apatite is an accessory phase.

RSS94 Basalt: feldspar-phyric
N
Large (~1 cm) poikilitic plagioclases in an intersertal textured groundmass of plagioclase, clinopyroxene, and a glassy mesostasis. Equant oxide, interstitial chlorite and accessory apatite are present as minor phases.

RSS96 Basalt: feldspar-phyric
N
Altered plagioclase phenocrysts (15%) in an altered groundmass of plagioclase (53%), intergranular clinopyroxene (7%) and equidimensional and acicular opaques (5%). Glassy material (5%), chlorite (15%) and some epidote is present interstitially.

RSS97 Basalt/Dolerite? sparsely amygdaloidal
N
Magnificent ophitic textured rock with rounded augites (40%) and plagioclases (56%), with minor anhedral opaque oxide (2%) and interstitial chlorite (2%).

RSS98 Basalt: amygdaloidal
HFE
Intersertal texture of plagioclase and glomeroporphyritic clinopyroxenes with interstitial brown glassy material and chlorite. Opaque-oxides are acicular in habit.

RSS99 Basalt: sparsely amygdaloidal
HFE
Intersertal texture of very altered plagioclases and glomeroporphyritic clinopyroxenes with interstitial glassy material. Opaques are acicular in habit.

RSS102 Welded Tuff
There are primarily four constituents making up this rock: (1) pumice fragments, (2) amygdales, (3) phenocrysts and (4) a glassy groundmass. Pumice fragments or lapilli are generally flattened and consist of micro-crystalline aggregates of quartz. The amygdales usually have a very irregular form and are probably the result of later filling in of spaces in what must have been a very porous rock-type. Amygdale minerals include quartz, epidote, calcite, zeolites and apatite. Both K-feldspar and plagioclase are present as phenocrysts. The feldspars are characterized by their pronounced poikilitic (commonly with epidote) nature and usually exhibit an embayed resorption texture. The groundmass comprises abundant crystallites of predominantly feldspar (hyalopilitic texture). Some melanocratic glassy fragments may represent mafic material sampled by the eruption.

RSS103 Basalt: feldspar-phyric
LFE
glomeroporphyritic plagioclase in a groundmass of plagioclase and intergranular clinopyroxene and equant and acicular opaques.

RSS107 Basalt: aphyric
LFE
Hyaloophitic texture of plagioclase (35%) and nodular clinopyroxene (25%) in glass (35%). Opaques (5%) are present as acicular minerals.

RSS108 Basalt: aphyric
LFE
Intersertal texture of plagioclase (35%), nodular glomeroporphyritic clinopyroxene (20%) in a brown glass (30%). Large acicular opaque-oxides (6%) and interstitial chlorite (9%) is also present.

RSS109 Dolerite: aphyric
N
Sub-ophitic texture of plagioclase and augite. Minor phases include equant oxides and some glassy material.

[B: Petrography]

RSS110 Basalt: aphyric
HFE
Fine-grained intergranular texture of plagioclase (55%), clinopyroxene (35%) and magnetite (10%). Accessory minerals include pseudomorphs (chlorite) after olivine and apatite. plagioclases have a dusting of kaolinite.

RSS111 Basalt: aphyric
HFE
Fine-grained intersertal texture of plagioclase (50%), clinopyroxene (34%), equant oxide (8%) and a glassy material (8%). Plagioclase is altered to kaolinite.

RSS112 Basalt: amygdaloidal, pyroxene- and feldspar-phyric
HFE
Fine-grained intersertal texture of plagioclase, clinopyroxene, glass, equant oxide and accessory quartz and chlorite.

RSS114 Basalt: micro-feldspar-phyric
N
Medium-grained intersertal texture of plagioclase (55%), clinopyroxene (20%), glass (18%), equant oxide (5%) and pseudomorphed olivine (2%). Some interstitial chlorite and hematite (oxidation) are present. Plagioclase is ubiquitously kaolinised.

RSS123 Dolerite
N
Sub-ophitic texture of plagioclase (50%), clinopyroxene (45%) and equant opaques (5%).

RSS127 Dolerite
N
Sub-ophitic texture of plagioclase, clinopyroxene, equidimensional opaques with interstitial glass and chlorite.

RSS137 Basalt: micro-phyric
LFE
glomeroporphyritic clinopyroxene microphenocrysts in a felted groundmass of plagioclase, clinopyroxene, glassy material and predominantly equidimensional opaques.

RSS138 Dolerite
LFE
Intersertal texture of plagioclase (60%), clinopyroxene (25%), glass (10%), and equant oxides (5%). Olivine (pseudomorphed) is an accessory phase. All minerals are relatively unaltered.

RSS144 Dolerite
LFE
Intergranular texture of plagioclase, clinopyroxene and acicular opaques, with some interstitial glassy material.

RSS147 Dolerite
HFE
Intergranular texture of plagioclase, clinopyroxene, equant (60%) and

acicular (40%) opaques.

RSS150 Dolerite
HFE
Intergranular texture of plagioclase (64%), clinopyroxene (30%) and opaques (6%). All minerals are relatively unaltered. Magnetites contain only sandwich lamellae (C1) and smaller discrete ilmenites are also present (R1).

RSS152 Dolerite
LFE
Sub-ophitic texture of plagioclase (55%), clinopyroxene (40%) and opaques (5%). Rock is extremely fresh. Magnetites have only sandwich ilmenite lamellae (C1) while discrete ilmenites do contain some Fe-rutile exsolution (R2).

RSS156 Dolerite
HFE
Intergranular texture of plagioclase (60%), clinopyroxene (37%) and both acicular and equidimensional opaque oxides (8%). Some interstitial chlorite is present. Rock is extremely fresh.

RSS157 Basalt: aphyric
LFE
Intersertal texture of glomeroporphyritic clinopyroxene, plagioclase, acicular opaques, minor pseudomorphed olivine and interstitial glass.

RSS160 Dolerite
HFE
Sub-ophitic texture of plagioclase (60%), clinopyroxene (30%), opaques (7%) and some glassy mesostasis (3%). Opaques consist of discrete grains and composite intergrowths of magnetite (C3) and ilmenite (R1). All minerals are unaltered.

RSS162 Dolerite
HFE
Medium-grained intergranular texture of plagioclase (55%), clinopyroxene (40%) and opaques (5%). Ilmenite (R1) is only present in intergrowths with, or as cores of, magnetite (C3) grains.

RSS165 Dolerite
HFE
Medium-grained intergranular texture of plagioclase (40%), clinopyroxene (35%), acicular and equidimensional opaque oxides (5%) and a glassy mesostasis (20%). All minerals are relatively unaltered.

RSS167 Basalt: aphyric
LFE
glomeroporphyritic clinopyroxenes, plagioclase and acicular opaques with some interstitial glass. Plagioclases are kaolinised. Orthopyroxene is a rare microphenocryst.

RSS168 Dolerite
HFE
Intergranular texture of clinopyroxene, plagioclase, equidimensional

opaques and some interstitial glassy material.

RSS169 Dolerite
N
Intergranular texture of plagioclase (60%), clinopyroxene (25%), equant oxide (5%) and a glassy mesostasis (10%). Some interstitial chlorite is present. All phases are relatively unaltered.

RSS180 Dolerite: phyric
N
Large plagioclase phenocrysts in a medium-grained sub-ophitic groundmass of plagioclase and augite with minor equant oxide and some glassy material.

RSS183 Dolerite
N
Sub-ophitic texture of plagioclase and augite, and minor equant opaques. Clinopyroxene is occasionally altered.

RSS184 Basalt: micro-phyric
LFE
glomeroporphyritic clusters of clinopyroxene in a black glass matrix containing abundant acicular opaques. Idiomorphic chlorite-filled shapes represent pseudomorphs after olivine. No plagioclase is present.

RSV3 Basalt: aphyric
LFE
Intersertal texture of plagioclase and clinopyroxene in a glassy groundmass.

RSV4 Basalt: aphyric
LFE
Hyaloophitic texture of plagioclase (50%), clinopyroxene (13%) and acicular opaques (6%) in a glass groundmass (30%). Microcrystalline aggregates of quartz and zeolite group mineral occupy idiomorphic spaces (2%). Calcite is an accessory phase. No alteration is present.

RSV6 Basalt: aphyric
LFE
Plagioclase and large acicular opaques with intergranular clinopyroxene and interstitial glass and chlorite.

RSV7 Dolerite: porphyritic
N?
glomeroporphyritic plagioclase phenocrysts in a sub-ophitic groundmass of plagioclase, clinopyroxene and acicular and equidimensional opaques.

RSV8 Composite Dyke
A felsic dyke containing mafic xenoliths of variable size representing varying degrees of assimilation. The dyke material is coarser-grained and contains plagioclase, poikilitic clinopyroxenes (augite), K-feldspar, equidimensional idiomorphic opaques (magnetite?) and

quartz. The mafic xenoliths are finer-grained and contain a typical basaltic assemblage of plagioclase, augite, minor acicular opaques (ilmenite?) and glassy material.

RSV11 Dolerite
N
Sub-ophitic plagioclase (55%), clinopyroxene (40%) and equant oxides (5%). All phases are unaffected by any alteration.

RSV14 Basalt: aphyric
LFE
Intersertal texture of plagioclase (46%), glomeroporphyritic clinopyroxene (20%), acicular opaques (5%) with interstitial glass (20%) and chlorite (7%). Olivine (pseudomorphed) is an accessory phase.

RSV16 Dolerite: aphyric
N
Sub-ophitic texture of plagioclase, clinopyroxene and minor magnetite with little or no alteration present. Estimated modes are plagioclase (55%), clinopyroxene (35%), magnetite (6%, C3) and a glassy mesostasis (4%).

RSV18 Basalt: aphyric
LFE
Intersertal and rarely sub-ophitic texture of plagioclase (45%), clinopyroxene (25%), and minor acicular oxides (7%) with interstitial dark brown glass (22%) and chlorite (1%). The rock is relatively unaltered.

RSV19 Basalt: aphyric
LFE
Intersertal and rarely sub-ophitic texture of plagioclase (45%), clinopyroxene (25%), and minor acicular oxides (7%) with interstitial dark brown glass (22%) and chlorite (1%). The rock is relatively unaltered.

RSV20 Basalt: aphyric
LFE
Intersertal and rarely sub-ophitic texture of plagioclase (45%), clinopyroxene (25%), and minor acicular opaques (7%) with interstitial dark brown glass (22%) and chlorite (1%). The rock is relatively unaltered.

RSV24 Dolerite
N?
Sub-ophitic plagioclase (55%), clinopyroxene (40%) and equant oxides (5%). All phases are unaffected by any alteration.

RSV27 Basalt: aphyric
LFE
Intersertal and rarely sub-ophitic texture of plagioclase (65%), clinopyroxene (10%) and acicular oxides (6%) with interstitial glass (15%), quartz (accessory) and zeolite (accessory).

RSV28 Basalt: aphyric
LFE
Intersertal and rarely sub-ophitic texture of plagioclase (45%), clinopyroxene (25%), and minor acicular opaques (7%) with interstitial dark brown glass (22%) and chlorite (1%). The rock is relatively unaltered. Olivine (pseudomorphed) as a minor constituent.

RSV30 Basalt: sparsely amygdaloidal.
LFE
Infrequent orthopyroxene (green colour suggesting some alteration) microphenocrysts in a very fine-grained groundmass of plagioclase, clinopyroxene, glass and acicular opaques, all often arranged in a spherulitic texture.

RSV31 Basalt: aphyric
LFE
A classic intersertal texture of plagioclase (46%), smaller clinopyroxenes (20%) and ilmenite (6%) with interstitial glass (20%) and chlorite (8%). The ilmenites are all acicular and have been ubiquitously oxidised to pseudobrookite (R7).

RSV35 Dolerite
N
Sub-ophitic plagioclase (55%), clinopyroxene (40%) and equant oxide (5%). All phases are unaffected by any alteration.

RSC2 Basalt: aphyric
LFE
Intergranular texture of plagioclase (60%), clinopyroxene (25%) and acicular oxide (5%) with interstitial chlorite (5%) and glassy material (5%).

RSC3 Basalt: aphyric
LFE
Intersertal texture of plagioclase, clinopyroxene and minor acicular opaques with interstitial glass and lesser chlorite and calcite. Plagioclase is remarkably unaltered.

RSC4 Dolerite: aphyric
N
Ophitic texture of plagioclase (60%) and augite (35%) with minor opaques (5%) and altered olivine. Opaques are predominantly magnetite (C2) with few discrete ilmenites. In some instances the olivines have small remnant fragments of fresh material contained within the altered mass.

RSC6 Basalt: aphyric
LFE
Intergranular texture of plagioclase, clinopyroxene, acicular oxides, interstitial chlorite and accessory quartz.

RSC7 Volcanoclastic
An interesting large section. The thin-section reveals a cyclic type of variation of two distinct alternately layered components. One contains sub-rounded quartz grains cemented with both a siliceous and

ferruginous cement. The other part contains predominantly plagioclase and long acicular needles of a mafic mineral with interstitial ferruginous material. It is suggested that these parts represent volcanic and lithic origins. The greater proportion of ferruginous cement in the coarse-grained lithic fraction is due to its proximity to the volcanic derived layer.

RSC8 Basalt: amygdaloidal
LFE
Microphenocrysts of clinopyroxene, often glomeroporphyritic, and more occasionally plagioclase are in a groundmass of plagioclase, clinopyroxene, chlorite, glassy material and ilmenite. Estimated modal abundances are: plagioclase 50%, clinopyroxene 12%, opaques 8%, chlorite 20% and glassy material 10%.

RSC22 Dolerite
N
Sub-ophitic plagioclase (50%), clinopyroxene (45%) and magnetite (3%, C3) and olivine - including **fresh** fragments - (2%). Infrequent microporphyritic clusters of plagioclase are also present. All phases are extremely fresh.

RSC25 Basalt: micro-phyric
HFE
Fine-grained intersertal texture of plagioclase, clinopyroxene and glassy material with minor small acicular opaques. Microphenocrysts of plagioclase are occasionally present. Plagioclase is relatively fresh.

RSC28 Dolerite?
N
Intergranular texture of plagioclase, small clinopyroxene, and minor pseudomorphed olivine, equidimensional opaques, apatite and interstitial glass.

RSC32 Basalt: phyric
N
glomeroporphyritic clusters of plagioclase in a medium-grained intergranular groundmass of plagioclase, clinopyroxene, lesser equant oxide and interstitial chlorite. Estimated modes are plagioclase 55%, clinopyroxene 32%, opaques 5% and chlorite 8%. Plagioclase is partially kaolinised.

RSC33 Basalt: phyric
N
Very fine-grained groundmass of plagioclase, clinopyroxene, glassy material and evenly dispersed equidimensional opaques. The groundmass adjacent plagioclase phenocrysts is typically even more fine-grained indicative of chilling.

RSC35 Basalt: phyric
HFE
Fine-grained altered groundmass of plagioclase, clinopyroxene, glassy material and abundant equant opaques (~10%). Plagioclase phenocrysts and plagioclase in the groundmass show a sub-alignment. Occasional

micro-amygdales containing quartz are present. Plagioclase is extensively altered to kaolinite.

RSC36 Basalt: aphyric
HFE
Fine-grained intersertal texture of plagioclase (altered), clinopyroxene, glass and minor equant oxides. Irregularly shaped amygdaloidal patches and large irregularly distributed patches of opaque oxide are present.

RSC37 Dolerite
HFE
Intersertal texture of plagioclase, clinopyroxene, acicular and equidimensional opaques and a glassy mesostasis. Plagioclase is altered to kaolinite

RSC38 Basalt: aphyric
HFE
Very fine-grained intersertal texture of plagioclase, clinopyroxene, glass and opaque oxide (equant).

RSC39 Basalt: amygdaloidal
HFE
Extremely fine-grained felted texture of plagioclase and glass. Amygdales are abundant (contain quartz and chlorite).

RSC40 Basalt: aphyric
HFE
Fine-grained intersertal texture of plagioclase, clinopyroxene, equant oxides and glass. Infrequent microphenocrysts of plagioclase are also present.

RSC43a Mafic intrusion (circular)
Altered medium-grained rock consisting of very long acicular needles of chlorite and an opaque phase (ilmenite?). Lathes of plagioclase and more rounded clinopyroxenes are also present. Apatite needles are relatively abundant (~0.5%) and quartz and K-feldspar is present interstitially.

RSC45 Komatipoort Gabbro
Coarse-grained ophitic texture of plagioclase and augite. Augite is brown and zoned (Ti-augite) with exsolution lamellae. Minor equant oxide and accessory apatite and quartz is present.

RSC49 Mafic: aphyric
HFE
Medium-grained intergranular texture of plagioclase, clinopyroxene, minor equant oxide and interstitial chlorite. Larger clinopyroxenes are often poikilitic with inclusions concentrated near their centers.

RSC50 Dolerite
N
Medium-grained sub-ophitic texture of plagioclase and clinopyroxene, both somewhat fragmented. Equidimensional oxides are an accessory phase.

RSC51 Mafic: feldspar-phyric, amygdaloidal
N
Abundant large plagioclase and smaller clinopyroxene phenocrysts, commonly altered and glomeroporphyritic, are set in a very fine-grained matrix of plagioclase, clinopyroxene, opaques and glass.

RSC55 Basalt: amygdaloidal
N
Altered plagioclase with interstitial clinopyroxene and minor pseudomorphed olivine and equant opaques.

RSC56 Basalt: feldspar-phyric
N
Large altered feldspar phenocrysts in a groundmass of altered plagioclase, clinopyroxene, equant oxides and interstitial glass. Olivine (pseudomorphed) is an accessory phase.

RSC69 Dolerite
HFE
Intersertal texture of plagioclase and clinopyroxene in an opaque-rich brown glass. Acicular and equidimensional opaque phases and interstitial chlorite and occasional micro-amygdales are present. Apatite is extremely abundant (*ca* 0.5-1.5%). Plagioclase is extensively kaolinised.

RSC70 Dolerite
HFE
Intersertal texture of plagioclase, clinopyroxene, acicular and equidimensional opaques and a glassy mesostasis. Plagioclase is partially kaolinised.

RSC71 Dolerite
N
Intergranular texture of plagioclase (50%), augite (27%), equant opaques (8%) and some glassy material (15%). Plagioclase is relatively fresh while clinopyroxene grains are somewhat altered.

RSC72 Dolerite
N
Intersertal texture of plagioclase (60%), augite (30%), equant opaques (5%) and some glassy material (5%). All minerals are relatively unaltered.

RSC73 Dolerite: feldspar-phyric
N?
Discrete kaolinised plagioclase phenocrysts in a very fine-grained glassy groundmass containing equant oxides, plagioclase and lesser chlorite. Occasional round amygdales appear pink in hand specimen.

RSC77 Basalt: amygdaloidal
N
Fine-grained intergranular texture of clinopyroxene, plagioclase and equidimensional opaques.

[B: Petrography]

RSC78 Basalt: aphyric
N
Intergranular texture of plagioclase, clinopyroxene and minor equidimensional opaques. Some infrequent pseudomorphs after olivine. Sample is relatively unaltered.

RSC79 Basalt: aphyric
N
Intergranular texture of plagioclase, clinopyroxene and minor equidimensional opaques.

RSC85 Dolerite
HFE
Intersertal texture of plagioclase (50%), clinopyroxene (28%), both acicular (ilmenite?) and equidimensional (sulphide?) opaques (7%) and a glassy mesostasis (15%) and accessory apatite. Some kaolinisation of plagioclase is present.

RSC86 Dolerite
N
Sub-ophitic texture of plagioclase (60%), clinopyroxene (35%) and equidimensional opaques (5%). Sample is relatively fresh.

RSC87 Dolerite
N
Sub-ophitic texture of plagioclase (50%), clinopyroxene (45%), and equant oxides (5%). Sample is relatively unaltered.

RSK2 Basalt: aphyric
N
Altered rock containing plagioclase (69%), clinopyroxene (15%), equant oxides (5%), glassy material (4%), interstitial chlorite (4%), and pseudomorphs after olivine (3%).

RSK4 Basalt: feldspar-phyric
N
Abundant plagioclase phenocrysts of variable size in an intergranular groundmass of plagioclase, clinopyroxene, and equant opaques. Some interstitial chlorite is present.

RSK6 Basalt: amygdaloidal
N
Intergranular texture of plagioclase (very altered), clinopyroxene, and minor equant opaques and irregular chlorite.

RSK7 Basalt: amygdaloidal
N
A very altered sample consisting of fine-grained completely kaolinised feldpar, interstitial opaques and large amygdales containing chlorite, calcite and quartz

RSK9 Basalt: aphyric
N
Considerably altered sample composed of plagioclase, clinopyroxene and minor equant oxides.

RSK10 Basalt: plagioclase-phyric
N
Large poikilitic plagioclase feldspars in a groundmass of plagioclase, clinopyroxene and minor acicular opaques.

RSK13 Basalt?: very amygdaloidal
?
Fine-grained felted groundmass of predominantly plagioclase and a glassy material. Amygdaloidal phases include zeolite (natrolite?), and quartz.

RSK14 Basalt: aphyric
HFE
Medium-grained sub-ophitic texture of plagioclase (59%), Ti-augite (20%), interstitial glassy material (8%), equant opaques (6%) and chlorite (5%). Apatite is a relatively abundant phase (2%). Ti-augite is zoned and contains exsolution lamellae.

RSK16 Basalt: aphyric
?
Very altered rock containing occasional unaltered clinopyroxenes.

RSK18 Basalt: aphyric
HFE
Intergranular texture of plagioclase, clinopyroxene and minor equidimensional opaques and apatite.

RSK19 Basalt: aphyric
N
Very fine-grained intergranular texture of plagioclase, clinopyroxene and minor opaque oxide.

RSK21 Basalt: microphyric (pyroxene + plagioclase)
LFE
Plagioclase and clinopyroxene microphenocrysts in a matrix of plagioclase, clinopyroxene, acicular opaques and some interstitial glass.

RSK22 Basalt: aphyric
N
Coarse-grained altered rock containing kaolinised feldspar, large sub-ophitic pyroxenes and a glassy groundmass.

RST1 Basalt: aphyric (Tshokwane)
LFE
Hyalopilitic texture of plagioclase, acicular opaques and interstitial micro-glomeroporphyritic clinopyroxenes in a glassy groundmass. Quartz is present interstitially as an accessory phase

FV3/FV4 Picrite Basalt: (Sweni River)
Medium-grained rock composed of olivine (30%), orthopyroxene (36%), acicular opaques (4%), plagioclase (10%), clinopyroxene (10%) and interstitial glass (10%). Orthopyroxene is present as large poikilitic phenocrysts, frequently zoned and infrequently mantled with clinopyroxene. Clinopyroxene, feldspar, opaques and glass are confined to the groundmass. Phenocrysts of olivine are only partially altered.

APPENDIX C. ANALYTICAL DATA

The following is an index to data given in Tables C1 to C4:

C1: Central Lebombo XRF data in order of sample number. Data is unnormalized with Fe reported as total Fe_2O_3 (as analysed). All major element oxides are in wt % and trace elements in ppm. The $^{143}Nd/^{144}Nd$ and $^{87}Sr/^{86}Sr$ ratios are calculated at 190 Ma. $^{206}Pb/^{204}Pb$, $^{207}Pb/^{204}Pb$ and $^{208}Pb/^{204}Pb$ are common lead determinations and the $\delta^{18}O$ is given in ‰ (all positive values). Height is the stratigraphic location of basalt flows in metres (Appendix D) and Mg# the Mg-number calculated assuming a Fe_2O_3/FeO ratio of .15 (see data on microfiche). Blank spaces indicate missing data.

C2: Spark-source mass spectrographic REE data (in ppm). Data is from S. R. Taylor, Australian National University, Canberra and Duncan *et al.* (1984a).

C2a: Spark-source mass spectrographic trace element data (in ppm). Data is from S. R. Taylor, Australian National University, Canberra and Duncan *et al.* (1984a).

C3: XRF analyses of soil overlying basalts just east of Satara, *ca* 100 km north of the Sabie River (Watkeys, pers. comm., 1986). Data is unnormalized with total Fe as Fe_2O_3.

C4: Central Lebombo Sr-, Nd-, Pb- and O-isotope data. Rb and Sr were determined by XRF, Sm and Nd by isotope dilution (unless otherwise stated) and $\delta^{18}O$ (‰) by H. S. Smith and C. Harris. Data is arranged in order of basaltic rock type: LFE group, HFE group, N group and N. Lebombo picrites. RSS86 is a felsic dyke intruding the base of the Jozini Formation in the Sabie River section.

[C: Data]

Data given on microfiche (inside back cover of this volume) is indexed in the following manner:

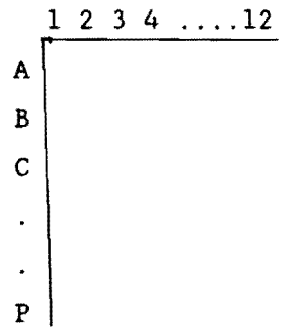

1. Whole-rock XRF data, normalized volatile-free with total Fe as FeO. Data is given for basaltic rocks and is grouped in terms of the basaltic rock types. SrI is the $^{87}Sr/^{86}Sr$ ratio calculated at 190 Ma, 206 Pb the common lead ratio $^{206}Pb/^{204}Pb$ and d-180 the $\delta^{18}O$ value (in ‰). Blank spaces indicate unavailable data

	location
LFE-group (n=54)	B1 - G1
HFE-group (n=40)	H1 - K1
N-group (n=46)	L1 - P1

2. Whole-rock major element XRF data with an assumed Fe_2O_3/FeO ratio of .15 and calculated Mg#. Data is unnormalized and is ordered in terms of sample number.

location
C2 - C3

3. Semi-quantitative slab data (XRF) for all samples analysed in the central Lebombo (n=360). Fe is reported as total Fe_2O_3. Samples are listed in order of sample number and the group with which each slab is geochemically affiliated is given along with its stratigraphic position (if a basalt).

location
E3 - I5

[C: Data]

All microprobe data is in order of sample number - RSS-, RSV- and RSC- for each species listed below

4. Olivine microprobe data: location
L5 - B6

samples : RSC4; RSC22
(N-group)

5. Pyroxene microprobe data: location
E6 - H8

samples:	LFE-group	HFE-group	N-group
	RSS2	RSS7	RSS35
	RSS8	RSS67	RSS162
	RSS26	RSS150	RSV16
	RSS36	RSS160	RSC4
	RSS152		RSC22
	RSV31		RSC32

6. Feldspar microprobe data: location
K8 - J10

samples:	LFE-group	HFE-group	N-group
	RSS2	RSS67	RSS35
	RSS8	RSS150	RSS63
	RSS36	RSS160	RSS162
	RSS152		RSV16
	RSV31		RSC4
			RSC22
			RSC32

7. Opaque oxide microprobe data: location
M10 -H12

samples:	LFE-group	HFE-group	N-group
	RSS2	RSS7	RSS162
	RSS14	RSS150	RSV16
	RSS36	RSS160	RSC4
	RSS41		RSC22
	RSS152		RSC32
	RSV31		

8. Glass microprobe data: location
K12 - L12
samples: RSS2, RSS8, RSV31

Table C1. Central Lebombo Whole Rock XRF Data (total Fe as Fe_2O_3t).

	RSS1	RSS2	RSS7	RSS8	RSS11	RSS13	RSS19	RSS20	RSS21	RSS22
SiO_2	50.68	51.75	49.38	51.50	49.97	52.23	50.70	51.03	50.45	50.66
TiO_2	3.14	3.25	4.08	3.10	3.00	3.14	2.88	2.89	2.83	2.89
Al_2O_3	11.76	12.91	12.73	12.34	11.84	11.43	12.89	13.12	12.81	12.85
Fe_2O_3t	11.30	11.42	16.27	11.33	11.02	11.20	12.08	11.83	11.89	12.03
MnO	.15	.15	.22	.17	.14	.15	.17	.15	.15	.13
MgO	6.88	4.91	4.41	5.51	5.99	6.19	5.88	5.32	5.90	5.81
CaO	7.41	8.64	8.63	7.54	8.95	7.71	7.00	7.72	8.06	7.97
Na_2O	2.17	1.89	2.24	2.08	1.97	2.42	1.43	2.84	2.38	2.63
K_2O	2.59	2.48	1.41	2.36	1.61	1.68	3.54	1.71	1.98	1.27
P_2O_5	.51	.54	.71	.51	.46	.46	.46	.46	.45	.45
H_2O-	.85	.52	.39	.73	1.01	.49	.41	.38	.47	.52
LOI	2.16	1.38	- .10	2.17	3.37	2.71	2.18	2.07	2.32	2.36
TOTAL	99.60	99.84	100.39	99.35	99.33	99.81	99.63	99.51	99.70	99.56
Mo	1.7	5.4	2.3	1.8	2.4	5.3	5.7	< 1.7	4.9	3.5
Nb	23	27	34	23	17.3	18.5	18.0	15.9	16.5	17.5
Zr	414	425	428	397	352	347	336	352	322	335
Y	34	37	64	34	36	34	34	37	35	36
Sr	574	1110	317	1055	658	621	801	621	652	626
U	< 3.5	1.5	< 3.9	< 1.1	< 3.5	< 4.7	< 4.7	< 3.6	< 4.6	< 4.7
Rb	54	50	36	60	36	34	101	40	45	25
Th	9.1	8.5	9.0	7.2	7.5	7.3	< 6.1	9.6	< 6.0	< 6.0
Pb	15.6	10.6	18.9	10.3	8.8	< 6.6	9.4	20	7.3	8.9
Ba	947	830	538	986	511	644	2100	642	883	432
Sc	24	23	32	23	25	26	24	21	23	23
La	58	56	43	50	37	38	39	41	41	42
Ce	126	125	106	110	85	86	84	90	87	89
Nd	83	84	70	77	62	62	61	65	61	61
Cs	3.7	< 3.6	4.5	< 3.5	< 3.5	< 3.4	< 3.6	4.0	< 3.5	< 3.4
Zn	117	117	146	115	113	116	123	121	119	122
Cu	106	113	430	106	73	86	51	55	51	53
Ni	129	61	53	73	109	97	112	106	112	111
Co	50	43	45	47	46	46	50	48	52	51
Cr	320	141	60	180	280	272	96	87	98	94
V	225	228	382	234	232	235	236	231	233	234
$^{143}Nd/^{144}Nd$		.51199								
$^{87}Sr/^{86}Sr$		.70628		.70617						
$^{206}Pb/^{204}Pb$		17.43								
$^{207}Pb/^{204}Pb$		15.41								
$^{208}Pb/^{204}Pb$		37.80								
$\delta^{18}O$		6.48								
Height	111	145		151	241	244	404	431	441	472
Mg#	57.8	49.2	37.7	52.3	55.0	55.4	52.3	50.2	52.7	52.0

RSS1 : amygdaloidal basalt
RSS2 : sparsely amyg. basalt (F)
RSS7 : dolerite (F)
RSS8 : amygdaloidal basalt (F)
RSS11 : amygdaloidal basalt
RSS13 : amygdaloidal basalt
RSS19 : sparsely amygdaloidal basalt
RSS20 : amygdaloidal basalt
RSS21 : amygdaloidal basalt
RSS22 : sparsely amygdaloidal basalt

Table C1. Central Lebombo Whole Rock XRF Data (total Fe as Fe_2O_3t).

	RSS26	RSS27	RSS31	RSS32	RSS33	RSS35	RSS36	RSS40	RSS41	RSS45
SiO_2	49.18	48.07	49.36	51.00	50.78	50.92	51.64	50.81	50.35	50.65
TiO_2	3.35	3.39	2.82	3.45	3.63	1.58	3.27	2.08	4.07	3.47
Al_2O_3	11.31	11.95	10.59	12.73	13.59	14.04	14.00	13.03	13.29	13.59
Fe_2O_3t	12.42	11.89	11.80	11.93	12.82	12.71	12.20	14.54	12.81	12.21
MnO	.15	.14	.13	.14	.14	.16	.14	.18	.15	.13
MgO	6.94	5.80	8.50	5.57	3.53	5.49	3.94	5.13	4.20	4.85
CaO	8.66	9.41	9.31	7.27	6.89	8.43	6.88	7.38	6.90	7.73
Na_2O	1.91	2.48	2.37	2.78	2.58	2.96	2.78	3.71	2.68	2.95
K_2O	1.88	.57	.49	2.50	2.75	.80	2.79	.99	3.09	2.16
P_2O_5	.51	.52	.40	.54	.78	.20	.70	.23	.69	.55
H_2O-	.63	.69	.71	.40	.45	.43	.22	.18	.34	.39
LOI	2.35	4.32	2.82	1.48	1.63	1.78	.98	1.92	1.32	1.43
TOTAL	99.30	99.22	99.31	99.79	99.59	99.51	99.55	100.18	99.89	100.10
Mo	4.6	< 1.7	< 1.7	< 1.7	4.8	2.8	6.7	4.2	6.0	2.3
Nb	20	18.4	15.0	18.9	34	7.6	30	6.5	29	19.9
Zr	374	378	290	392	517	129	466	158	460	380
Y	35	37	33	43	46	25	46	33	45	40
Sr	682	966	453	1040	1050	642	1100	262	875	1290
U	< 1.1	< 3.5	< 3.5	< 3.7	< 4.8	< 4.6	< 4.7	< 1.1	< 4.9	< 3.6
Rb	41	12.2	10.0	55	51	18.2	55	28	72	52
Th	5.2	8.5	5.2	9.9	11.0	< 6.0	11.4	2.2	8.1	12.2
Pb	7.8	13.5	8.7	10.7	11.8	< 6.6	11.8	3.5	10.3	18.3
Ba	627	179	222	709	1045	263	1055	178	891	680
Sc	28	30	26	24	18.7	23	16.9	24	19.0	20
La	43	43	31	41	62	14.4	60	11.2	52	44
Ce	98	92	75	91	142	32	138	46	122	98
Nd	73	70	55	70	99	21	92	33	88	72
Cs	3.7	3.6	< 3.5	< 3.5	< 3.6	< 3.3	< 3.5	< 2.6	< 3.6	< 3.5
Zn	121	119	114	128	139	109	129	122	137	122
Cu	106	84	88	93	193	80	132	93	88	74
Ni	101	83	264	111	45	103	76	65	73	80
Co	53	47	56	46	39	52	39	58	44	46
Cr	267	210	474	202	10.1	81	83	38	29	88
V	276	265	247	244	219	242	207	327	241	243
$^{143}Nd/^{144}Nd$								.51218		
$^{87}Sr/^{86}Sr$	.70519							.70549		
$^{206}Pb/^{204}Pb$								16.89		
$^{207}Pb/^{204}Pb$								15.36		
$^{208}Pb/^{204}Pb$								37.97		
$\delta^{18}O$								4.50		
Height	738	759	930	970	1000	1032	1072	1315	1328	1394
Mg#	55.7	52.4	61.9	51.1	38.4	49.3	42.1	44.3	42.4	47.1

RSS26 : amygdaloidal basalt (F)
RSS27 : amygdaloidal basalt
RSS31 : amygdaloidal basalt
RSS32 : massive basalt
RSS33 : felsphyric (glom.) basalt
RSS35 : amyg. felsphyric basalt
RSS36 : felsphyric (glom.) basalt?
RSS40 : massive basalt
RSS41 : feldsparphyric basalt
RSS45 : massive basalt? (F)

Table C1. Central Lebombo Whole Rock XRF Data (total Fe as Fe_2O_3t).

	RSS47	RSS63	RSS66	RSS67	RSS70	RSS73	RSS74	RSS75	RSS76	RSS78
SiO_2	50.67	50.83	48.72	48.69	49.13	48.41	44.89	46.73	46.73	49.55
TiO_2	3.50	1.91	1.97	3.66	1.84	2.19	3.78	3.74	3.89	3.69
Al_2O_3	13.54	13.86	12.85	12.37	14.23	12.63	12.91	12.24	12.56	12.32
Fe_2O_3t	12.28	13.50	15.55	15.90	11.93	15.56	16.64	16.33	16.56	15.03
MnO	.14	.16	.20	.19	.17	.19	.22	.21	.22	.18
MgO	4.81	5.18	5.39	4.52	6.86	5.60	3.65	4.13	4.10	3.71
CaO	7.95	8.41	7.25	7.22	8.96	8.53	8.77	8.67	7.97	6.77
Na_2O	2.43	3.05	4.20	3.41	3.28	3.46	3.06	2.30	3.30	3.00
K_2O	2.07	1.16	.27	1.18	1.33	.68	1.30	.82	.74	1.56
P_2O_5	.57	.22	.25	.57	.21	.29	1.26	.77	.84	.87
H_2O-	.37	.31	.49	.91	.32	.40	.49	.53	.49	.53
LOI	1.73	1.40	1.97	1.39	2.05	2.11	2.25	3.39	2.26	1.96
TOTAL	100.07	99.99	99.10	100.02	100.32	100.05	99.21	99.88	99.65	99.15
Mo	5.8	3.5	5.7	5.3	3.8	5.3	5.2	3.3	< 1.8	8.4
Nb	23	7.3	7.7	25	7.4	12.0	35	29	31	37
Zr	383	139	148	253	119	165	344	326	333	386
Y	40	33	39	44	24	37	55	52	53	49
Sr	1145	424	133	541	569	233	325	317	282	414
U	< 4.7	< 1.1	< 4.8	< 4.9	< 4.7	< 4.9	< 5.0	< 3.8	< 3.8	< 3.2
Rb	42	26	8.9	28	46	26	30	21	17.8	51
Th	8.4	2.8	< 6.2	6.9	< 6.0	< 6.4	8.0	6.3	5.9	< 3.8
Pb	13.7	3.8	< 6.8	8.2	6.6	< 7.0	8.3	12.3	15.9	4.9
Ba	729	390	84	588	267	167	618	458	426	771
Sc	22	25	36	27	27	38	27	27	28	24
La	44	12.6	12.5	30	9.6	17.1	48	35	33	47
Ce	106	34	24	70	21	38	112	90	87	117
Nd	74	21	19.4	49	14.5	27	84	64	66	76
Cs	< 3.5	< 3.4	< 3.4	< 3.5	< 3.3	3.7	4.1	3.7	4.0	< 3.8
Zn	126	124	130	124	101	121	154	166	167	131
Cu	77	170	282	323	223	278	160	292	247	306
Ni	74	119	86	65	126	70	17.5	43	54	29
Co	44	53	54	46	50	54	40	48	48	41
Cr	78	87	119	32	273	93	7.7	29	34	< 2.5
V	257	262	337	359	272	361	251	312	325	248
$^{143}Nd/^{144}Nd$										
$^{87}Sr/^{86}Sr$		.70599								
$^{206}Pb/^{204}Pb$										
$^{207}Pb/^{204}Pb$										
$^{208}Pb/^{204}Pb$										
$\delta^{18}O$										
Height	1418	1543	1675	1698	1930	2050	1919	2085	2099	2130
Mg#	46.7	46.2	43.8	39.0	56.3	44.7	33.1	36.4	35.8	35.7

RSS47 : massive basalt
RSS63 : amyg. felsphyric (glom.) basalt
RSS66 : amyg. felsphyric basalt
RSS67 : massive basalt
RSS70 : amygdaloidal basalt
RSS73 : ropy basalt
RSS74 : amygdaloidal basalt
RSS75 : ropy basalt
RSS76 : ropy basalt
RSS78 : massive basalt

Table C1. Central Lebombo Whole Rock XRF Data (total Fe as Fe_2O_3t).

	RSS80	RSS81	RSS82	RSS86	RSS87	RSS88	RSS91	RSS92	RSS93	RSS96
SiO_2	51.55	49.29	54.92	70.07	59.54	48.92	51.76	48.78	46.93	51.18
TiO_2	2.77	3.38	1.86	.62	1.84	2.96	1.52	3.70	3.78	1.82
Al_2O_3	12.47	12.38	12.32	12.99	12.95	14.86	13.44	12.54	12.45	14.80
Fe_2O_3t	15.17	15.79	15.07	4.49	10.23	14.05	12.48	16.06	16.46	12.50
MnO	.21	.20	.24	.10	.16	.19	.16	.23	.21	.16
MgO	2.62	3.36	1.60	.36	2.24	3.03	5.94	4.84	4.20	5.02
CaO	6.31	6.77	4.87	1.65	4.61	7.73	6.68	9.12	8.85	6.97
Na_2O	2.57	2.50	3.23	3.32	2.80	2.99	4.73	2.25	3.89	3.50
K_2O	2.52	2.36	2.64	4.72	3.36	1.66	.32	1.01	.23	1.94
P_2O_5	1.35	1.06	.75	.15	.55	1.10	.17	.75	.56	.22
H_2O-	.44	.80	.32	.38	.41	.57	.32	.64	.43	.51
LOI	1.94	1.65	1.72	.74	1.00	1.84	2.11	.09	1.91	1.47
TOTAL	99.92	99.54	99.54	99.61	99.68	99.91	99.62	100.01	99.90	100.08
Mo	2.6	2.0	4.6	< 1.5	2.3	< 1.7	2.9	2.3	4.9	< 1.6
Nb	46	44	57	91	58	35	6.7	25	26	8.0
Zr	510	483	683	953	680	417	105	345	262	138
Y	71	63	86	110	91	64	27	68	43	31
Sr	1045	424	264	170	315	535	258	261	136	530
U	< 3.7	< 3.8	5.9	4.6	< 3.3	< 3.7	< 4.5	< 1.2	< 4.9	< 3.4
Rb	65	71	69	141	92	45	7.4	23	5.5	59
Th	10.2	9.3	11.2	16.6	12.2	5.4	< 5.8	3.1	< 6.4	5.0
Pb	14.5	11.0	13.8	21	14.8	7.4	< 6.4	4.9	< 7.0	8.6
Ba	938	787	840	1500	1055	567	120	476	53	243
Sc	21	23	21	8.9	22	24	23	42	28	24
La	62	53	74	110	78	47	12.1	33	29	14.8
Ce	146	124	162	226	164	109	21	75	71	34
Nd	106	88	114	131	102	80	14.5	54	49	23
Cs	< 3.5	4.0	3.9	< 2.8	< 3.3	4.6	< 3.2	< 3.7	< 3.6	< 3.3
Zn	159	177	199	95	122	146	109	133	150	115
Cu	304	388	165	12.0	90	256	126	251	306	127
Ni	< 2.2	10.0	< 2.2	< 1.5	12.9	7.1	156	55	33	101
Co	34	40	19.1	4.5	23	35	56	44	47	52
Cr	< 2.4	< 2.5	< 2.1	< 1.6	6.6	< 2.4	105	71	< 2.5	80
V	104	205	9.3	4.1	110	135	250	397	372	246
$^{143}Nd/^{144}Nd$										
$^{87}Sr/^{86}Sr$								.70447		
$^{206}Pb/^{204}Pb$										
$^{207}Pb/^{204}Pb$										
$^{208}Pb/^{204}Pb$										
$\delta^{18}O$				6.57						
Height	2160	2171					1568		1561	1415
Mg#	28.0	32.3	19.4	15.3	33.1	32.6	51.6	40.4	36.4	47.5

RSS80 : sparsely amygdaloidal basalt
RSS81 : sparsely amygdaloidal basalt
RSS82 : basaltic?
RSS86 : granophyric dyke - center
RSS87 : granophyric dyke - margin
RSS88 : mafic rock at dyke contact
RSS91 : amygdaloidal basalt
RSS92 : dolerite (F)
RSS93 : sparsely amygdaloidal basalt
RSS96 : amyg. felsphyric (glom.) basalt

Table C1. Central Lebombo Whole Rock XRF Data (total Fe as Fe_2O_3t).

	RSS97	RSS98	RSS99	RSS102	RSS103	RSS107	RSS109	RSS110	RSS111	RSS112
SiO_2	50.70	50.49	51.00	68.36	51.40	51.03	49.32	48.81	48.05	49.57
TiO_2	.99	2.90	2.80	.77	3.21	3.49	2.49	4.04	3.84	3.36
Al_2O_3	14.26	12.86	12.68	10.89	13.66	12.41	13.70	12.37	12.33	12.39
Fe_2O_3t	11.90	11.96	11.69	7.91	12.15	11.53	14.61	15.76	15.73	15.58
MnO	.16	.14	.14	.14	.15	.15	.21	.18	.19	.19
MgO	6.48	5.61	5.54	.50	3.82	6.06	5.94	3.91	3.80	3.08
CaO	9.30	7.13	8.18	4.08	6.19	7.69	9.65	6.77	7.96	6.58
Na_2O	2.93	3.38	2.59	3.43	2.70	1.77	2.18	2.32	1.93	2.94
K_2O	.48	2.28	1.65	1.95	2.50	3.53	.89	3.17	1.57	2.94
P_2O_5	.13	.46	.45	.24	.71	.52	.41	.84	.93	1.07
H_2O-	.68	.39	.39	.31	.73	.43	.32	.34	.49	.29
LOI	2.28	1.88	2.68	1.49	2.09	1.48	.75	1.55	3.11	1.39
TOTAL	100.29	99.48	99.79	100.08	99.30	100.09	100.48	100.05	99.92	99.41
Mo	< 1.6	4.6	2.8	< 1.5	1.8	1.9	< 1.8	9.7	9.2	9.2
Nb	3.0	17.5	18.3	64	29	20	18.4	40	39	45
Zr	75	340	330	749	485	386	272	450	432	480
Y	23	35	36	78	48	40	55	55	52	59
Sr	234	402	624	355	873	724	335	875	962	409
U	< 3.4	< 4.6	< 4.7	< 3.1	< 3.5	< 3.7	< 3.8	< 1.2	< 3.3	< 3.3
Rb	12.7	47	34	55	57	91	28	87	41	68
Th	< 4.2	9.3	< 6.0	12.4	9.8	5.3	5.3	6.5	6.3	6.1
Pb	7.5	10.8	7.5	22	14.8	6.6	12.2	6.7	6.7	7.8
Ba	174	1195	764	1215	1115	1060	350	1080	914	736
Sc	36	25	23	9.7	17.7	24	37	23	24	25
La	7.8	40	36	67	61	38	26	43	47	56
Ce	16.6	88	81	147	134	89	57	120	118	129
Nd	11.4	62	61	96	93	65	40	81	82	86
Cs	< 3.3	< 3.4	< 3.4	< 2.9	< 3.4	4.4	< 3.5	< 4.0	< 3.9	< 4.0
Zn	88	121	115	152	139	119	120	153	165	177
Cu	122	59	53	37	151	113	318	339	348	412
Ni	75	98	102	< 1.7	70	117	86	41	26	8.9
Co	49	50	48	3.5	39	44	49	46	42	37
Cr	199	101	98	< 1.8	69	225	158	13.5	5.8	< 2.5
V	270	237	231	3.9	204	262	288	278	244	204
$^{143}Nd/^{144}Nd$										
$^{87}Sr/^{86}Sr$								.70435		
$^{206}Pb/^{204}Pb$										
$^{207}Pb/^{204}Pb$										
$^{208}Pb/^{204}Pb$										
$\delta^{18}O$										
Height	1110	490	502		1032	827		2177	2175	2165
Mg#	55.1	51.3	51.7	12.1	41.5	54.2	47.7	35.8	35.1	30.6

RSS97 : massive basalt?
RSS98 : amygdaloidal basalt?
RSS99 : amygdaloidal basalt
RSS102 : volcanoclastic (tuff?)
RSS103 : amyg. felsphyric (glom.) basalt
RSS107 : massive basalt (F)
RSS109 : basaltic
RSS110 : massive basalt
RSS111 : massive basalt
RSS112 : ropy basalt

Table C1. Central Lebombo Whole Rock XRF Data (total Fe as Fe_2O_3t).

	RSS114	RSS123	RSS127	RSS137	RSS138	RSS139	RSS144	RSS147	RSS150	RSS152
SiO_2	49.15	48.96	48.00	50.28	51.93	53.92	50.84	49.07	48.99	50.77
TiO_2	3.41	2.46	2.28	3.49	3.37	2.38	2.88	3.76	4.28	2.87
Al_2O_3	12.03	13.09	14.18	13.70	13.53	12.40	13.06	13.14	12.70	13.72
Fe_2O_3t	15.67	15.57	15.99	12.12	12.58	14.58	12.06	15.08	15.86	12.85
MnO	.24	.22	.20	.14	.15	.21	.15	.22	.21	.18
MgO	3.38	5.68	5.99	4.82	3.87	2.52	5.69	4.62	4.64	5.16
CaO	7.39	9.72	10.01	7.73	7.39	5.86	7.24	8.51	8.65	9.31
Na_2O	2.47	2.52	2.47	2.69	2.56	3.27	2.55	2.74	2.50	2.68
K_2O	2.07	.65	.34	1.96	2.12	2.01	2.67	1.31	1.43	1.32
P_2O_5	1.27	.33	.21	.57	.71	.96	.45	.67	.68	.49
H_2O-	.32	.27	.20	.24	.28	.29	.34	.27	.34	.35
LOI	2.19	- .03	.49	1.90	1.48	1.39	1.80	.90	- .03	.51
TOTAL	99.61	99.48	100.36	99.62	99.98	99.79	99.71	100.29	100.29	100.22
Mo	8.4	7.7	7.3	8.2	8.8	8.6	6.7	9.6	9.3	9.1
Nb	35	13.4	4.4	21	23	40	15.5	33	34	35
Zr	351	195	135	384	401	448	334	302	402	338
Y	51	46	33	39	42	63	34	38	59	38
Sr	698	216	269	1255	1080	370	907	651	317	697
U	< 1.2	< 3.2	< 3.3	< 3.1	< 1.2	< 3.1	< 3.1	< 3.3	1.5	< 1.2
Rb	45	16.7	7.6	42	48	52	63	22	35	29
Th	5.1	< 3.9	< 3.9	7.8	6.6	7.0	5.0	< 3.9	6.0	6.4
Pb	6.6	< 4.6	< 4.6	10.6	9.9	< 4.4	5.3	5.2	6.6	7.8
Ba	1010	281	70	731	669	804	789	678	512	657
Sc	25	39	28	22	18.8	18.7	22	25	32	24
La	47	18.7	4.5	45	49	56	37	43	43	46
Ce	116	45	25	107	118	136	93	103	105	106
Nd	80	31	21	70	78	87	60	66	67	63
Cs	< 3.9	< 3.9	< 3.8	< 3.8	< 3.8	< 3.7	< 3.8	< 4.0	< 4.1	< 3.8
Zn	156	124	117	125	131	147	119	125	135	118
Cu	125	286	288	74	33	174	49	157	386	156
Ni	8.5	64	132	82	27	< 2.4	110	48	61	66
Co	36	48	58	45	43	30	49	46	41	42
Cr	< 2.5	76	179	75	4.5	< 2.3	89	7.3	56	57
V	196	341	338	256	238	96	232	351	366	246
$^{143}Nd/^{144}Nd$					.51211				.51241	.51233
$^{87}Sr/^{86}Sr$	.70473				.70514				.70467	.70487
$^{206}Pb/^{204}Pb$					16.45				17.72	17.46
$^{207}Pb/^{204}Pb$					15.22				15.54	15.51
$^{208}Pb/^{204}Pb$					37.05				38.21	38.24
$\delta^{18}O$									5.42	5.51
Height	2080			1315						
Mg#	32.7	45.0	45.8	47.0	40.9	27.8	51.5	40.9	39.7	47.4

RSS114 : massive basalt
RSS123 : dolerite (F)
RSS127 : dolerite
RSS137 : massive basalt
RSS138 : dolerite (F)
RSS139 : dolerite
RSS144 : dolerite (F)
RSS147 : dolerite (F)
RSS150 : dolerite (F)
RSS152 : dolerite (F)

Table C1. Central Lebombo Whole Rock XRF Data (total Fe as Fe_2O_3t).

	RSS156	RSS157	RSS160	RSS162	RSS165	RSS167	RSS168	RSS169	RSS183	RSS184
SiO_2	48.71	51.69	50.06	50.17	51.07	49.63	49.28	49.88	49.77	49.45
TiO_2	3.66	2.89	3.21	2.29	3.46	3.35	4.11	2.58	2.62	2.93
Al_2O_3	13.17	12.87	12.77	13.10	12.61	11.47	12.62	12.53	12.82	10.88
Fe_2O_3t	14.73	12.05	15.53	15.86	15.14	12.17	15.59	17.31	16.19	11.22
MnO	.20	.16	.23	.22	.21	.15	.25	.24	.23	.16
MgO	4.76	5.74	5.00	5.64	3.64	7.11	4.64	4.84	5.34	7.15
CaO	8.90	6.99	8.84	9.93	7.81	8.76	8.38	9.26	9.35	9.10
Na_2O	2.56	2.96	2.46	2.43	2.55	3.85	2.66	2.50	2.46	1.69
K_2O	1.47	2.82	1.08	.17	1.86	.61	1.47	.74	.76	1.87
P_2O_5	.67	.46	.46	.25	.95	.49	.80	.38	.38	.48
H_2O-	.29	.35	.51	.38	.41	.38	.22	.29	.30	.69
LOI	.93	1.46	.26	- .04	.57	2.26	.33	.06	.20	4.58
TOTAL	100.04	100.43	100.41	100.44	100.28	100.21	100.36	100.60	100.42	100.19
Mo	9.9	6.7	8.5	7.3	10.0	7.1	9.9	8.7	8.5	8.3
Nb	33	16.0	25	9.1	41	18.8	32	13.4	13.1	21
Zr	313	329	300	148	428	360	312	211	221	366
Y	38	35	46	32	55	34	42	46	52	31
Sr	707	988	357	309	536	522	824	208	227	1240
U	< 1.2	< 3.1	< 1.2	< 1.2	< 1.2	< 3.1	< 3.3	< 1.2	< 3.3	1.0
Rb	28	67	23	2.7	40	12.1	31	17.4	18.0	23
Th	6.4	5.2	3.5	2.2	6.9	4.7	< 4.0	3.1	< 3.9	8.2
Pb	7.7	7.1	4.4	2.2	7.8	5.9	6.8	3.4	4.9	10.5
Ba	681	979	408	106	678	254	763	213	350	879
Sc	23	21	32	33	23	28	26	35	41	24
La	43	38	30	9.9	54	41	46	15.9	22	52
Ce	109	93	79	37	130	96	112	50	55	122
Nd	67	62	51	26	85	65	73	35	39	75
Cs	< 3.9	< 3.7	< 3.9	< 3.8	< 3.9	< 3.7	< 4.0	< 3.9	< 3.9	< 3.8
Zn	129	122	124	127	137	119	119	134	120	110
Cu	205	47	252	240	274	88	252	348	306	96
Ni	48	114	54	62	23	108	140	47	47	159
Co	47	50	47	52	36	51	47	49	49	49
Cr	141	110	67	45	55	269	< 2.6	45	51	420
V	326	225	340	359	216	262	298	393	354	221
$^{143}Nd/^{144}Nd$			.51240	.51258	.51245					
$^{87}Sr/^{86}Sr$	.70513		.70419	.70422	.70477			.70504		.70636
$^{206}Pb/^{204}Pb$			17.77		17.75					
$^{207}Pb/^{204}Pb$			15.54		15.53					
$^{208}Pb/^{204}Pb$			38.43		38.44					
$\delta^{18}O$			5.34	5.76						
Height		491				757				1
Mg#	42.0	51.6	42.0	44.4	35.0	56.8	40.1	38.6	42.4	58.8

RSS156 : dolerite (F)
RSS157 : massive basalt (F)
RSS160 : dolerite (F)
RSS162 : dolerite (F)
RSS165 : dolerite (F)
RSS167 : massive basalt
RSS168 : dolerite (F)
RSS169 : dolerite (F)
RSS183 : dolerite? (F)
RSS184 : massive basalt (F)

Table C1. Central Lebombo Whole Rock XRF Data (total Fe as Fe_2O_3t).

	RSV4	RSV8	RSV8M	RSV11	RSV14	RSV16	RSV18	RSV19	RSV20	RSV21
SiO_2	49.88	61.34	51.40	49.14	51.03	50.65	51.54	50.73	50.84	53.19
TiO_2	2.99	1.53	3.10	2.27	2.88	2.00	2.89	2.84	2.96	2.72
Al_2O_3	11.42	13.08	13.07	13.34	12.99	14.02	13.29	12.96	13.48	12.45
Fe_2O_3t	11.43	9.92	13.80	15.14	12.03	14.27	11.81	12.11	11.75	11.02
MnO	.16	.18	.26	.23	.15	.22	.15	.14	.16	.15
MgO	6.76	1.72	3.85	6.40	5.63	5.52	5.29	5.67	5.30	5.17
CaO	9.39	4.39	9.01	10.41	7.35	10.20	9.63	7.20	9.55	7.07
Na_2O	1.11	3.16	2.83	2.50	2.49	2.36	1.78	2.75	1.59	2.48
K_2O	1.25	3.30	1.47	.48	2.84	.69	1.96	2.41	2.11	1.81
P_2O_5	.47	.30	.48	.28	.46	.29	.47	.46	.48	.41
H_2O-	.71	.27	.24	.36	.79	.29	.66	.64	.59	.93
LOI	4.14	.59	.51	- .09	1.21	.03	.88	1.77	1.23	2.07
TOTAL	99.71	99.76	100.01	100.55	99.85	100.54	100.36	99.68	100.04	99.48
Mo	4.0	3.6	9.3	7.4	5.3	< 1.7	2.1	< 1.7	1.7	< 1.7
Nb	17.5	69	44	9.6	17.1	10.5	16.8	15.7	16.7	16.6
Zr	346	891	490	162	347	181	346	331	355	330
Y	32	102	62	41	37	46	37	36	36	36
Sr	891	316	359	218	957	197	795	1040	741	738
U	< 1.1	< 3.3	< 3.2	< 1.2	< 4.8	< 1.2	< 1.2	< 3.5	< 1.2	< 3.5
Rb	16.7	90	34	11.1	64	17.7	32	54	41	37
Th	5.9	14.0	5.6	1.6	8.9	1.7	5.8	9.4	6.3	5.6
Pb	7.4	15.9	6.1	3.9	7.1	2.6	8.8	13.9	9.0	19.5
Ba	579	1120	538	183	976	260	653	879	640	858
Sc	28	18.4	28	38	22	42	24	22	24	20
La	39	92	52	12.9	41	20	40	38	40	35
Ce	89	196	124	39	89	40	84	83	91	80
Nd	67	125	74	28	62	28	58	61	65	54
Cs	5.4	4.4	< 3.9	< 3.9	< 3.5	< 3.6	< 3.5	< 3.4	< 3.6	< 3.4
Zn	110	153	156	114	123	110	119	121	126	114
Cu	89	107	110	245	55	275	50	51	45	50
Ni	115	14.3	45	75	115	54	121	119	115	93
Co	44	15.7	37	50	52	48	51	50	50	46
Cr	322	22	63	96	100	96	119	117	119	85
V	240	95	281	315	235	317	238	215	244	229
$^{143}Nd/^{144}Nd$				.51233		.51228	.51201			
$^{87}Sr/^{86}Sr$	.70627			.70449		.70567	.70656		.70556	
$^{206}Pb/^{204}Pb$				17.00		17.35	17.26			
$^{207}Pb/^{204}Pb$				15.36		15.49	15.44			
$^{208}Pb/^{204}Pb$				37.50		37.98	37.84			
$\delta^{18}O$						5.75	6.17			
Height	93				239		272	272	295	296
Mg#	57.1	28.3	38.7	48.8	51.3	46.6	50.2	51.3	50.2	51.2

RSV4 : massive basalt (F)
RSV8 : felsic dyke + mafic xenoliths
RSV8M : mafic xen. in above
RSV11 : dolerite (F)
RSV14 : massive basalt (F)
RSV16 : dolerite F)
RSV18 : auto-intr. in RSV19 (F)
RSV19 : massive basalt
RSV20 : auto-intr. in RSV21 (F)
RSV21 : amygdaloidal basalt

Table C1. Central Lebombo Whole Rock XRF Data (total Fe as Fe_2O_3t).

	RSV24	RSV26	RSV27	RSV30	RSV31	RSV35	RSC3	RSC4	RSC6	RSC8
SiO_2	50.03	50.85	50.89	50.49	51.31	50.95	49.73	49.86	52.55	51.17
TiO_2	2.11	3.59	3.03	2.99	3.24	2.12	2.74	1.71	3.05	3.02
Al_2O_3	13.42	12.51	13.48	11.20	11.17	13.58	12.85	14.49	13.38	11.51
Fe_2O_3t	14.56	11.41	11.88	11.73	12.14	14.24	11.89	13.27	11.90	11.68
MnO	.22	.14	.14	.15	.15	.21	.13	.19	.14	.14
MgO	5.98	5.64	5.26	8.26	6.66	5.93	5.74	6.66	5.19	7.13
CaO	10.28	7.08	7.66	9.15	8.51	9.91	8.39	10.83	7.75	7.93
Na_2O	2.42	2.39	1.53	1.10	1.84	2.65	1.59	2.48	2.58	2.20
K_2O	.59	2.07	2.45	.96	2.01	.83	1.62	.44	2.05	1.42
P_2O_5	.30	.53	.48	.44	.49	.26	.43	.23	.45	.46
H_2O-	.31	.72	.39	.56	.24	.29	.54	.36	.33	.42
LOI	.18	2.37	2.32	2.68	1.99	.14	4.10	.26	1.15	2.66
TOTAL	100.38	99.29	99.50	99.71	99.76	101.08	99.75	100.77	100.51	99.76
Mo	6.9	< 1.7	6.2	4.1	4.8	7.2	< 1.7	< 1.7	8.5	2.5
Nb	10.3	24	15.4	14.0	19.4	8.3	16.1	8.4	14.1	19.7
Zr	181	414	343	313	362	160	316	119	334	342
Y	45	38	38	35	35	37	35	31	36	36
Sr	189	454	1000	630	1075	279	838	253	935	780
U	< 3.2	< 3.5	< 4.8	< 4.6	< 1.2	< 1.2	< 3.5	< 1.1	< 3.1	< 4.7
Rb	13.0	37	70	17.8	40	19.5	29	9.4	52	24
Th	< 3.8	10.3	9.5	6.4	6.0	< 1.5	7.9	< 1.4	4.4	< 6.1
Pb	< 4.5	18.9	14.0	9.4	8.2	2.9	10.4	2.2	10.4	< 6.7
Ba	240	760	1170	506	799	254	604	195	777	607
Sc	42	22	23	25	27	39	23	35	21	25
La	14.5	43	36	33	41	14.2	36	15.7	38	39
Ce	39	105	87	71	94	42	83	30	94	89
Nd	27	75	61	55	66	28	58	21	60	62
Cs	< 3.8	< 3.5	3.8	< 3.5	< 3.5	< 3.8	< 3.4	< 3.5	< 3.8	< 3.4
Zn	112	120	123	111	121	103	120	93	122	118
Cu	267	123	45	94	98	202	49	169	43	85
Ni	60	112	71	278	100	62	120	88	74	196
Co	48	45	48	52	49	47	50	51	47	49
Cr	114	245	121	443	277	67	132	210	118	329
V	318	243	252	237	255	305	220	273	227	253
$^{143}Nd/^{144}Nd$					.51204			.51219		
$^{87}Sr/^{86}Sr$					.70498	.70479		.70466		
$^{206}Pb/^{204}Pb$					17.46			16.65		
$^{207}Pb/^{204}Pb$					15.48			15.41		
$^{208}Pb/^{204}Pb$					37.67			37.30		
$\delta^{18}O$					6.17					
Height		349	436	485	562		97		136	225
Mg#	47.9	52.6	49.8	61.4	55.2	48.4	52.0	53.1	49.6	57.8

RSV24 : dolerite (F)
RSV26 : amygdaloidal basalt
RSV27 : sparsely amygdaloidal basalt
RSV30 : massive basalt
RSV31 : massive basalt? (F)
RSV35 : dolerite (F)
RSC3 : massive basalt
RSC4 : dolerite (F)
RSC6 : massive basalt (F)
RSC8 : massive basalt

Table C1. Central Lebombo Whole Rock XRF Data (total Fe as Fe_2O_3t).

	RSC18	RSC19	RSC22	RSC25	RSC28	RSC32	RSC33	RSC35	RSC36	RSC37
SiO_2	45.95	50.30	50.02	53.24	50.21	48.67	49.13	49.09	48.52	50.56
TiO_2	3.93	2.26	1.51	2.39	3.28	1.66	1.82	2.89	3.76	3.41
Al_2O_3	13.09	13.92	14.06	11.86	12.07	14.54	13.36	11.95	12.05	12.09
Fe_2O_3t	15.66	12.97	13.21	16.07	17.48	13.48	14.58	17.72	16.24	15.95
MnO	.23	.16	.19	.29	.23	.20	.20	.24	.20	.25
MgO	4.66	5.22	6.43	2.13	3.86	6.18	5.65	4.12	3.87	3.92
CaO	7.90	6.95	10.94	6.73	6.94	9.52	8.76	6.91	6.80	7.55
Na_2O	2.32	4.62	2.57	2.44	2.77	3.12	2.80	2.76	2.64	2.71
K_2O	1.18	.15	.48	1.89	2.11	.29	.42	1.27	2.12	1.64
P_2O_5	.74	.25	.18	1.19	1.10	.19	.22	.58	.81	1.10
H_2O-	.92	.71	.30	1.05	.30	.28	.64	.53	.48	.36
LOI	2.40	2.15	.13	.53	.05	2.12	1.97	1.76	1.93	.97
TOTAL	98.96	99.67	100.02	99.80	100.40	100.26	99.56	99.81	99.42	100.51
Mo	1.8	< 1.7	7.0	4.6	9.8	3.8	4.2	6.6	6.0	10.6
Nb	32	11.5	6.5	48	35	6.2	6.2	24	40	35
Zr	319	155	107	607	385	94	118	301	441	453
Y	45	36	30	137	60	27	32	59	62	73
Sr	419	464	241	306	405	546	364	403	306	419
U	< 3.8	< 3.5	< 1.1	< 3.7	< 3.3	< 1.2	< 4.8	< 1.2	< 5.0	< 3.3
Rb	26	4.8	8.8	50	51	4.3	13.4	40	56	41
Th	10.9	< 4.3	1.6	11.0	< 4.0	2.1	< 6.2	4.4	< 6.4	5.4
Pb	15.7	< 4.7	2.4	11.5	< 4.7	1.7	< 6.8	5.5	< 7.1	9.2
Ba	742	57	211	782	712	98	186	431	622	530
Sc	28	27	41	34	32	35	39	36	27	32
La	49	12.9	12.8	83	47	10.0	9.5	29	50	46
Ce	108	30	33	187	118	16.8	25	69	114	113
Nd	75	24	21	138	82	13.9	17.1	50	81	79
Cs	3.7	< 3.3	< 3.7	< 3.6	< 3.9	< 3.4	< 3.4	< 3.6	< 3.6	< 3.9
Zn	121	118	92	227	155	99	114	154	156	142
Cu	295	229	170	9.1	321	184	202	405	384	131
Ni	26	109	68	< 2.3	29	68	64	34	30	21
Co	50	52	48	20	41	54	52	52	46	39
Cr	< 2.6	276	151	< 2.4	9.9	101	95	10.6	< 2.4	3.0
V	335	284	283	22	203	321	344	321	284	204
$^{143}Nd/^{144}Nd$			.51215			.51257		.51246		
$^{87}Sr/^{86}Sr$			.70525			.70426		.70455		
$^{206}Pb/^{204}Pb$			16.73			18.90		18.65		
$^{207}Pb/^{204}Pb$			15.34			15.64		15.61		
$^{208}Pb/^{204}Pb$			37.55			38.11		38.36		
$\delta^{18}O$			5.68					5.97		
Height	2327	2308			2560	2617	2781	2549	2522	
Mg#	40.1	47.6	52.3	23.0	33.2	50.7	46.5	34.2	34.9	35.5

RSC18 : amygdaloidal basalt
RSC19 : felsphyric (glom.) basalt
RSC22 : dolerite (F)
RSC25 : intermediate basaltic
RSC28 : feldsparphyric basalt?
RSC32 : feldsparphyric basalt (F)
RSC33 : amygdaloidal basalt
RSC35 : sparsely amygdaloidal basalt
RSC36 : sparsely amygdaloidal basalt
RSC37 : dolerite

Table C1. Central Lebombo Whole Rock XRF Data (total Fe as Fe_2O_3t).

	RSC38	RSC39	RSC40	RSC45	RSC50	RSC55	RSC56	RSC59	RSC69	RSC70
SiO_2	49.72	47.88	49.87	50.09	50.14	49.85	52.78	52.04	48.77	50.40
TiO_2	3.71	3.65	3.49	1.89	2.47	1.16	1.60	3.42	3.49	3.32
Al_2O_3	12.20	11.93	11.90	15.48	13.03	13.99	13.91	12.16	11.33	12.08
Fe_2O_3t	16.53	16.24	16.33	13.87	15.56	12.56	12.64	11.44	17.86	15.64
MnO	.20	.26	.23	.21	.25	.18	.15	.15	.27	.24
MgO	3.57	3.95	3.39	3.21	5.56	6.31	4.98	6.18	3.68	3.85
CaO	7.21	7.52	7.37	8.85	9.59	9.02	8.11	7.54	7.51	7.43
Na_2O	3.03	2.51	2.60	2.84	2.53	3.81	3.33	2.11	2.64	2.75
K_2O	1.22	.93	1.54	1.12	.71	.53	1.32	2.33	1.74	1.60
P_2O_5	.84	.82	.91	.56	.33	.15	.19	.51	1.58	1.08
H_2O-	.35	.53	.36	.37	.39	.47	.33	.42	.35	.50
LOI	1.30	2.82	1.50	1.62	.05	2.50	1.16	1.62	1.32	.96
TOTAL	99.87	99.05	99.49	100.11	100.62	100.53	100.50	99.91	100.54	99.85
Mo	3.1	5.2	7.4	5.1	7.3	6.1	5.9	7.6	10.3	10.0
Nb	37	40	45	26	11.8	4.6	7.4	19.5	36	35
Zr	458	433	500	337	203	91	132	375	449	456
Y	63	59	69	52	48	26	30	36	68	72
Sr	521	219	523	397	202	192	518	971	448	426
U	< 1.2	< 5.0	< 5.1	< 4.7	< 3.3	< 3.0	< 3.1	< 3.1	< 3.4	< 1.2
Rb	40	20.0	40	28	15.6	12.0	44	52	40	38
Th	6.7	< 6.5	8.5	6.1	< 3.9	< 3.6	< 3.7	3.7	5.9	6.7
Pb	7.4	10.2	< 7.2	< 6.7	< 4.6	< 4.2	4.8	6.2	7.5	6.8
Ba	695	289	738	437	284	146	207	769	809	529
Sc	27	31	29	29	40	36	22	26	29	31
La	50	49	55	37	16.0	4.3	11.2	38	54	48
Ce	116	109	126	85	46	15.6	32	100	137	119
Nd	80	78	89	63	31	12.0	23	67	95	81
Cs	3.8	< 3.6	< 3.7	< 3.4	< 3.9	< 3.5	< 3.5	< 3.8	< 4.0	< 3.9
Zn	169	164	171	121	123	97	109	117	174	140
Cu	367	325	443	151	273	140	96	106	314	124
Ni	33	33	16.2	26	51	79	138	95	14.5	19.8
Co	45	44	40	31	47	51	54	45	39	39
Cr	2.9	3.5	< 2.4	26	86	213	68	205	< 2.6	< 2.5
V	286	290	206	152	357	279	229	257	150	197
$^{143}Nd/^{144}Nd$	.51249									.51243
$^{87}Sr/^{86}Sr$	.70451									.70443
$^{206}Pb/^{204}Pb$										17.66
$^{207}Pb/^{204}Pb$										15.50
$^{208}Pb/^{204}Pb$										38.21
$\delta^{18}O$										
Height	2492	2495	2500			1150	976	929		
Mg#	32.8	35.4	31.8	34.3	44.5	53.0	47.1	54.8	31.6	35.4

RSC38 : ropy basalt
RSC39 : amygdaloidal basalt
RSC40 : ropy basalt
RSC45 : gabbro
RSC50 : dolerite
RSC55 : sparsely amygdaloidal basalt
RSC56 : amyg. felsphyric (glom.) basalt
RSC59 : massive basalt
RSC69 : dolerite
RSC70 : dolerite

Table C1. Central Lebombo Whole Rock XRF Data (total Fe as Fe_2O_3t).

	RSC71	RSC72	RSC75	RSC77	RSC78	RSC79	RSC85	RSC86	RSC87	RSK1
SiO_2	48.70	49.23	49.90	50.74	49.40	49.44	49.45	50.23	49.29	55.16
TiO_2	1.84	1.89	3.21	1.67	1.71	1.89	3.62	2.11	1.90	1.82
Al_2O_3	13.41	13.34	12.06	13.68	14.62	12.81	11.81	13.48	13.68	11.34
Fe_2O_3t	14.89	14.92	16.17	12.74	13.74	13.96	17.18	14.44	14.71	17.29
MnO	.23	.22	.22	.17	.20	.20	.25	.23	.21	.34
MgO	6.48	6.17	3.27	5.62	6.07	6.27	3.96	5.98	6.36	1.03
CaO	10.30	10.94	7.22	8.63	10.78	9.39	7.97	10.18	10.55	5.77
Na_2O	2.49	2.20	2.52	3.48	2.30	2.82	2.25	2.34	2.55	2.64
K_2O	.35	.22	1.80	1.18	.31	.38	1.41	.60	.40	2.49
P_2O_5	.20	.20	1.08	.20	.19	.20	.79	.29	.17	.77
H_2O-	.37	.29	.48	.42	.31	.70	.38	.36	.35	.83
LOI	.98	.69	1.89	1.49	.87	2.09	.85	.23	.14	.38
TOTAL	100.24	100.30	99.82	100.03	100.51	100.14	99.93	100.44	100.29	99.87
Mo	7.6	8.0	9.5	5.6	6.3	6.3	10.2	7.9	7.3	5.5
Nb	6.1	5.7	45	5.1	6.1	7.5	37	11.0	4.1	55
Zr	115	117	515	135	107	119	447	181	110	788
Y	31	31	69	27	28	29	80	44	31	104
Sr	288	224	345	468	251	448	266	183	260	350
U	< 3.2	< 1.2	< 3.3	< 3.0	< 3.2	< 3.1	1.6	< 1.2	< 1.2	< 3.9
Rb	9.0	4.3	44	39	4.7	11.4	29	14.2	9.9	69
Th	< 3.8	2.1	6.2	< 3.6	< 3.8	< 3.7	5.4	1.8	< 1.5	10.1
Pb	< 4.5	1.7	6.3	< 4.2	< 4.4	< 4.4	6.2	2.7	3.2	10.6
Ba	106	79	619	222	100	148	473	242	114	1005
Sc	36	38	27	23	32	38	35	42	37	28
La	5.9	10.3	60	11.7	5.5	7.4	43	14.3	4.7	87
Ce	22	21	143	32	17.7	25	109	38	21	191
Nd	18.0	16.0	95	21	17.2	21	74	26	15.4	136
Cs	< 3.7	< 3.8	< 3.9	< 3.5	< 3.7	< 3.6	< 4.0	< 3.8	< 3.8	5.1
Zn	112	112	171	105	97	110	144	105	100	222
Cu	206	214	412	89	205	176	79	263	233	50
Ni	78	69	18.6	91	69	62	26	61	81	< 2.4
Co	56	54	40	52	52	51	41	48	50	13.3
Cr	126	129	6.3	50	92	65	< 2.6	116	137	< 2.3
V	348	349	151	248	306	334	226	330	363	< 3.3
$^{143}Nd/^{144}Nd$										
$^{87}Sr/^{86}Sr$		.70424					.70616	.70519	.70442	
$^{206}Pb/^{204}Pb$										
$^{207}Pb/^{204}Pb$										
$^{208}Pb/^{204}Pb$										
$\delta^{18}O$										
Height			2532	1480	2640	2656				
Mg#	49.5	48.1	31.3	49.6	49.6	50.2	34.0	48.2	49.4	12.0

RSC71 : dolerite
RSC72 : dolerite (F)
RSC75 : massive basalt
RSC77 : amygdaloidal basalt
RSC78 : massive basalt (F)
RSC79 : feldsparphyric basalt (F)
RSC85 : dolerite (F)
RSC86 : dolerite (F)
RSC87 : dolerite (F)
RSK1 : gabbro

Table C1. Central Lebombo Whole Rock XRF Data (total Fe as Fe_2O_3t).

	RSK2	RSK4	RSK6	RSK9	RSK10	RSK14	RSK18	RSK21	RSK22	FV1
SiO_2	50.73	51.20	51.66	51.22	51.68	48.38	49.77	50.07	50.67	51.02
TiO_2	2.42	1.63	1.98	1.37	1.73	3.19	3.19	3.44	1.20	3.05
Al_2O_3	13.41	17.26	12.96	13.76	17.15	11.66	12.38	13.21	13.90	11.74
Fe_2O_3t	13.04	11.18	13.45	12.22	10.65	17.65	16.17	12.05	12.64	11.75
MnO	.16	.12	.16	.17	.13	.25	.20	.13	.18	.13
MgO	4.44	3.81	4.83	5.56	2.57	3.55	3.13	5.55	6.21	6.61
CaO	7.68	9.17	7.56	7.89	8.27	6.65	6.67	6.83	9.22	7.83
Na_2O	2.41	2.83	3.32	3.16	2.95	2.44	3.00	2.51	2.75	2.99
K_2O	.96	.56	1.42	1.95	1.41	1.97	1.62	2.41	.47	1.99
P_2O_5	.32	.20	.24	.18	.28	1.69	1.08	.57	.16	.48
H_2O-	.57	.49	.38	.31	.34	.53	.65	.44	.47	.42
LOI	2.86	1.21	1.77	1.83	2.80	1.39	1.74	2.65	2.50	1.77
TOTAL	99.01	99.66	99.72	99.61	99.95	99.36	99.60	99.86	100.37	99.79
Mo	3.4	< 1.6	5.0	4.0	< 1.6	7.4	2.2	8.2	5.3	4.5
Nb	12.8	6.5	8.9	6.3	8.8	40	46	23	3.1	23
Zr	206	140	152	109	196	456	545	414	92	350
Y	41	26	34	26	36	73	73	36	26	35
Sr	316	487	363	498	364	544	289	966	196	930
U	< 4.7	< 3.4	< 4.8	< 4.6	< 3.4	< 5.1	< 3.8	< 3.1	< 3.0	< 4.7
Rb	32	18.0	47	53	42	50	44	51	13.0	39
Th	< 6.1	4.9	< 6.2	< 6.0	4.3	8.5	11.1	7.3	< 3.6	10.0
Pb	< 6.7	10.0	< 6.8	< 6.5	14.9	9.8	14.0	7.7	< 4.2	9.6
Ba	245	152	214	393	293	821	555	899	126	741
Sc	24	18.4	25	24	21	33	25	21	38	25
La	22	16.5	15.6	12.5	16.1	58	65	49	5.3	43
Ce	47	32	36	24	39	139	147	117	16.9	97
Nd	34	24	23	16.6	26	106	103	77	14.6	66
Cs	< 3.3	< 3.3	< 3.4	< 3.3	< 3.3	< 3.7	< 3.6	< 3.8	< 3.5	< 3.4
Zn	128	97	118	106	103	176	178	125	98	119
Cu	58	66	81	65	145	221	444	93	166	105
Ni	66	79	65	89	61	4.3	16.6	90	68	125
Co	50	46	51	52	35	38	38	42	48	49
Cr	32	90	34	51	36	< 2.3	5.8	111	215	284
V	278	221	296	263	198	114	151	247	291	244
$^{143}Nd/^{144}Nd$										
$^{87}Sr/^{86}Sr$										
$^{206}Pb/^{204}Pb$										
$^{207}Pb/^{204}Pb$										
$^{208}Pb/^{204}Pb$										
$\delta^{18}O$										
Height	1868	758	931	684	1896	2472	2549	167	777	
Mg#	43.3	43.6	44.8	50.5	35.4	31.1	30.5	50.9	52.4	55.8

RSK2 : amygdaloidal basalt
RSK4 : amyg. felsphyric basalt
RSK6 : ropy basalt
RSK9 : sparsely amygdaloidal basalt
RSK10 : amyg. felsphyric basalt
RSK14 : sparsely amyg. metam. basalt
RSK18 : sparsely amyg. basalt?
RSK21 : amygdaloidal basalt
RSK22 : massive basalt
FV1 : sparsely amygdaloidal basalt

Table C1. Central Lebombo Whole Rock XRF Data (total Fe as Fe_2O_3t).

	FV2	FV4	FV5	CL100	CL102	CL105	CL108	CL110	CL111	CL113
SiO_2	50.59	45.88	46.65	54.06	52.19	49.39	50.64	50.39	51.38	50.54
TiO_2	3.69	2.04	2.73	3.15	3.19	4.00	2.96	3.01	2.92	2.93
Al_2O_3	12.91	6.36	11.32	12.42	12.07	13.17	12.98	13.19	13.13	12.97
Fe_2O_3t	12.40	13.38	11.01	11.03	11.41	14.80	11.84	11.98	11.79	12.02
MnO	.15	.16	.14	.15	.15	.21	.14	.16	.14	.15
MgO	4.82	18.08	5.19	4.98	6.39	4.34	6.23	5.47	6.02	6.00
CaO	6.91	5.94	8.80	7.70	8.09	8.59	7.76	8.25	8.05	8.01
Na_2O	2.81	.80	1.75	2.20	1.94	2.39	2.00	1.88	1.88	1.86
K_2O	3.49	.69	1.28	2.60	2.05	1.44	1.97	2.57	2.08	1.82
P_2O_5	.58	.29	.45	.51	.48	.69	.41	.49	.47	.40
H_2O-	.32	1.08	.40	.36	.34	.21	.38	.53	.41	.23
LOI	1.33	2.93	9.38	1.41	1.61	.63	2.05	1.69	1.60	1.76
TOTAL	99.99	97.64	99.10	100.59	99.91	99.86	99.36	99.61	99.87	98.71
Mo	4.6	3.5	2.9							
Nb	26	11.9	19.7	19.2	13.0	32	13.2	12.3	13.2	15.7
Zr	421	210	311	396	355	343	333	351	329	414
Y	40	21	31	31	30	38	31	33	30	38
Sr	1120	435	460	1100	1095	805	803	1090	768	900
U	< 4.7	< 4.5	< 4.4							
Rb	85	20	27	54	44	28	42	54	39	50
Th	8.6	< 5.9	6.0	5.4						
Pb	12.8	< 6.4	9.6	11.8						
Ba	1040	272	583	955	608	845	492	833	705	1270
Sc	24	17.2	27	23	24	24	22	22	23	24
La	49	25	39							
Ce	118	54	84							
Nd	80	38	58							
Cs	4.0	3.3	4.3							
Zn	125	117	111	106	109	124	112	117	116	136
Cu	137	73	60	112	57	129	47	47	42	58
Ni	84	1070	70	68	96	11.9	104	99	107	127
Co	42	101	43	44	46	44	49	52	52	50
Cr	106	1145	134	172	256	23	94	89	102	100
V	260	163	228	200	203	273	224	207	210	220
$^{143}Nd/^{144}Nd$										
$^{87}Sr/^{86}Sr$						.70504		.70672		
$^{206}Pb/^{204}Pb$										
$^{207}Pb/^{204}Pb$										
$^{208}Pb/^{204}Pb$										
$\delta^{18}O$										
Height				39			185	232	332	371
Mg#	46.7	75.2	51.4	50.4	55.8	39.9	54.2	50.7	53.4	52.8

FV2 : massive basalt (F)
FV4 : picrite basalt
FV5 : amygdaloidal basalt
CL100 : basalt
CL102 : dolerite (F)
CL105 : dolerite
CL108 : basalt
CL110 : basalt
CL111 : basalt
CL113 : basalt

Table C1. Central Lebombo Whole Rock XRF Data (total Fe as Fe_2O_3t).

	CL115	CL118	CL120	CL132	CL143	CL156	CL267	CL356	CL360	CL372
SiO_2	49.58	47.95	51.24	51.00	49.96	48.78	49.16	49.14	47.30	51.47
TiO_2	3.63	4.31	2.91	3.28	1.95	3.67	2.14	2.35	2.65	1.70
Al_2O_3	13.41	12.91	13.00	12.14	13.15	12.48	13.05	12.60	13.20	16.54
Fe_2O_3t	14.88	15.02	12.04	15.58	15.03	15.88	16.00	16.35	14.03	11.60
MnO	.19	.20	.14	.22	.23	.21	.24	.24	.21	.14
MgO	4.45	4.65	5.65	3.42	5.86	4.81	5.06	5.63	7.21	4.02
CaO	8.97	8.58	7.22	7.12	10.13	7.26	9.83	9.96	11.50	9.28
Na_2O	2.39	2.20	2.60	2.75	2.45	3.02	3.25	2.18	1.63	2.74
K_2O	1.21	1.43	2.81	1.63	.50	1.66	.77	.50	.39	.61
P_2O_5	.52	.59	.49	.88	.20	.51	.15	.29	.20	.17
H_2O-	.17	.20	.32	.29	.19	.18	.61	.21	.15	.19
LOI	.41	1.13	1.54	1.05	.15	1.24	.45	.16	.93	1.28
TOTAL	99.81	99.17	99.96	99.36	99.80	99.70	100.71	99.61	99.40	99.74
Mo										
Nb	27	29	27	37	8.3	24	19.7	10.8	11.9	7.2
Zr	325	320	333	347	143	246	259	180	120	142
Y	35	36	35	48	38	40	53	47	26	28
Sr	681	751	1140	509	204	541	167	193	355	406
U	1.1		1.1							
Rb	24	30	60	36	10.6	38	19.7	13.0	4.0	15.8
Th	4.9		4.8							
Pb	8.4		17.7							
Ba	644	616	1175	660	202	773	247	254	182	232
Sc	25	26	22	24	41	27	43	45	38	20
La										
Ce										
Nd										
Cs	.5		.2							
Zn	110	132	113	133	104	114	129	125	99	102
Cu	207	258	44	126	219	320	393	244	432	96
Ni	47	55	103	9.6	67	72	50	63	109	1.0
Co	48	50	53	39	52	47	47	54	55	48
Cr	13.3	40	112	12.5	105	51	50	61	151	91
V	310	380	219	218	347	365	395	367	366	228
$^{143}Nd/^{144}Nd$	.51225		.51198							.51194
$^{87}Sr/^{86}Sr$	.70500		.70637							.70790
$^{206}Pb/^{204}Pb$	17.39									
$^{207}Pb/^{204}Pb$	15.48									
$^{208}Pb/^{204}Pb$	38.03									
$\delta^{18}O$			4.65							
Height	378		479	966		1947		310	603	742
Mg#	40.1	40.9	51.3	33.1	46.6	40.5	41.6	43.8	53.6	43.9

CL115 : basalt (F)
CL118 : dolerite
CL120 : basalt
CL132 : basalt
CL143 : dolerite (F)
CL156 : basalt
CL267 : dolerite
CL356 : dolerite (F)
CL360 : basalt (F)
CL372 : basalt (F)

Table C1. Central Lebombo Whole Rock XRF Data (total Fe as Fe_2O_3t).

	CL376
SiO_2	52.75
TiO_2	1.98
Al_2O_3	13.17
Fe_2O_3t	13.52
MnO	.17
MgO	4.92
CaO	8.50
Na_2O	2.41
K_2O	.93
P_2O_5	.19
H_2O-	.19
LOI	1.16
TOTAL	99.89
Mo	
Nb	7.4
Zr	150
Y	28
Sr	318
U	
Rb	21
Th	
Pb	
Ba	179
Sc	22
La	
Ce	
Nd	
Cs	
Zn	110
Cu	132
Ni	83
Co	55
Cr	55
V	286
$^{143}Nd/^{144}Nd$	
$^{87}Sr/^{86}Sr$	
$^{206}Pb/^{204}Pb$	
$^{207}Pb/^{204}Pb$	
$^{208}Pb/^{204}Pb$	
$\delta^{18}O$	
Height	1236
Mg#	45.0

CL376 : basalt

Table C2. Central Lebombo REE data from spark-source mass spectrography.

	LFE-group				HFE-group			N-group	
	RSV31	RSS2	CL100	CL120	RSC35	RSC38	CL115	RSC32	RSS40
La	51.9	64.1	57.0	46.0	28.2	53.3	54.0	9.79	14.7
Ce	117	139	138	110	68.4	118	122	23.8	35.3
Pr	13.5	17.4	18.3	14.1	9.56	16.5	15.6	3.15	5.15
Nd	59.2	72.0	70.0	60.0	44.3	72.4	68.0	14.5	23.5
Sm	12.9	13.6	13.6	13.2	10.6	15.9	13.2	3.95	5.87
Eu	3.63	3.82	3.85	3.86	2.98	4.13	3.50	1.39	1.94
Gd	9.80	10.1	9.50	9.70	10.2	13.0	10.9	4.23	5.75
Tb	1.46	1.46	1.37	1.39	1.72	2.21	1.60	.73	1.01
Dy	7.71	7.63	7.10	7.60	10.5	12.7	8.90	4.38	6.17
Ho	1.24	1.28	1.25	1.38	2.05	2.31	1.60	.89	1.14
Er	2.95	3.00	2.96	3.30	5.64	5.80	3.90	2.24	2.96
Tm			.36	.41			.45		
Yb	2.12	2.09	2.32	2.73	4.76	4.48	3.30	1.76	2.49

Table C2a. Central Lebombo trace element data from spark-source mass spectrography (data in ppm unnormalized).

	LFE-group				HFE-group			N-group	
	RSV31	RSS2	CL100	CL120	RSC35	RSC38	CL115	RSC32	RSS40
U	.85	1.24	1.13	1.10	.87	1.11	1.13	.18	.33
Th	3.94	5.42	5.4	4.8	3.06	5.45	4.9	.52	1.74
Bi	-	.31	-	-	.12	.18	-	.07	.25
Pb	6.2	8.1	11.8	17.7	4.1	8.2	8.4	1.02	3.6
Hf	9.1	10.4	9.6	8.8	7.58	12.1	8.5	2.54	5.37
Cs	.15	.32	.41	.17	.16	.55	.48	.26	.07
Sn	6.7	6.7	3.64	2.98	6.7	9.0	3.32	2.4	4.1

Table C3. XRF analyses of soils overlying LFE-group basalts.

	C1	C2	C3	C4	D1	D2	D3	D4
SiO_2	51.79	52.32	51.08	52.13	48.46	50.18	50.24	49.05
TiO_2	4.79	4.58	4.67	4.89	5.39	5.52	4.91	4.97
Al_2O_3	12.68	12.27	12.25	12.02	12.63	12.55	12.37	12.32
Fe_2O_3	12.08	11.99	11.71	11.66	12.01	11.83	11.58	12.24
MnO	.17	.16	.17	.17	.16	.17	.15	.15
MgO	1.31	1.25	1.26	1.46	1.53	1.63	1.67	1.60
CaO	2.99	2.72	2.73	3.10	2.06	2.36	2.25	2.51
Na_2O	.76	.75	.73	.81	.59	.66	.62	.60
K_2O	1.89	1.93	1.74	1.89	2.02	2.12	1.71	1.87
P_2O_5	.30	.30	.26	.33	.33	.31	.40	.23
H_2O+	11.75	11.74	13.16	10.20	14.75	13.65	14.40	12.97
TOTAL	100.51	100.01	99.76	98.66	99.93	100.98	100.30	98.50
Nb	34	32	34	36	34	32	30	33
Zr	420	404	407	408	426	413	414	407
Y	29	29	29	26	30	29	29	29
Sr	962	776	801	931	627	639	611	608
Rb	46	46	43	41	51	51	43	41
Zn	92	88	96	89	96	101	97	97
Cu	121	113	115	115	134	130	132	137
Ni	106	126	127	122	160	161	161	163
Co	48	53	50	73	53	47	49	49
Cr	242	241	235	229	313	302	306	316
V	221	224	220	222	241	234	232	303
CIA	61.1	61.7	62.1	59.1	67.1	64.2	67.0	63.5

Table C4. Central Lebombo Isotope Data.

Strontium Naturals

Name	Rb	Sr	Rb/Sr	$^{87}Rb/^{86}Sr$	$^{87}Sr/^{86}Sr_m$	$^{87}Sr/^{86}Sr_i$	ϵ_{Sr}
RSS2	50	1110	0.0450	0.1302	0.70663 ±1	0.70628 ±1	25.7
RSS8	60	1055	0.0569	0.1644	0.70661 ±2	0.70617 ±2	24.1
RSS26	41	682	0.0601	0.1738	0.70566 ±1	0.70519 ±1	10.2
RSS138	48	1080	0.0444	0.1285	0.70549 ±1	0.70514 ±1	9.6
RSS152	29	697	0.0416	0.1203	0.70519 ±1	0.70487 ±1	5.6
RSS184	23	1240	0.0185	0.0536	0.70650 ±1	0.70636 ±1	26.8
RSV4	16.7	891	0.0187	0.0542	0.70642 ±1	0.70627 ±1	25.6
RSV18	32	795	0.0403	0.1164	0.70687 ±1	0.70656 ±1	29.6
RSV20	41	741	0.0564	0.1630	0.70600 ±1	0.70556 ±1	15.5
RSV31	40	1075	0.0372	0.1076	0.70527 ±1	0.70498 ±1	7.2
CL110+	54	1093	0.0494	0.1428	0.70711 ±5	0.70672 ±5	32.0
CL120+	60	1144	0.0524	0.1519	0.70678 ±4	0.70637 ±4	27.0
RSS92	23	261	0.0881	0.2547	0.70516 ±3	0.70447 ±3	0.0
RSS110	87	875	0.0994	0.2874	0.70513 ±1	0.70435 ±1	-1.7
RSS114	45	698	0.0645	0.1864	0.70523 ±1	0.70473 ±1	3.6
RSS150	35	317	0.1104	0.3192	0.70553 ±1	0.70467 ±1	2.8
RSS156	28	707	0.0396	0.1145	0.70544 ±1	0.70513 ±1	9.4
RSS160	23	357	0.0644	0.1862	0.70469 ±1	0.70419 ±1	-4.0
RSS165	40	536	0.0746	0.2157	0.70535 ±1	0.70477 ±1	4.2
RSC35	40	403	0.0993	0.2869	0.70533 ±1	0.70455 ±1	1.2
RSC38	40	521	0.0768	0.2219	0.70511 ±1	0.70451 ±1	0.6
RSC70	38	426	0.0892	0.2578	0.70513 ±1	0.70443 ±1	-0.5
RSC85	29	266	0.1090	0.3152	0.70701 ±2	0.70616 ±2	24.0
CL105+	28	805	0.0348	0.1005	0.70531 ±5	0.70504 ±5	8.1
CL115+	24	681	0.0347	0.1002	0.70527 ±6	0.70500 ±6	7.5
RSS40	28	262	0.1069	0.3090	0.70632 ±2	0.70549 ±2	14.4
RSS63	26	424	0.0613	0.1773	0.70647 ±1	0.70599 ±1	21.6
RSS162	2.7	309	0.0087	0.0253	0.70429 ±2	0.70422 ±2	-3.5
RSS169	17.4	208	0.0837	0.2418	0.70569 ±3	0.70504 ±3	8.0
RSV11	11.1	218	0.0509	0.1472	0.70489 ±1	0.70449 ±1	0.3
RSV16	17.7	197	0.0898	0.2597	0.70637 ±1	0.70567 ±1	17.0
RSV35	19.5	279	0.0699	0.2020	0.70534 ±9	0.70479 ±9	4.6
RSC4	9.4	253	0.0372	0.1074	0.70495 ±1	0.70466 ±1	2.7
RSC22	8.9	241	0.0369	0.1068	0.70554 ±1	0.70525 ±1	11.1
RSC32	7.8	546	0.0143	0.0413	0.70437 ±1	0.70426 ±1	-3.0
RSC72	4.3	224	0.0192	0.0555	0.70439 ±1	0.70424 ±1	-3.3
RSC86	14.2	183	0.0776	0.2243	0.70580 ±1	0.70519 ±1	10.3
RSC87	9.9	260	0.0381	0.1101	0.70472 ±1	0.70442 ±1	-0.7
CL372#	15.8	406	0.0389	0.1125	0.70820	0.70790	48.6
KA24	30	902	0.0333	0.0961	0.70531 ±1	0.70505 ±1	8.2
KP111	101	1168	0.0865	0.2500	0.70548 ±1	0.70480 ±1	4.8
KP121	45	831	0.0542	0.1565	0.70576 ±1	0.70534 ±1	12.3
KS47	29	843	0.0344	0.0994	0.70505 ±1	0.70478 ±1	4.4
KP112+	61	795	0.0767	0.2218	0.70590 ±5	0.70530 ±5	11.8
KS3+	58	842	0.0689	0.1991	0.70533 ±4	0.70479 ±4	4.6

/Table C4

Nd Naturals

Name	Sm	Nd	Sm/Nd	$^{147}Sm/^{144}Nd$	$^{143}Nd/^{144}Nd_m$	$^{143}Nd/^{144}Nd_i$	ϵ_{Nd}	T_{CHUR} (Ma)
RSS2*	13.6	72.0	0.189	0.114	0.512127 ±6	0.511985 ±6	-7.98	940
RSS138	13.6	65.8	0.207	0.125	0.512235 ±14	0.512080 ±14	-6.13	860
RSS152	11.3	56.8	0.199	0.120	0.512472 ±6	0.512322 ±6	-1.40	330
RSV18	11.0	53.2	0.207	0.125	0.512129 ±8	0.511974 ±8	-8.20	1080
RSV31*	12.9	59.2	0.218	0.132	0.512205 ±5	0.512041 ±5	-6.8	1020
CL120+	13.2	60	0.220	0.133	0.512140 ±20	0.511975 ±20	-8.2	1190
RSS150	12.5	57.1	0.219	0.132	0.512568 ±11	0.512403 ±11	.18	170
RSS160	9.83	43.6	0.226	0.136	0.512575 ±10	0.512406 ±10	.22	160
RSS165	15.3	70.4	0.217	0.131	0.512616 ±8	0.512453 ±8	1.14	50
RSC35*	10.6	44.3	0.239	0.145	0.512643 ±6	0.512463 ±6	1.35	-20
RSC38*	15.9	72.4	0.220	0.133	0.512654 ±10	0.512489 ±10	1.85	-40
RSC70	15.5	68.3	0.227	0.137	0.512576 ±8	0.512405 ±8	.22	160
CL115+	13.2	68	0.194	0.117	0.512400 ±10	0.512254 ±10	-2.73	460
RSS40	6.19	23.7	0.261	0.158	0.512334 ±9	0.512138 ±9	-5.00	1190
RSS162	4.92	22.0	0.224	0.135	0.512746 ±11	0.512578 ±11	3.59	-270
RSV11	6.23	23.3	0.267	0.162	0.512506 ±11	0.512305 ±11	-1.74	580
RSV16	5.91	23.6	0.250	0.151	0.512460 ±9	0.512272 ±9	-2.39	600
RSC4	4.86	18.8	0.259	0.156	0.512370 ±23	0.512176 ±23	-4.26	1010
RSC22	4.13	16.8	0.246	0.149	0.512325 ±10	0.512140 ±10	-4.95	990
RSC32	4.18	14.4	0.290	0.176	0.512741 ±8	0.512523 ±8	2.51	-750
CL372#	6.1	23.4	0.261	0.158	0.512140	0.511940	-8.8	1930
KS47					0.512278 ±11			
KP112+	12.3	61	0.202	0.122	0.512130 ±20	0.511978 ±20	-8.11	1030
KS3+	12.6	59	0.214	0.129	0.512270 ±20	0.512109 ±20	-5.55	830

* Sm and Nd determined by spark source mass spectrography.

/Table C4

Pb Naturals

Name	$^{206}Pb/^{204}Pb$	$^{207}Pb/^{204}Pb$	$^{208}Pb/^{204}Pb$	$^{207}Pb/^{206}Pb$
RSS2	17.427 ±11	15.414 ±13	37.80 ±3	0.88465 ±28
RSS138	16.452 ±11	15.222 ±12	37.05 ±3	0.92546 ±30
RSS152	17.459 ±9	15.514 ±7	38.24 ±2	0.88855 ±18
RSV18	17.260 ±8	15.441 ±10	37.84 ±2	0.89428 ±38
RSV31	17.455 ±7	15.479 ±7	37.67 ±2	0.88641 ±28
RSS150	17.719 ±5	15.538 ±5	38.21 ±1	0.87682 ±5
RSS160	17.766 ±5	15.543 ±6	38.43 ±2	0.87486 ±12
RSS165	17.750 ±13	15.533 ±10	38.44 ±3	0.87512 ±28
RSC35	18.651 ±7	15.613 ±6	38.36 ±2	0.83712 ±22
RSC70	17.656 ±4	15.495 ±4	38.21 ±1	0.87755 ±10
CL115[+]	17.39	15.48	38.03	
RSS40	16.888 ±3	15.358 ±5	37.97 ±1	0.90946 ±14
RSV11	16.998 ±3	15.360 ±4	37.50 ±1	0.90378 ±11
RSV16	17.346 ±5	15.485 ±5	37.98 ±1	0.89250 ±12
RSC4	16.650 ±7	15.413 ±6	37.30 ±2	0.91968 ±24
RSC22	16.725 ±6	15.337 ±6	37.55 ±2	0.91738 ±28
RSC32	18.905 ±7	15.642 ±6	38.11 ±2	0.82743 ±6
KS3[+]	17.42	15.53	37.60	

$\delta^{18}O$

RSS2	+6.48	RSS150	+5.42	RSS40	+4.50
RSS152	+5.51	RSS160	+5.34	RSS162	+5.76
RSV18	+6.17	RSC35	+5.97	RSV16	+5.75
RSV31	+6.17			RSC22	+5.68
CL120	+4.65				
KP112	+6.80	RSS86	+6.57		
KS3	+8.23				

[+] from Erlank (1984)
[#] from Hawkesworth (pers. com., 1987)

APPENDIX D. SAMPLE LOCALITIES

Figure D1. Sample locality maps for the central Lebombo. The first page is a map index for succeeding pages (p80-89) with each locality map indexed in increasing numerical order from north to south. Also located on the index map on pg 79 are samples not located on the succeeding sheets: FV-samples on the Sweni River north of the Sabie River, RST1 at Tshokwane and RSS89 near the Mozambique Border on the Sabie River.

/Figure D1

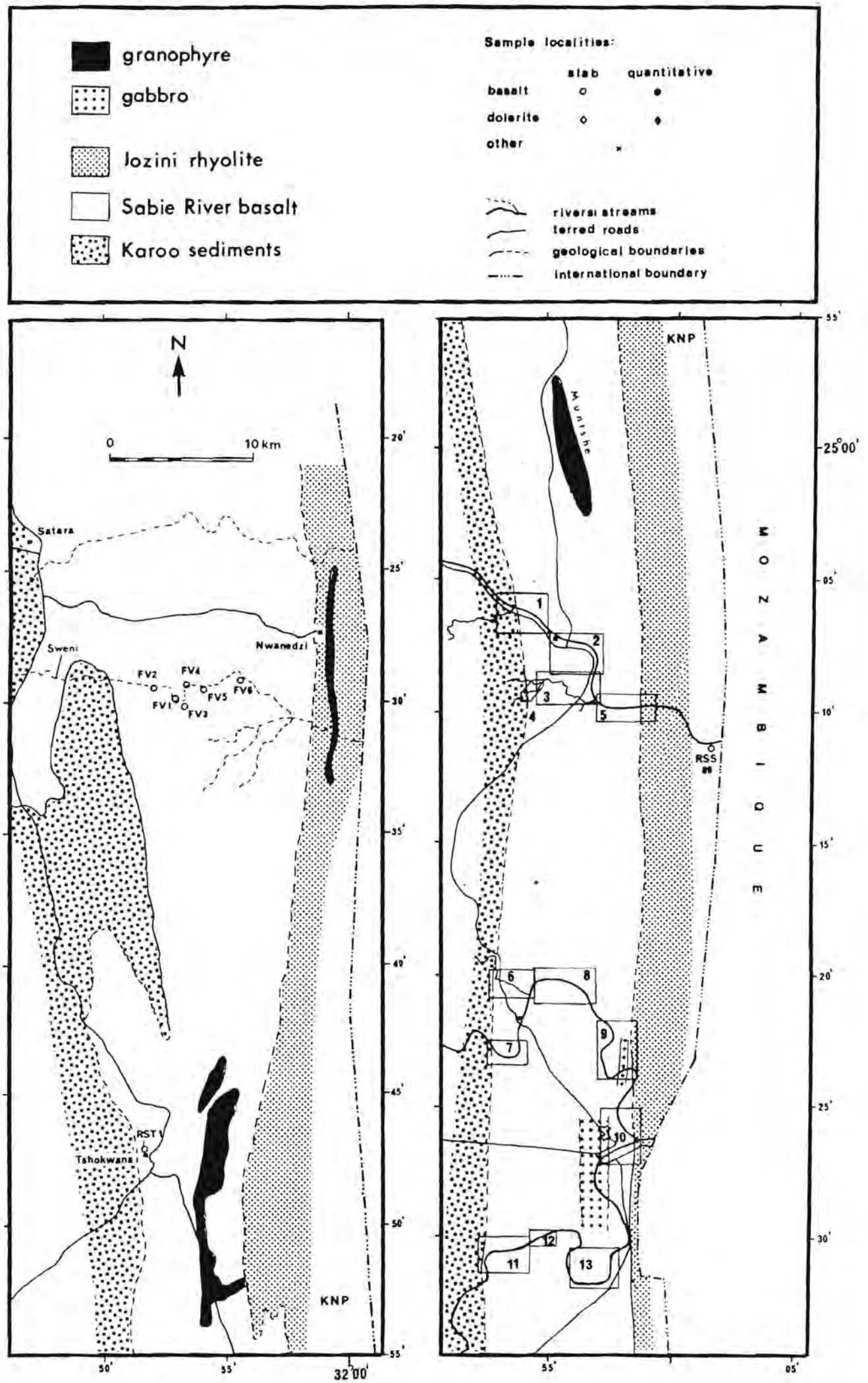
granophyre
gabbro
Nozini rhyolite
Sabie River basalt
Karoo sediments
Sample localities:
slab
quantitative
basalt
dolerite
other
rivers/ streams
tarred roads
geological boundaries
international boundary
N
0
10 km
Satara
Sweni
Nwanedzi
FV1
FV2
FV3
FV4
FV5
FV6
RST1
Tshokwane
KNP
32°00'
Munishe
MOZAMBIQUE
RSS
1
2
3
4
5
6
7
8
9
10
11
12
13
20'
25'
30'
35'
40'
45'
50'
55'
25°00'
05'
10'
15'
20'
25'
30'

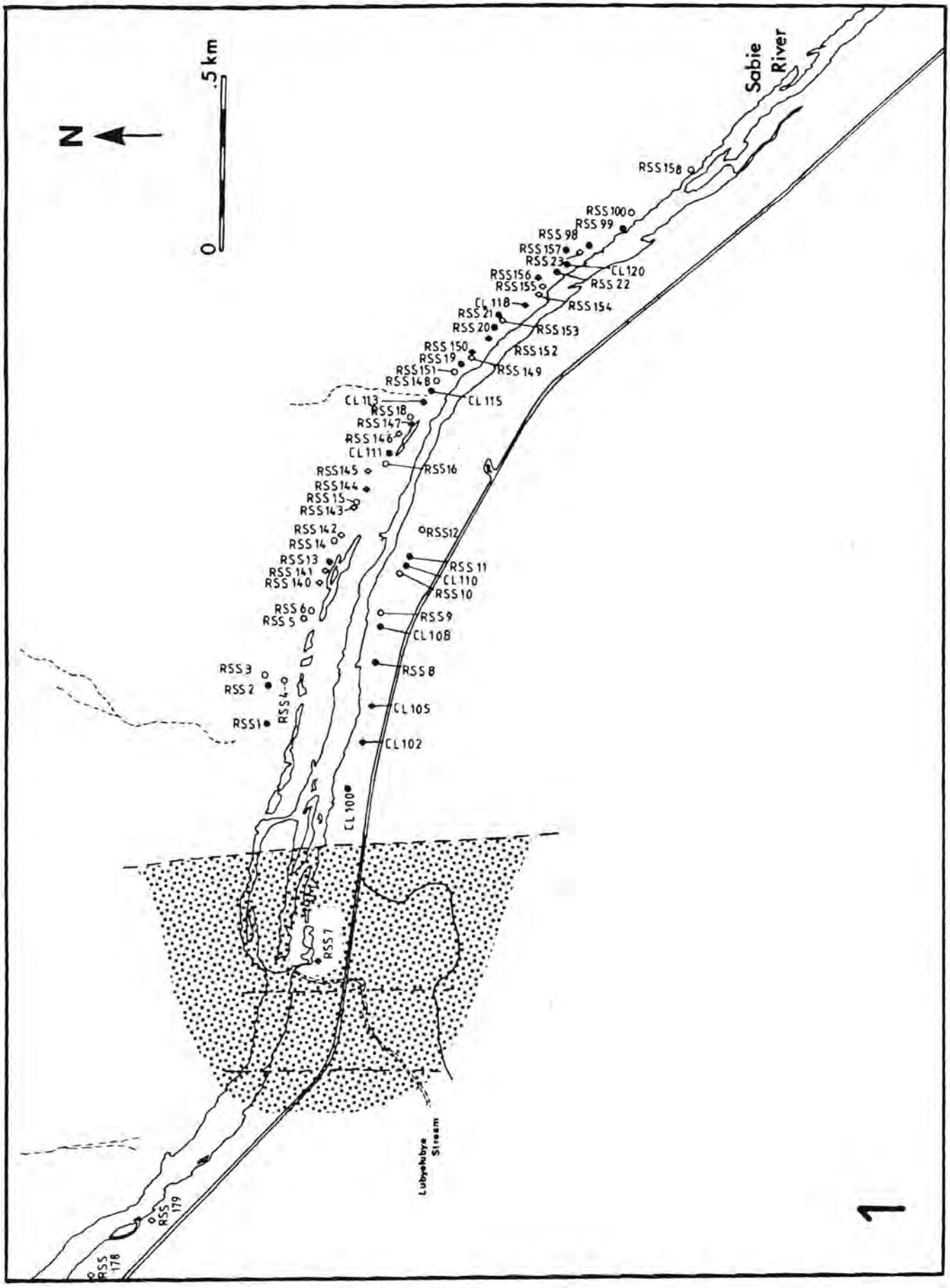
N
0
.5 km
Sabie River
RSS 158
RSS 100
RSS 99
RSS 98
RSS 157
RSS 23
CL 120
RSS 156
RSS 155
RSS 22
CL 118
RSS 154
RSS 21
RSS 20
RSS 153
RSS 150
RSS 19
RSS 152
RSS 151
RSS 149
RSS 148
CL 113
CL 115
RSS 18
RSS 147
RSS 146
CL 111
RSS 16
RSS 145
RSS 144
RSS 15
RSS 143
RSS 142
RSS 14
RSS 12
RSS 13
RSS 11
RSS 141
CL 110
RSS 140
RSS 10
RSS 6
RSS 5
RSS 9
CL 108
RSS 3
RSS 8
RSS 2
RSS 4
CL 105
RSS 1
CL 102
CL 100
RSS 7
Lubyelubye Stream
RSS 179
RSS 178
1

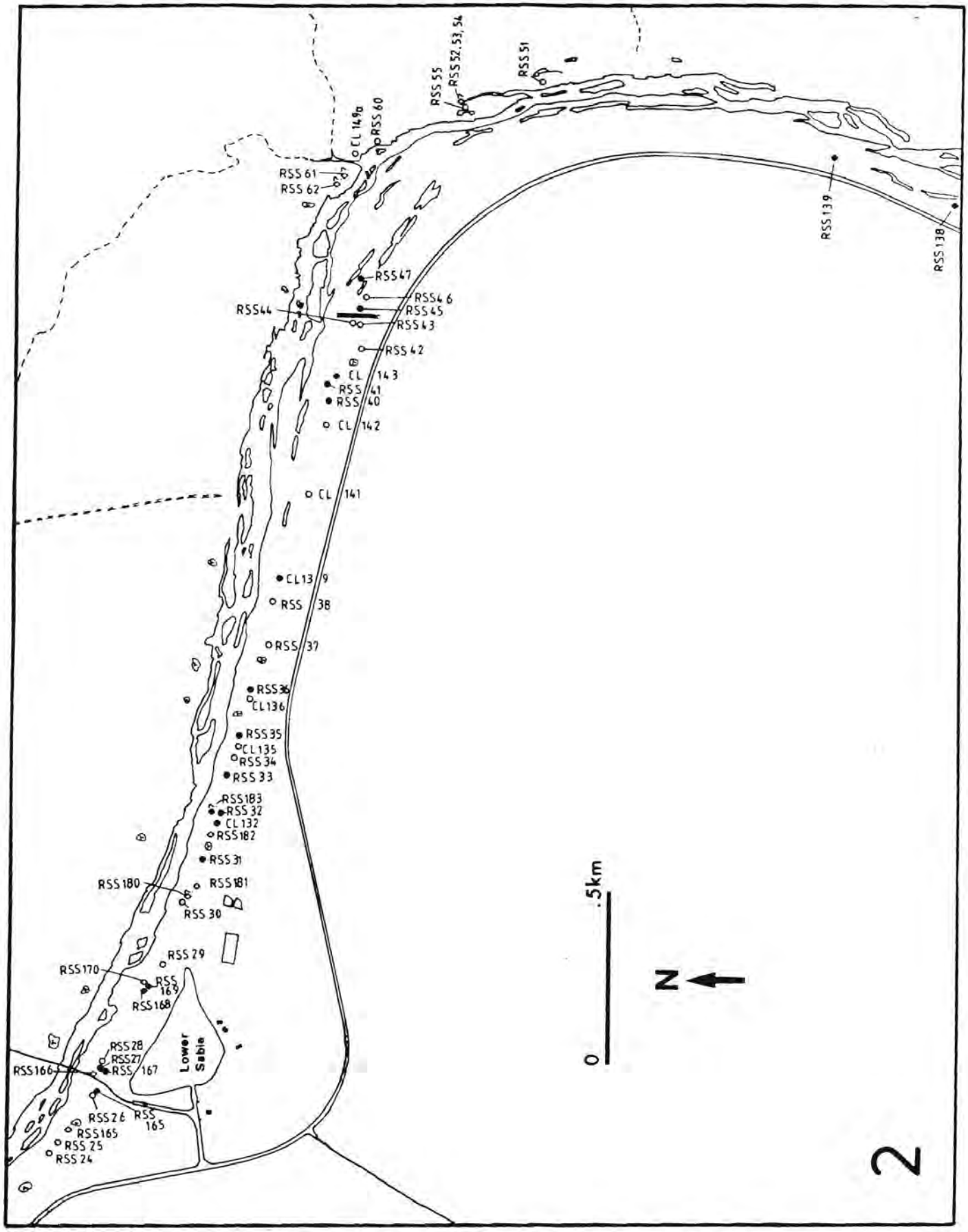
RSS 55
RSS 52, 53, 54
RSS 51
CL 149a
RSS 60
RSS 61
RSS 62
RSS 139
RSS 138
RSS 47
RSS 46
RSS 45
RSS 44
RSS 43
RSS 42
CL 143
RSS 41
RSS 40
CL 142
CL 141
CL 139
RSS 38
RSS 37
RSS 36
CL 136
RSS 35
CL 135
RSS 34
RSS 33
RSS 183
RSS 32
CL 132
RSS 182
RSS 31
RSS 180
RSS 181
RSS 30
RSS 29
RSS 170
RSS 169
RSS 168
RSS 28
RSS 27
RSS 166
RSS 167
Lower Sabia
RSS 26
RSS 165
RSS 165
RSS 25
RSS 24
0
.5km
N
2

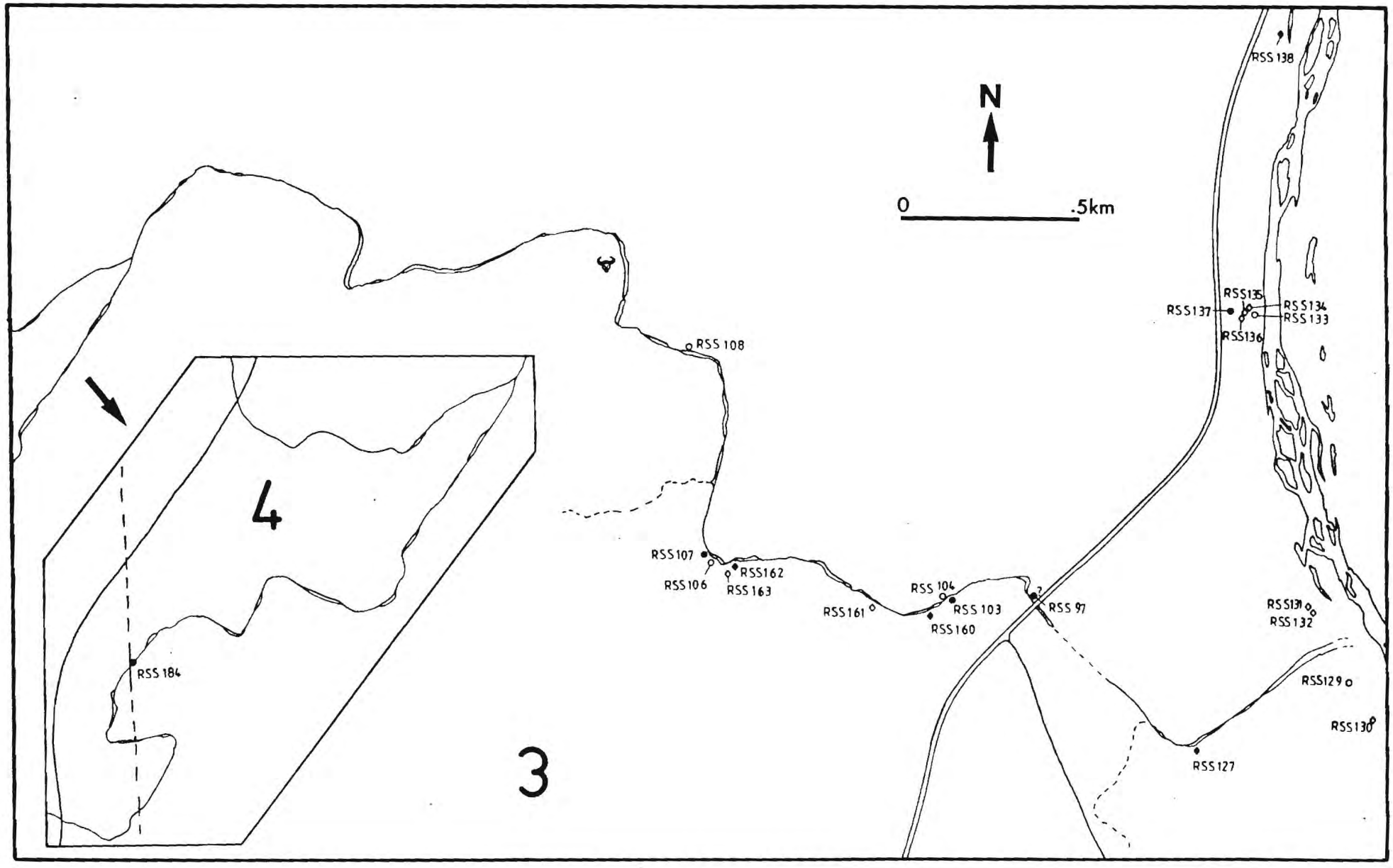
N
0
.5km
RSS 138
RSS 135
RSS 137
RSS 134
RSS 133
RSS 136
RSS 108
RSS 107
RSS 106
RSS 162
RSS 163
RSS 161
RSS 104
RSS 103
RSS 160
RSS 97
RSS 131
RSS 132
RSS 129
RSS 130
RSS 127
RSS 184
4
3

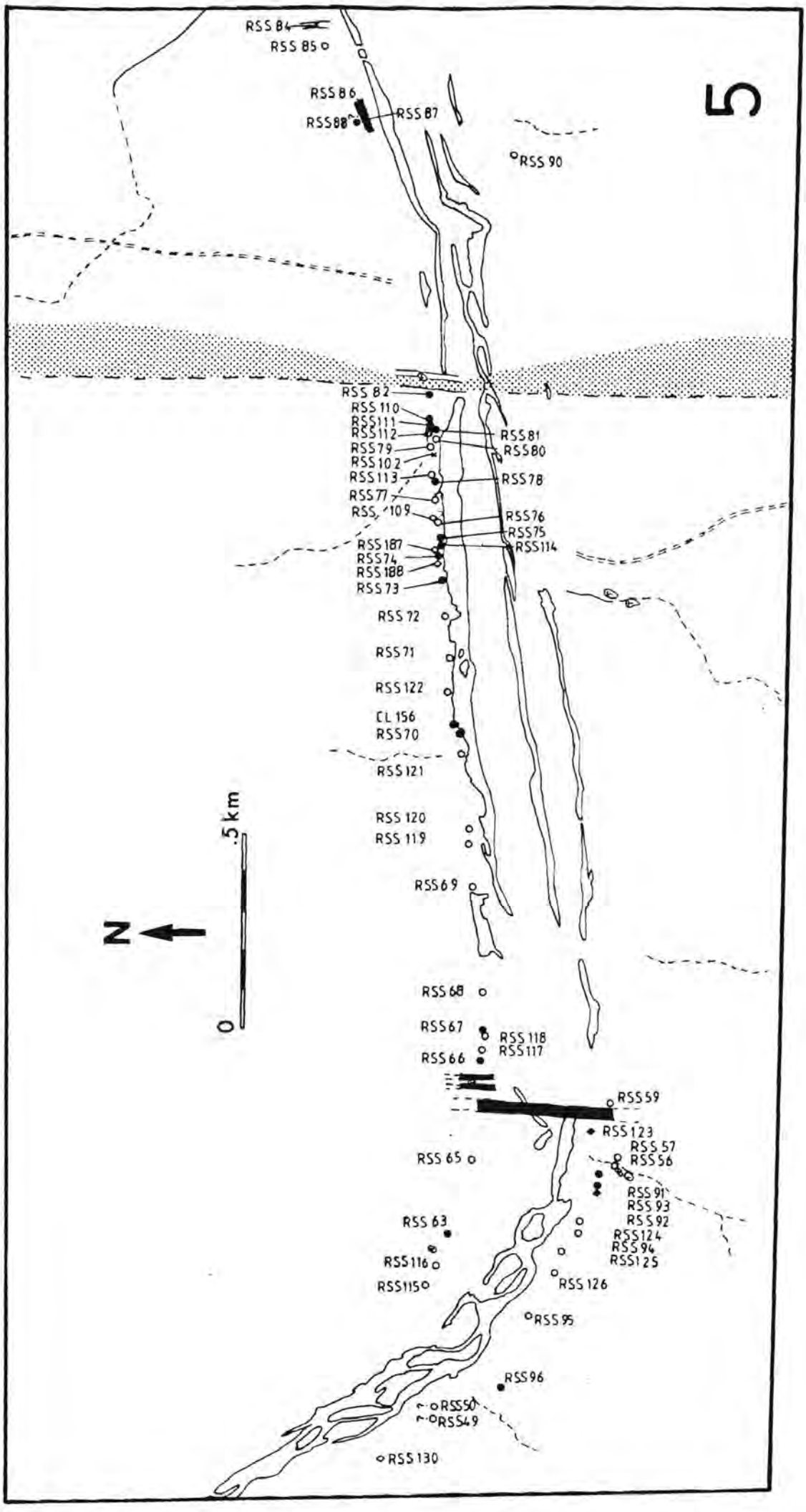
5
RSS 84
RSS 85
RSS 86
RSS 87
RSS 88
RSS 90
RSS 82
RSS 110
RSS 111
RSS 112
RSS 81
RSS 79
RSS 80
RSS 102
RSS 113
RSS 78
RSS 77
RSS 109
RSS 76
RSS 75
RSS 187
RSS 114
RSS 74
RSS 188
RSS 73
RSS 72
RSS 71
RSS 122
CL 156
RSS 70
RSS 121
RSS 120
RSS 119
RSS 69
RSS 68
RSS 67
RSS 118
RSS 117
RSS 66
RSS 59
RSS 123
RSS 57
RSS 56
RSS 65
RSS 91
RSS 93
RSS 92
RSS 63
RSS 124
RSS 94
RSS 116
RSS 125
RSS 115
RSS 126
RSS 95
RSS 96
RSS 50
RSS 49
RSS 130
N
.5 km
0

Nd	0.14	gabbro	pheno/trace	(25)
U	0.063	rhyolitic	pheno/matrix	(5)
Th	0.427	rhyolitic	pheno/matrix	(5)
Ni	6.86	basaltic	pheno/trace	(32)
	39.5	basaltic	pheno/trace	(32)
Cr	6	syn. lunar bas.	.1% doping	(39)
Co	2.22	gabbro	pheno/trace	(25)
	2.2	basaltic	pheno/trace	(25)
	1.46	basaltic	pheno/trace	(32)
Sc	1.8	gabbro	pheno/trace	(25)
	0.62	basaltic	pheno/trace	(32)
	6.43	basaltic	pheno/trace	(32)
V	0.29	basaltic	pheno/trace	(32)
	61	basaltic	pheno/trace	(32)
Zn	0.38	gabbro	pheno/trace	(25)
	2.76	basaltic	pheno/trace	(32)
	2.94	basaltic	pheno/trace	(32)
Cu	1.46	gabbro	pheno/trace	(25)

K-feldspar

element	D	composition	method	reference
Ti	0.008	gabbro	pheno/trace	(33)
Ce	0.044	rhyolitic	compilation	(43)
Nd	0.025	rhyolitic	compilation	(43)
Rb	1.85	granodior.	pheno/trace	(10)
	0.34	rhyolitic	compilation	(43)
	0.659	rhyolitic	pheno/matrix	(16)
Ba	6.12	rhyolitic	compilation	(43)
	6.4	granitic	% doping	(44)
	14.0	granitic	% doping	(44)
Sr	3.87	rhyolitic	compilation	(43)
	1.2	granitic	% doping	(44)
	5.0	granitic	% doping	(44)
U	0.0143	granodior.	pheno/trace	(12)
Pb	0.85	rhyolitic	pheno/matrix	(37)

	1.37	rhyolitic	pheno/matrix	(37)
Cr	1	gabbro	pheno/trace	(33)
Sc	0.29	gabbro	pheno/trace	(33)
V	0.024	gabbro	pheno/trace	(33)

Magnetite

element	D	composition	method	reference
Ti	29.3	trachybasalt	pheno/matrix	(27)
	32.9	trachybasalt	pheno/trace	(27)
Nb	13.1	basaltic	pheno/trace	(19)
	0.4	basic	compilation	(32)
Zr	3.21	basaltic	pheno/trace	(19)
	1.80	trachyte	pheno/matrix	(28)
	0.1	basic	compilation	(32)
Y	1.44	trachyte	pheno/matrix	(28)
	0.2	basic	compilation	(32)
La	0.015	gabbro	pheno/trace	(25)
	0.446	andesite	pheno/matrix	(29)
Ce	0.0146	gabbro	pheno/trace	(25)
Nd	0.026	gabbro	pheno/trace	(25)
K	0.043	dacitic	pheno/matrix	(26)
Rb	0.004	rhyolitic	pheno/trace	(28)
Ba	0.4	basaltic	pheno/trace	(19)
Sr	0.6	trachyandesite	pheno/matrix	(7)
U	0.15	trachyandesite	pheno/matrix	(7)
	0.10	dacitic	compilation	(32)
Th	8.0	basaltic	pheno/trace	(19)
	0.17	trachyandesite	pheno/matrix	(7)
	0.10	dacitic	compilation	(32)
Ni	1.39	basaltic	pheno/trace	(19)
	19.4	basaltic	1% doping	(40)
Cr	5.0	basaltic	pheno/trace	(19)
	84.4	trachyandesite	pheno/trace	(27)
	100	alkali bas.	% doping	(41)
Co	3.4	gabbro	pheno/trace	(25)

Sc	9.7	trachybasalt	pheno/trace	(27)
	16.8	trachybasalt	pheno/matrix	(27)
	17.6	trachybasalt	pheno/trace	(27)
	24	trachybasalt	pheno/trace	(27)
	0.73	basaltic	pheno/trace	(25)
V	16.5	trachybasalt	pheno/trace	(27)
	17.5	basaltic	pheno/trace	(19)
	0.11	alkali bas.	% doping	(41)
	67	alkali bas.	% doping	(41)
Zn	11.9	basaltic	pheno/trace	(19)
	2.6	basaltic	pheno/trace	(25)
Cu	5.47	basaltic	pheno/trace	(19)

Olivine

element	D	composition	method	reference
Ti	0.037	basaltic	pheno/matrix	(18)
	0.03	basaltic	pheno/matrix	(19)
	0.17	syn. bas.		(49)
Nb	0.15	basaltic	pheno/trace	(19)
	0.45	basaltic	pheno/matrix	(19)
	0.05	alkali bas.	pheno/matrix	(32)
Zr	0.04	basaltic	pheno/matrix	(19)
	0.03	alkali bas.	pheno/matrix	(32)
Y	0.13	alkali bas.	pheno/matrix	(32)
La	0.0005	basaltic	pheno/trace	(23)
	0.0018	basaltic	pheno/matrix	(22)
	0.0026	basaltic	pheno/matrix	(25)
Ce	0.0008	basaltic	pheno/trace	(23)
	0.0005	peridotite	compilation	(50)
	<0.00001	basaltic	% doping	(47)
Nd	0.0018	basaltic	pheno/matrix	(22)
	0.0013	basaltic	pheno/trace	(23)
	0.001	peridotite	compilation	(50)
	0.000007	basaltic	% doping	(47)
Sm	0.0013	peridotite	compilation	(50)
Eu	0.0016	peridotite	compilation	(50)
Gd	0.0015	peridotite	compilation	(50)
Dy	0.0017	peridotite	compilation	(50)

[E: Partition Coefficients]

Eu	0.0015	peridotite	compilation	(50)
K	0.0017	basaltic	pheno/matrix	(21)
	0.0056	basaltic	pheno/matrix	(16)
	0.0710	basaltic	pheno/matrix	(21)
Rb	0.0023	basaltic	pheno/matrix	(21)
	0.0113	basaltic	pheno/matrix	(16)
	0.188	basaltic	pheno/matrix	(21)
Ba	0.0013	basaltic	pheno/matrix	(22)
	0.09	basaltic	pheno/trace	(19)
	0.27	basaltic	pheno/matrix	(19)
	0.0112	basaltic	pheno/matrix	(16)
Sr	0.0012	basaltic	pheno/matrix	(21)
	0.07	basaltic	pheno/matrix	(19)
	0.12	basaltic	pheno/trace	(19)
	0.0185	basaltic	pheno/matrix	(16)
U	0.003	basaltic	pheno/matrix	(15)
	0.004	basaltic	pheno/matrix	(15)
Th	0.25	basaltic	pheno/matrix	(19)
Ni	(124/MgO)-.9	basic	.5% doping	(42)
	4.51	basaltic	pheno/trace	(19)
	12.2	basaltic	pheno/matrix	(18)
	17.0	basaltic	pheno/matrix	(30)
Cr	1.10	basaltic	pheno/matrix	(18)
	3.07	basaltic	pheno/trace	(19)
	0.6	alkali bas.	% doping	(41)
	0.72	alkali bas.	pheno/matrix	(32)
Co	2.75	basaltic	pheno/matrix	(17)
	3.00	basaltic	pheno/trace	(17),(31)
	5.17	basaltic	pheno/matrix	(6)
Sc	0.13	basaltic	pheno/matrix	(17)
	0.15	basaltic	pheno/matrix	(17),(30)
	0.22	basaltic	pheno/matrix	(30)
V	0.03	basaltic	pheno/matrix	(6)
	0.088	basaltic	pheno/matrix	(18)
	0.21	basaltic	pheno/trace	(19)
Zn	0.67	basaltic	pheno/matrix	(6)
	3.20	basaltic	pheno/matrix	(19)
Cu	0.11	basaltic	pheno/matrix	(18)
	1.63	basaltic	pheno/trace	(19)
	4.31	basaltic	pheno/trace	(19)
	0.34	basaltic	pheno/matrix	(19)

Orthopyroxene

element	D	composition	method	reference
Ti	0.1	basic	compilation	(32)
Nb	0.04	basaltic	pheno/trace	(32)
	0.11	basaltic	pheno/trace	(32)
Zr	0.003	basaltic	pheno/trace	(32)
	0.014	basaltic	pheno/trace	(32)
Y	0.20	basic	compilation	(32)
La	0.0005	basaltic	pheno/trace	(23)
Ce	0.0009	basaltic	pheno/trace	(23)
	0.024	basaltic	compilation	(44)
	0.003	peridotite	compilation	(50)
Nd	0.0019	basaltic	pheno/trace	(23)
	0.053	basaltic	compilation	(44)
	0.0068	peridotite	compilation	(50)
Sm	0.01	peridotite	compilation	(50)
Eu	0.013	peridotite	compilation	(50)
Gd	0.016	peridotite	compilation	(50)
Dy	0.022	peridotite	compilation	(50)
Er	0.030	peridotite	compilation	(50)
Yb	0.049	peridotite	compilation	(50)
K	0.008	bas. andesite	pheno/matrix	(15)
	0.00908	bas. andesite	pheno/matrix	(16)
	0.014	basaltic	compilation	(44)
Rb	0.0287	basaltic	pheno/matrix	(16)
	0.022	basaltic	compilation	(44)
Ba	0.0141	basaltic	pheno/matrix	(16)
	0.013	basaltic	compilation	(44)
Sr	0.0104	basaltic	pheno/matrix	(16)
	0.017	basaltic	compilation	(44)
Ni	3.15	basaltic	pheno/trace	(32)
	18.1	basaltic	pheno/trace	(32)
Cr	8.0	andesitic	pheno/trace	(45)

Co	2.08	basaltic	pheno/matrix	(34)
	1.61	basaltic	pheno/trace	(32)
	6.43	basaltic	pheno/trace	(32)
Sc	1.23	trachy-andes.	pheno/matrix	(34)
V	0.01	basaltic	pheno/trace	(32)
	1.23	basaltic	pheno/trace	(32)
Zn	2.10	basaltic	pheno/trace	(32)
Cu	0.25	basaltic	pheno/trace	(32)

Plagioclase

element	D	composition	method	reference
Ti	0.038	basaltic	pheno/matrix	(18)
	0.02	basaltic	pheno/matrix	(19)
Nb	0.12	basaltic	pheno/matrix	(19)
	0.20	basaltic	pheno/matrix	(19)
	0.03	andesi-bas.	pheno/matrix	(32)
Zr	0.03	basaltic	pheno/matrix	(19)
Y	0.13	basaltic	pheno/matrix	(19)
	0.18	asb	pheno/matrix	(32)
La	0.09	trachybasalt	pheno/matrix	(7)
Ce	0.023	basaltic	pheno/matrix	(11)
	0.278	basaltic	pheno/matrix	(11)
	0.12	basaltic	compilation	(44)
Nd	0.023	basaltic	pheno/matrix	(11)
	0.199	basaltic	pheno/matrix	(11)
	0.081	basaltic	compilation	(44)
K	0.08	basaltic	pheno/matrix	(35)
	0.15	basaltic	pheno/matrix	(35)
	0.23	basaltic	pheno/matrix	(21)
	0.174	basaltic	pheno/matrix	(21)
	0.151	basaltic	pheno/matrix	(16)
	0.1	dac./rhy.	pheno/matrix	(48)
Rb	0.0509	basaltic	pheno/matrix	(16)
	0.07	basaltic	pheno/matrix	(14)
	0.12	basaltic	pheno/matrix	(14)
	0.26	basaltic	pheno/matrix	(36)
	0.046	basaltic	pheno/matrix	(21)
	0.05	basaltic	pheno/matrix	(19)
	0.0294	basaltic	pheno/matrix	(16)

	0.118	basaltic	pheno/matrix	(16)
	0.041	dac./rhy.	pheno/matrix	(48)
Ba	0.242	basaltic	pheno/matrix	(16)
	0.18	basaltic	pheno/matrix	(36)
	0.33	basaltic	pheno/matrix	(36)
	0.77	basaltic	pheno/matrix	(36)
	0.407	basaltic	pheno/matrix	(21)
	0.15	basaltic	pheno/matrix	(19)
	0.60	basaltic	pheno/matrix	(19)
	0.151	basaltic	pheno/matrix	(16)
	0.31	dac./rhy.	pheno/matrix	(48)
Sr	1.66	basaltic	pheno/matrix	(16)
	1.69	basaltic	pheno/matrix	(36)
	1.56	basaltic	pheno/matrix	(21)
	1.04	basaltic	pheno/matrix	(19)
	2.22	basaltic	pheno/matrix	(19)
	1.36	basaltic	pheno/matrix	(16)
	4.4	dac./rhy.	pheno/matrix	(48)
U	0.012	basaltic	pheno/matrix	(15)
	0.007	basaltic	pheno/matrix	(15)
Th	0.67	trachybasalt	pheno/matrix	(19)
	0.06	trachybasalt	pheno/matrix	(7)
Pb	0.14	basaltic	pheno/matrix	(37)
	0.67	basaltic	pheno/matrix	(37)
	0.11	basaltic	pheno/matrix	(37)
	0.10	basaltic	pheno/matrix	(37)
	0.53	basaltic	pheno/matrix	(19)
	2.8	basaltic	pheno/matrix	(19)
Ni	0.06	basaltic	pheno/matrix	(18)
	0.10	basaltic	pheno/matrix	(19)
Cr	0.02	basaltic	pheno/matrix	(18),(19)
	0.05	andesi-bas.	pheno/matrix	(32)
Co	0.10	basaltic	pheno/matrix	(18)
	0.03	basaltic	pheno/trace	(25)
Sc	0.03	trachybasalt	pheno/matrix	(7)
	0.01	basaltic	pheno/trace	(25)
V	0.10	basaltic	pheno/matrix	(18)
	0.01	basaltic	pheno/matrix	(19)
Zn	0.11	basaltic	pheno/matrix	(18)
	0.04	basaltic	pheno/matrix	(19)
	0.14	basaltic	pheno/matrix	(19)
Cu	0.17	basaltic	pheno/matrix	(18)
	0.52	basaltic	pheno/matrix	(19)

Quartz

element	D	composition	method	reference
Zr	0.14	granitic	pheno/trace	(3)
	0.01	granitic	pheno/trace	(3)
La	0.0073	granitic	pheno/trace	(3)
	0.0053	granitic	pheno/trace	(3)
	0.015	rhyolitic	pheno/matrix	(39)
Ce	0.0078	granitic	pheno/trace	(3)
	0.0046	granitic	pheno/trace	(3)
Nd	0.023	rhyolitic	pheno/matrix	(39)
Rb	0.015	rhyolitic	pheno/matrix	(39)
Ba	0.055	rhyolitic	pheno/matrix	(39)
U	0.014	rhyolitic	pheno/matrix	(39)
Th	0.018	granitic	pheno/trace	(3)
	0.005	granitic	pheno/trace	(3)
Sc	0.013	granitic	pheno/trace	(3)
	0.019	granitic	pheno/trace	(3)

Phlogopite

element	D	composition	method	reference
Ti	0.9	basic	compilation	(32)
Nb	1.0	basic	compilation	(32)
	0.09	basic	pheno/trace	(32)
	0.26	basic	pheno/trace	(32)
Zr	0.6	basic	compilation	(32)
	0.01	basic	pheno/trace	(32)
	0.11	basic	pheno/trace	(32)
Ni	6.04			
	34.8			
Co	3.83			
Sc	0.06			
	0.61	basic	pheno/trace	(32)
V	0.77			

Zn	0.94	
	1.0	
Cu	0.30	
	0.38	

References

1. De Pieri, (1980). Mineral. Mag., 43, 985-988.
2. Higuchi and Nagasawa, (1969). Earth Planet. Sci. Lett., 7, 281-287.
3. Buma, Frey and Wones, (1971). Contrib. Min. Pet., 31, 300-320.
4. Andriambololona, Lefevre and Dupuy (1975). C. R. Acad. Sci. Paris, 281, Ser. D., 1797-1800.
5. Mahood and Hildreth, (1983). Geochim. Cos. Acta, 47, 11-30.
6. Matsui *et al.*, (1977). Bull. Soc. Fr. Min. Crystallog., 100, 315-324.
7. Villemant *et al.*, (1980). Bull. Min., 103, 267-286.
8. Crecraft, Nash and Evans, (1981). J. Geophys. Res., 86, 10303-10320.
9. Zielinski and Lipman, (1976). Bull. Geol. Soc. Amer., 87, 1477-1485.
10. Dupuy and Allegre, (1976). Geochim. Cos. Acta, 36, 437-458.
11. Schnetzler and Philpotts, (1970). Geochim. Cos. Acta, 34, 331-340.
12. Dostal and Capedri, (1975). Chem. Geol., 15, 285-294.
13. Hart and Brooks, (1974), Geochim. Cos. Acta, 38, 1799-1806.
14. Goodman, (1972), Geochim. Cos. Acta, 36, 303-317.
15. Dostal, Capedri and Dupuy, (1976). Lithos, 9, 179-183.
16. Philpotts and Schnetzler, (1970). Geochim. Cos. Acta, 34, 307-322.
17. Dale and Henderson, (1972). 24th Int. Geol. Cong. Montreal, Sect. 10, Proc., 105-111.
18. Bougault and Hekinian, (1974). Earth Planet. Sci. Lett., 24, 249-261.
19. Ross, (1977). Unpub. PhD thesis, Univ. of Queensland.
20. Hakli and Wright, (1967). Geochim. Cos. Acta, 31, 877-884.
21. Griffin and Rama Murthy, (1969). Geochim. Cos. Acta, 33, 1389-1414.
22. Gorton, (1974). Unpub. PhD thesis, Aust. National Univ.
23. Frey, Green and Roy, (1978). J. Petrol., 19, 463-513.
24. Nagasawa, (1973). Contrib. Min. Petrol., 39, 301-308.
25. Paster, Schanwecker and Haskin, (1974). Geochim. Cos. Acta, 38, 1549-1577.
26. Okamoto, (1979). J. Geol. Soc. Japan, 85, 525-535.
27. Leeman *et al.*, (1978). Contrib. Min. Petrol., 65, 269-272.
28. Ewart, (1982). J. Petrol., 23, 344-382.
29. Luhr and Carmichael, (1980). Contrib. Min. Petrol., 71, 343-372.
30. Leeman and Scheidegger, (1977). Earth Planet. Sci. Lett., 35, 247-257.
31. Gunn, (1971). Chem. Geol., 8, 1-13.
32. Le Roex, (1980). Unpub. PhD thesis, Univ. of Cape Town.
33. Mason, (1971). New Z. J. Geol. Geophys., 15, 465-475.
34. Onuma *et al.*, (1978). Earth Planet. Sci. Lett., 5, 47-51.
35. Goodman, (1972). Geochim. Cos. Acta, 36, 303-317.
36. Dupuy and Coulon, (1973). C. R. Acad. Sci. Paris, 277, Ser. D, 1593-1596.

37. Leeman, (1979). Geochim. Cos. Acta, **43**, 171-175.
38. Irving and Frey, (1978). Geochim. Cos. Acta, **42**, 771-787.
39. Ringwood, (1970). J. Geophys. Res., **75**, 6453-6479.
40. Leeman, (1974). Unpub. PhD thesis, Univ. of Oregon.
41. Lindstrom, (1976). Unpub. PhD thesis, Univ. of Oregon.
42. Hart and Davis, (1978). Earth Planet. Sci. Lett., **40**, 203-219.
43. Arth, (1976). J. Res. U. S. Geol. Surv., **4**(1), 41-47.
44. Long, (1978). Geochim. Cos. Acta, **42**, 838-846.
45. Ewart and Taylor, (1969). Contrib. Min. Petrol., **22**, 127-146.
46. McCallum and Charette, (1978). Geochim. Cos. Acta, **42**, 859-969.
47. McKay, (1986). Geochim. Cos. Acta, **50**, 69-79.
48. Nagasawa and Schnetzler, (1971). Geochim. Cos. Acta., **35**, 953-968.
49. Dunn (1987). Contrib. Min. Petrol., **96**, 476-484.
50. Hanson (1980). Ann. Rev. Earth Planet. Sci., **8**, 371-406.

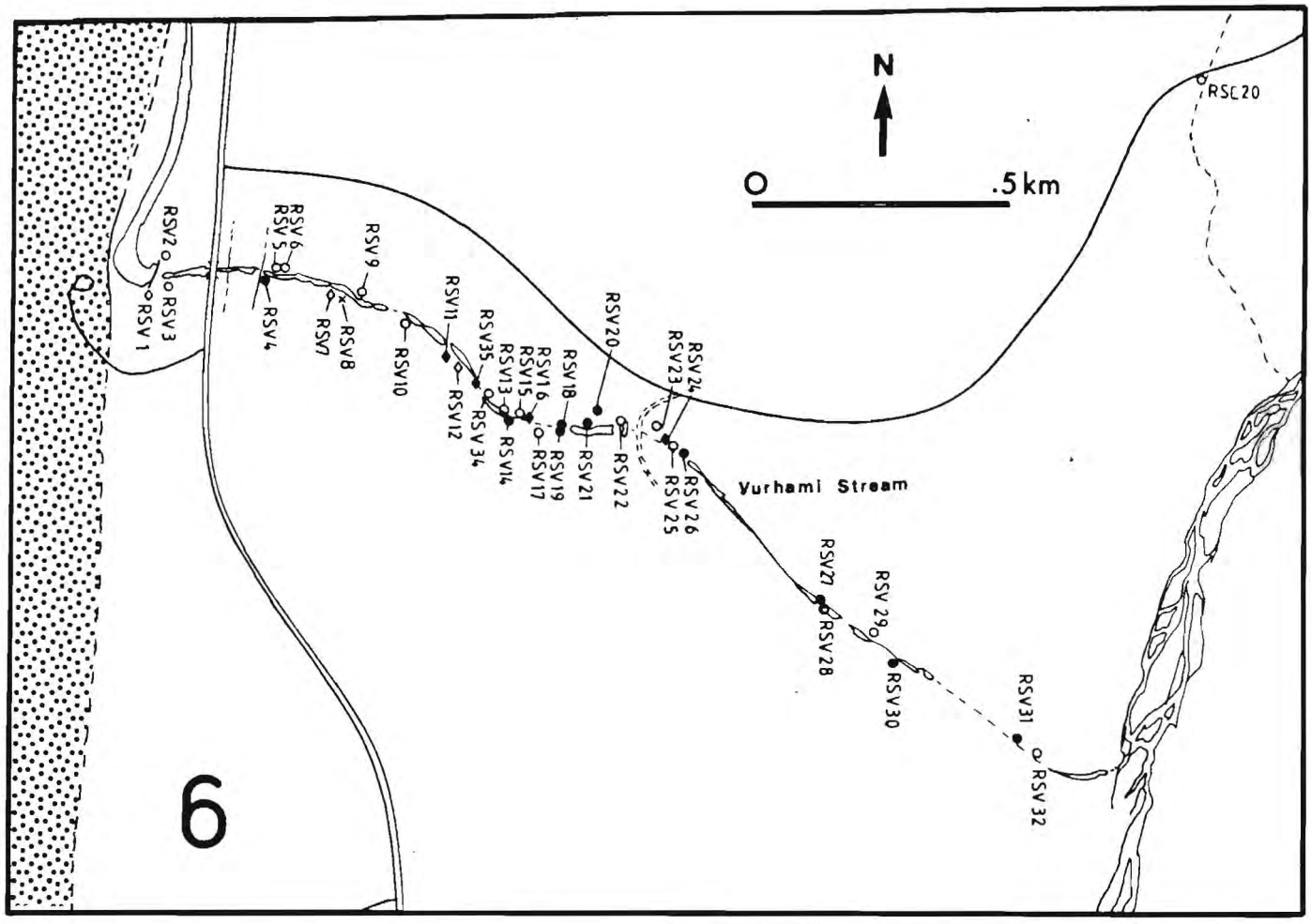
N
.5km
RSC20
RSV2
RSV3
RSV 1
RSV 6
RSV 5
RSV4
RSV9
RSV7
RSV8
RSV10
RSV11
RSV12
RSV35
RSV 34
RSV13
RSV14
RSV16
RSV15
RSV17
RSV18
RSV19
RSV21
RSV20
RSV22
RSV24
RSV23
RSV 26
RSV 25
Yurhami Stream
RSV27
RSV 29
RSV28
RSV30
RSV31
RSV 32
6

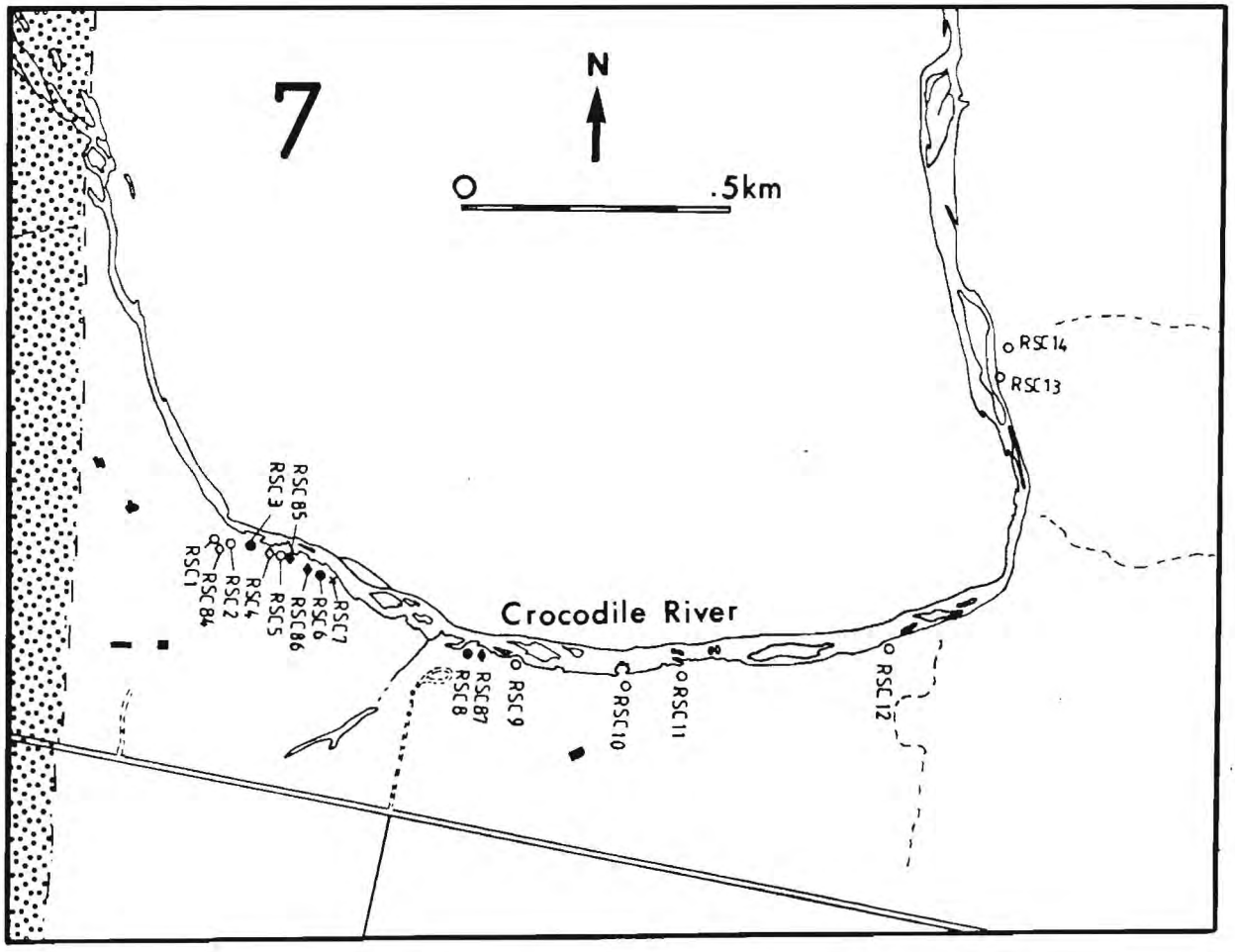
7
N
.5km
RSC14
RSC13
RSC B5
RSC 3
RSC1
RSC B4
RSC 2
RSC 4
RSC 5
RSC B6
RSC 6
RSC 7
Crocodile River
RSC B7
RSC 8
RSC 9
RSC 10
RSC 11
RSC 12

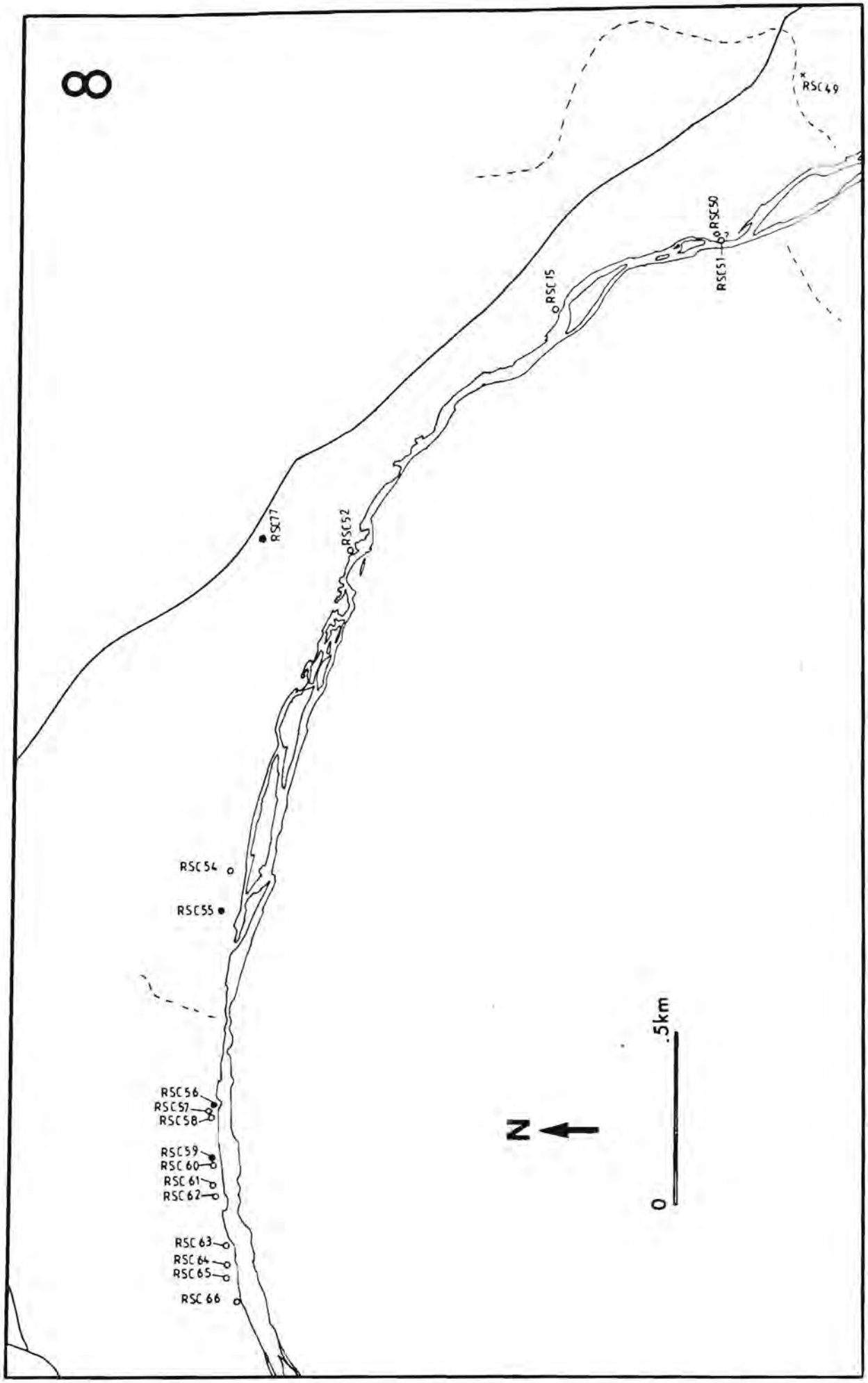
8
RSC49
RSC50
RSC51
RSC15
RSC52
RSC77
RSC54
RSC55
RSC56
RSC57
RSC58
RSC59
RSC60
RSC61
RSC62
RSC63
RSC64
RSC65
RSC66
N
.5km
0

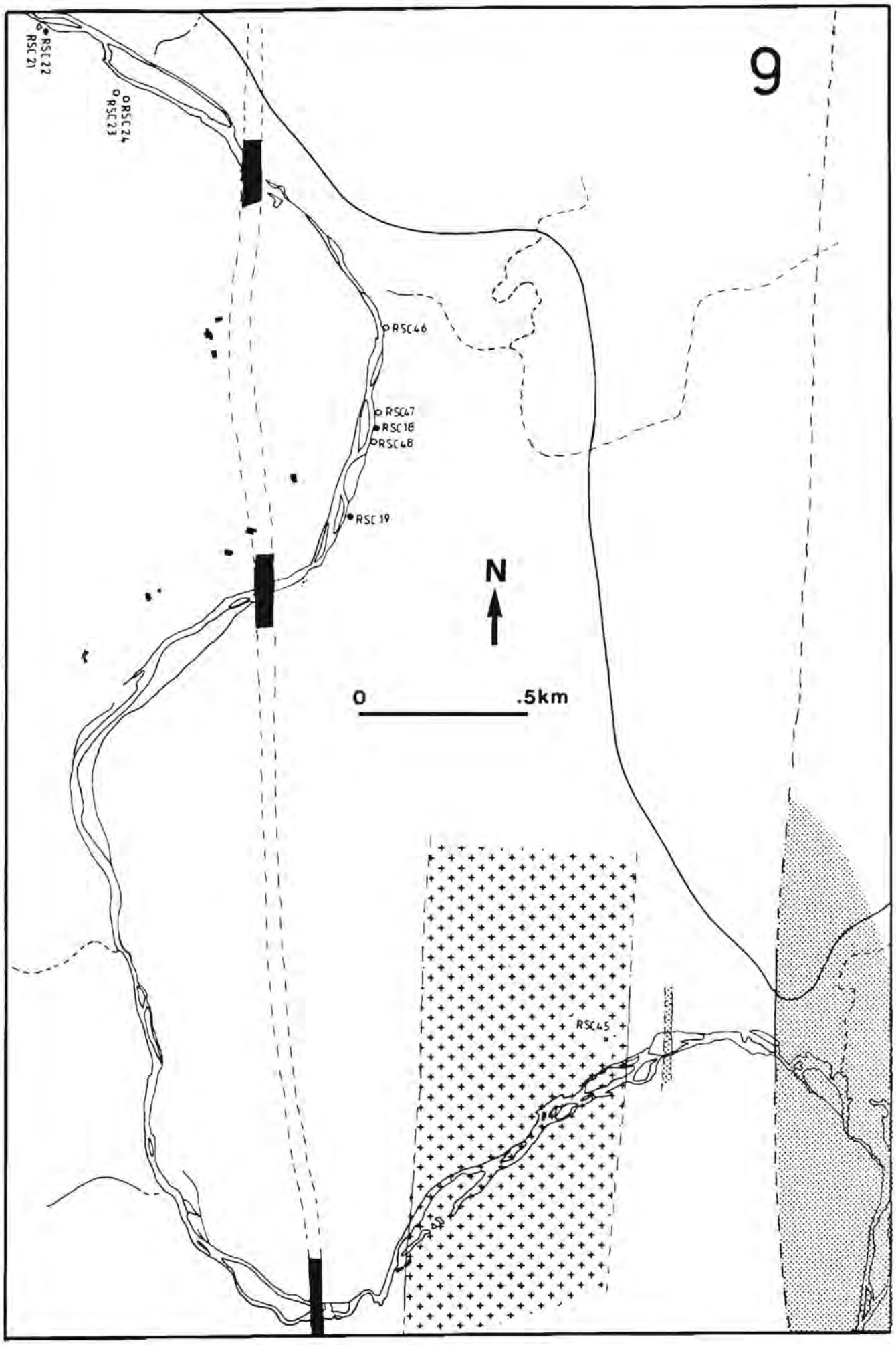
9
RSC22
RSC21
RSC24
RSC23
RSC46
RSC47
RSC18
RSC48
RSC19
N
0
.5km
RSC45

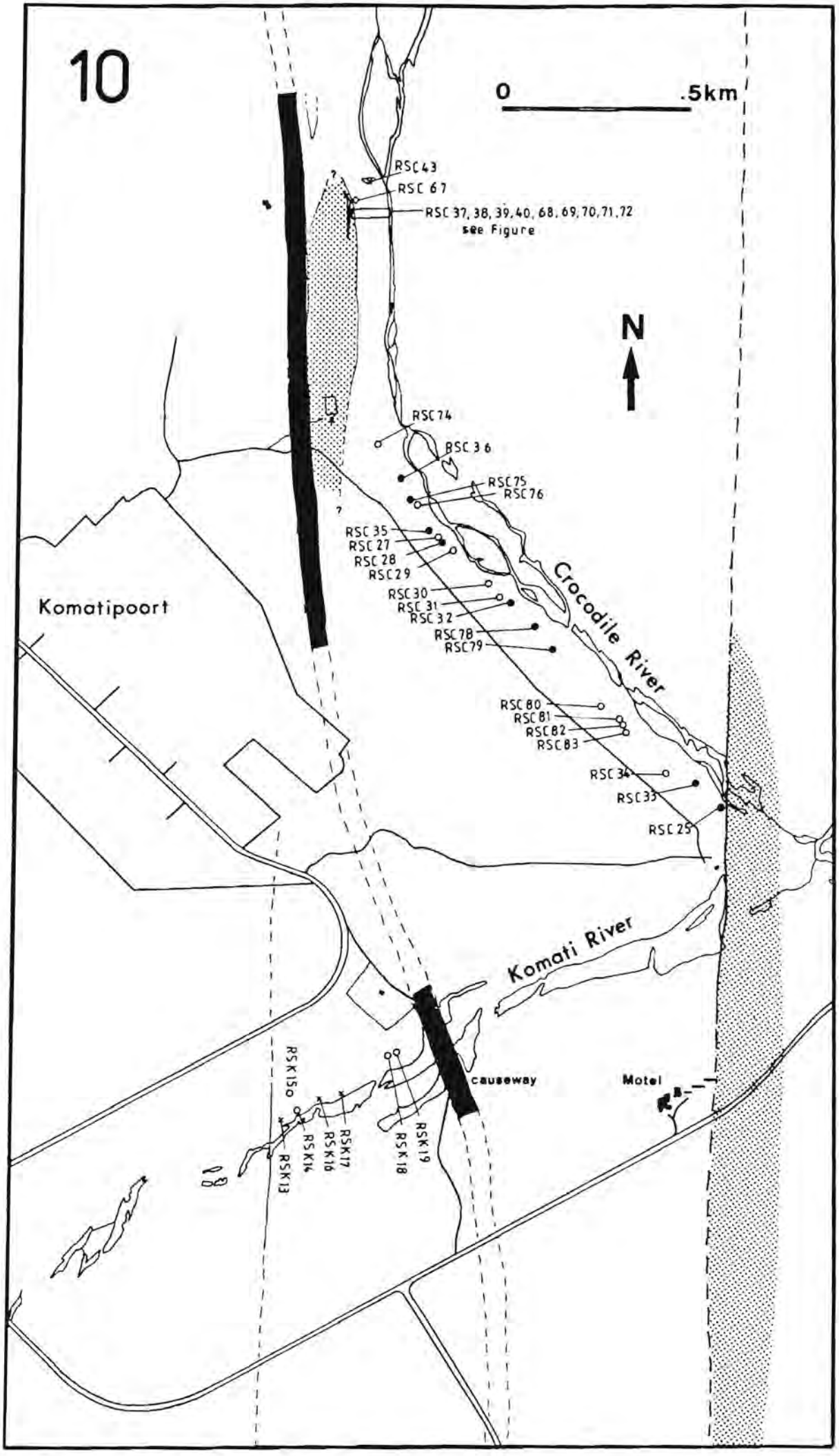
10
0
.5km
RSC43
RSC 67
RSC 37, 38, 39, 40, 68, 69, 70, 71, 72
see Figure
N
RSC74
RSC 36
RSC75
RSC76
RSC 35
RSC 27
RSC 28
RSC 29
RSC 30
RSC 31
RSC 32
RSC78
RSC79
Crocodile River
Komatipoort
RSC80
RSC81
RSC82
RSC83
RSC 34
RSC33
RSC 25
Komati River
causeway
Motel
RSK15o
RSK13
RSK14
RSK16
RSK17
RSK18
RSK19

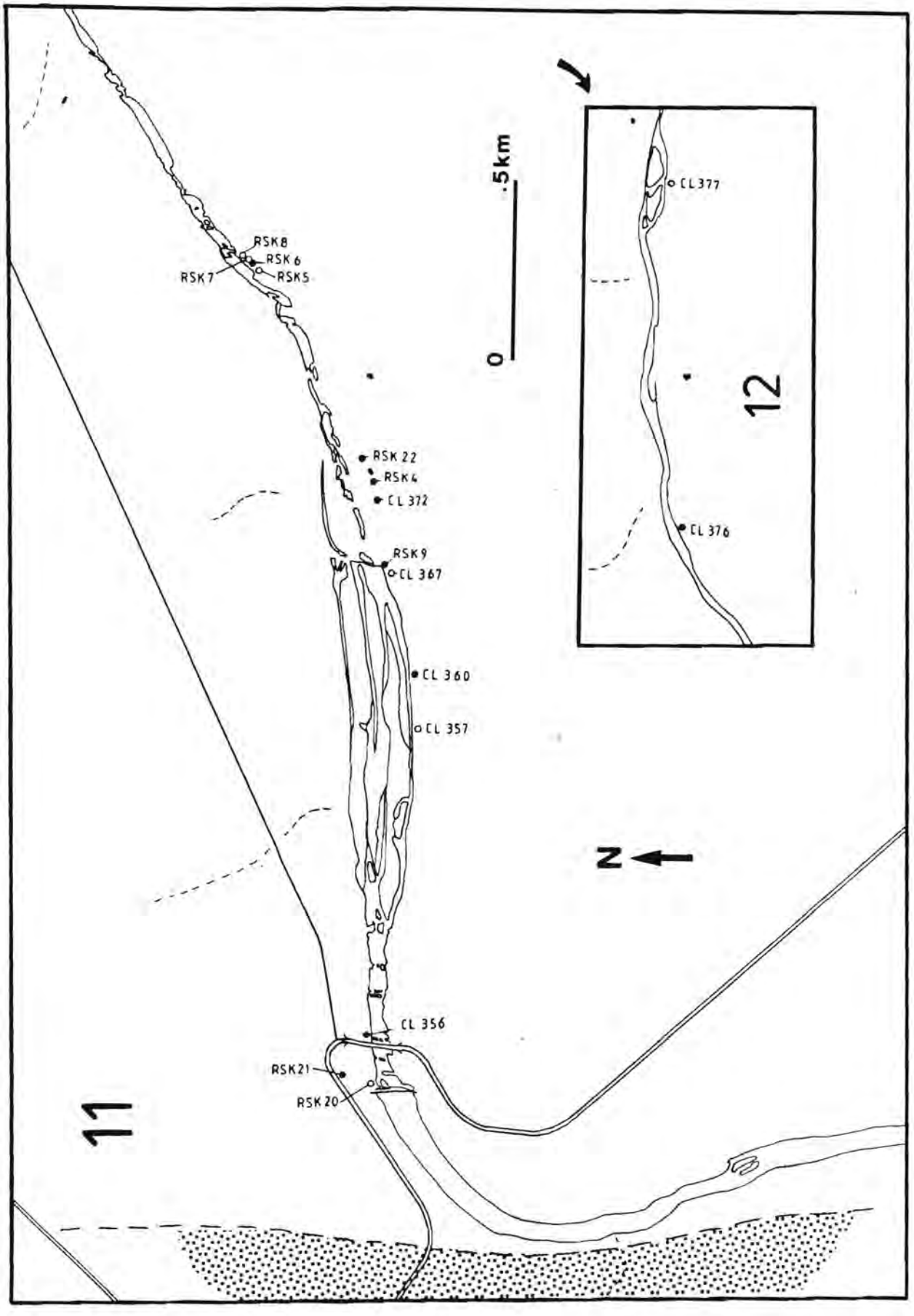
RSK8
RSK 6
RSK7
RSK5
RSK 22
RSK4
CL 372
RSK9
CL 367
CL 360
CL 357
CL 356
RSK21
RSK 20
11
0
.5km
N
CL377
CL 376
12

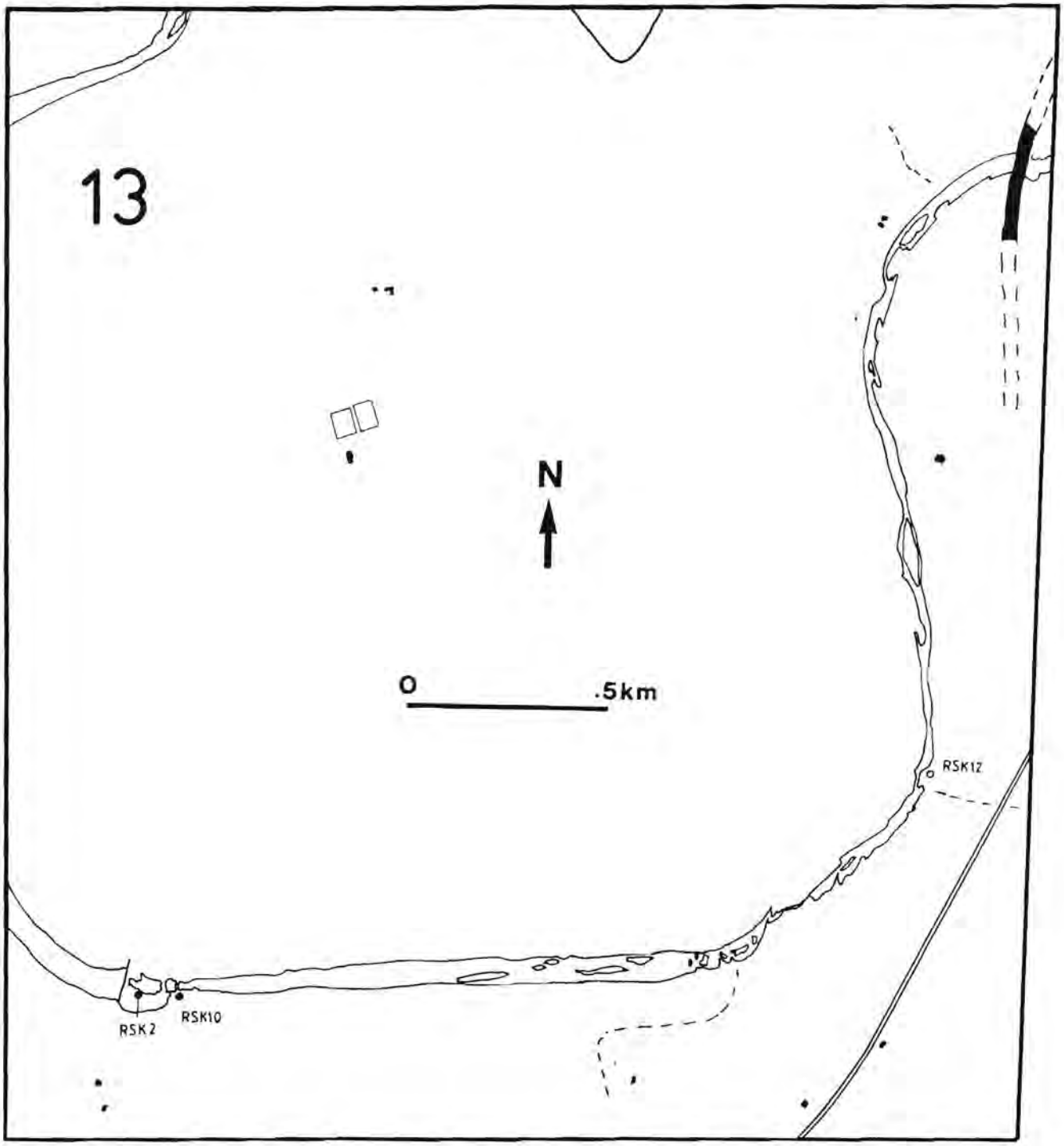
13
N
0
.5km
RSK12
RSK10
RSK2

Figure D2. Stratigraphic location of basaltic samples in the central Lebombo (excluding dolerites). Samples for which quantitative data are avalailable have their sample names located on the left-hand side of each stratigraphic section. Samples for which only semi-quantitative data (slab) are available are located on the right-hand side. The upper portion of the Crocodile and Komati River sections are both off-set to allow for the approximate contribution to section thickness made by the intrusion of the Komatipoort Gabbroic Complex. Stratigraphic heights were calculated using the distance of each sample from the base of the Sabie River Basalt Formation (contact with sandstone, as located on Fig. D1) and an average dip of 18° to the east.

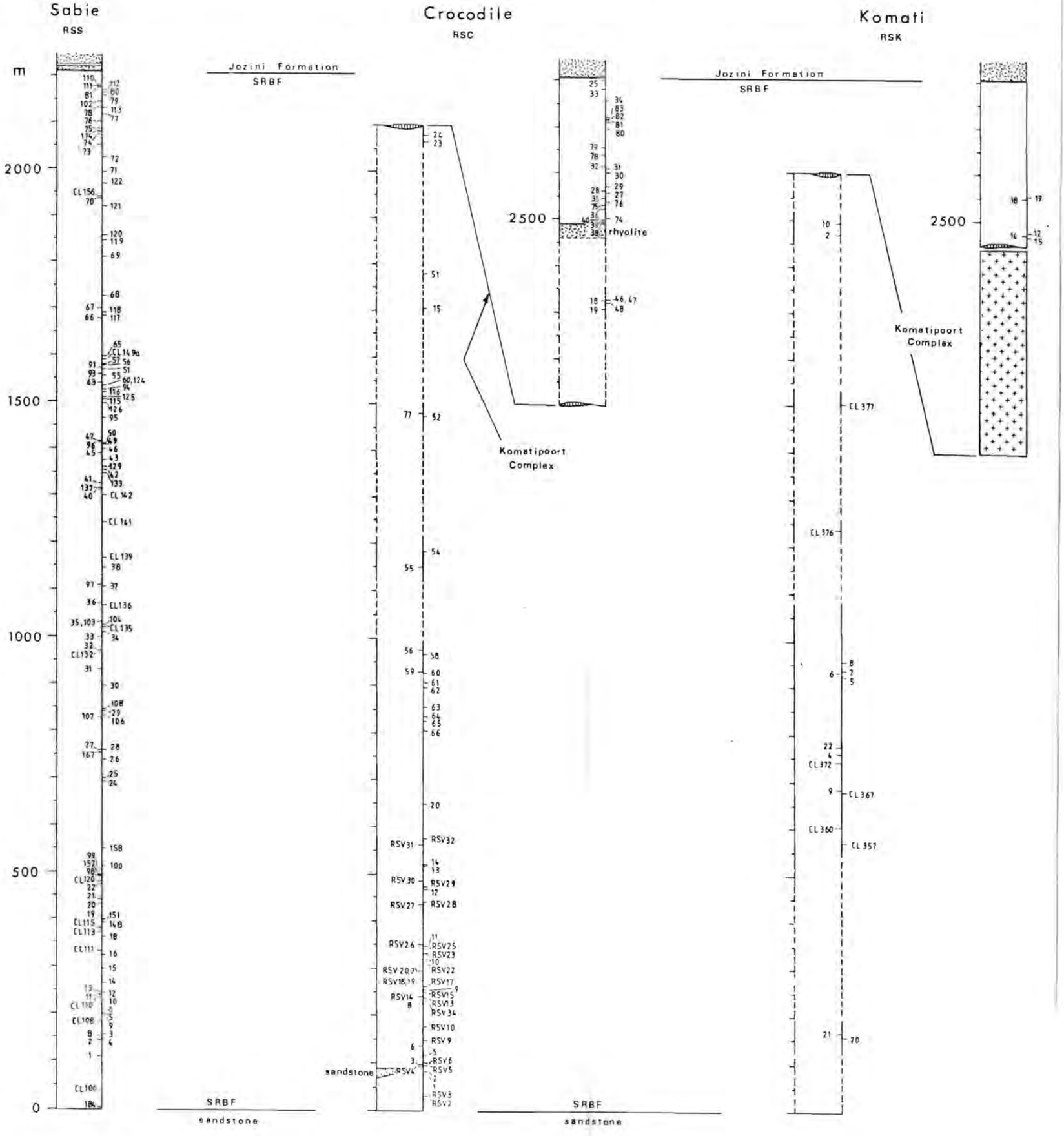
Sabie
RSS
Crocodile
RSC
Komati
RSK
m
2000
1500
1000
500
0
2500
Jozini Formation
SRBF
Komatipoort Complex
rhyolite
sandstone
SRBF
sandstone
SRBF
sandstone

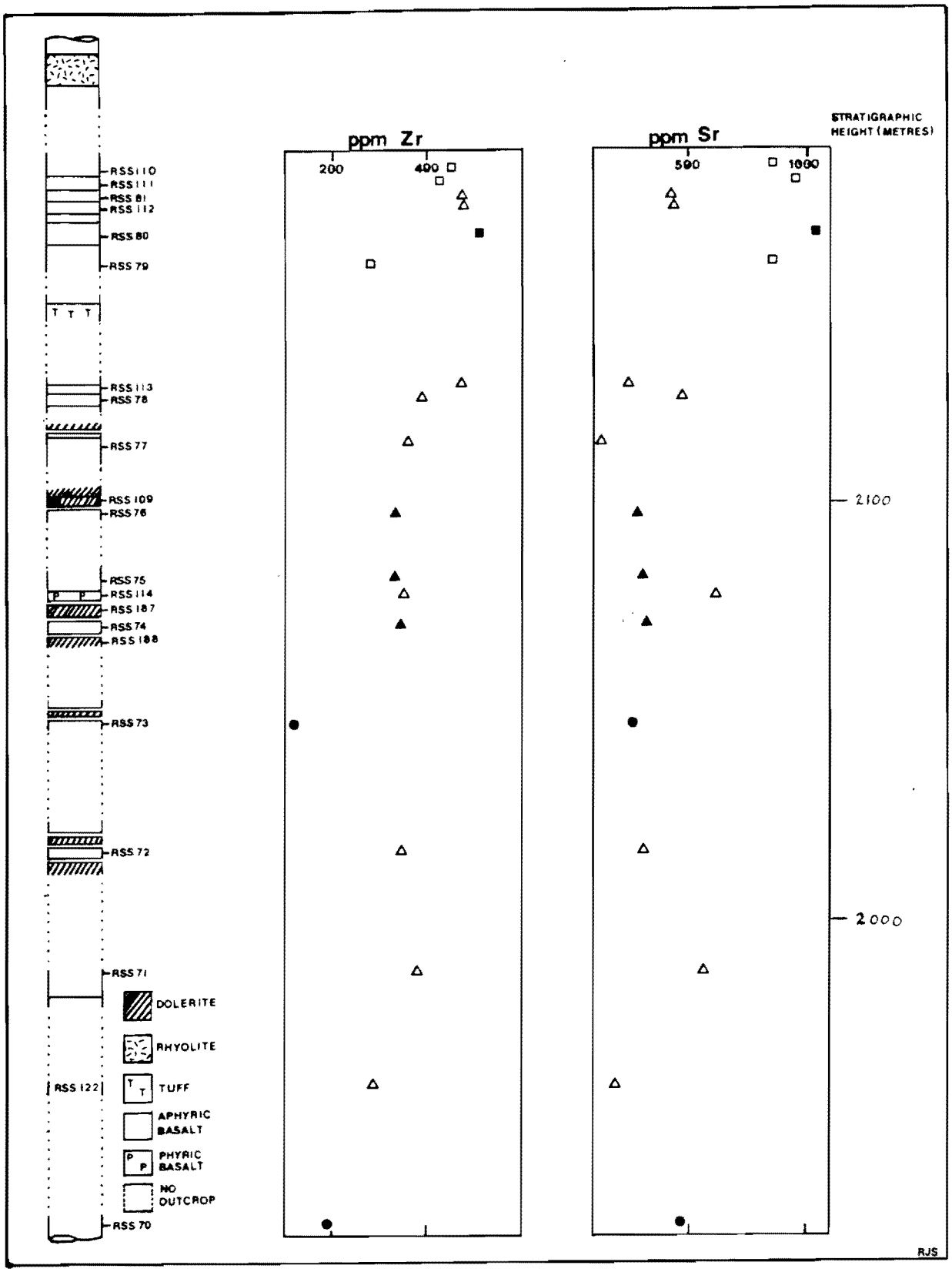

Figure D3. Detailed stratigraphy in Sabie River Section. Filled symbols represent quantitative data and open symbols semi-quantitative (slab) data.

APPENDIX E. PARTITION COEFFICIENT COMPILATION

Biotite

element	D	composition	method	reference
Ti	22.8	rhyolitic	pheno/matrix	(4)
	16.0	rhyolitic	pheno/matrix	(1)
Nb	1.8	int.-acidic	compilation	(32)
	3.0	int.-acidic	compilation	(32)
Zr	1.2	int.-acidic	compilation	(32)
	2.2	int.-acidic	compilation	(32)
Y	1.2	int.-acidic	compilation	(32)
	2.0	int.-acidic	compilation	(32)
La	1.02	granitic	pheno/trace	(3)
Ce	1.21	granitic	pheno/trace	(3)
	0.32	rhyolitic	pheno/matrix	(2)
Nd	0.044	dacitic	pheno/matrix	(11)
	0.29	rhyolitic	pheno/matrix	(2)
Na	0.18	rhyolite	pheno/matrix	(1)
K	2.5	rhyolite	pheno/matrix	(2)
	1.7	rhyolitic	pheno/matrix	(1)
Rb	2.7	rhyolitic	pheno/matrix	(9)
	3.2	granodior.	pheno/trace	(10)
	3.06	basaltic	pheno/matrix	(6)
Sr	.12	dac/rhy	pheno/matrix	(16)
Ba	7.0	rhyolitic	pheno/matrix	(5)
	6.36	dac/rhy.	pheno/matrix	(16)
U	0.0596	granodior.	pheno/trace	(12)
Th	1.54	granitic	pheno/trace	(3)
Ni	1.22	rhyolitic	pheno/matrix	(7)
	12.9	rhyolitic	pheno/matrix	(4)
Cr	3.7	rhyolitic	pheno/matrix	(5)
	19.0	rhyolitic	pheno/matrix	(6)
Co	25.2	rhyolitic	pheno/matrix	(4)
	79.0	rhyolitic	pheno/matrix	(6)

Sc	19.7	granitic	pheno/trace	(3)
V	50.0	rhyolitic	pheno/matrix	(4)
Cu	2.9	rhyolitic	pheno/matrix	(4)
Zn	9.8	rhyolitic	pheno/matrix	(4)
	20	rhyolitic	pheno/matrix	(6)
	50	rhyolitic	pheno/matrix	(8)

Clinopyroxene

element	D	composition	method	reference
Ti	0.20	basaltic	pheno/matrix	(18)
	0.93	basaltic	pheno/trace	(19)
	0.99	basaltic	pheno/trace	(19)
	0.69	basaltic	pheno/matrix	(19)
	0.40	syn. bas.		(49)
Nb	0.043	basaltic	pheno/matrix	(22)
	0.07	basaltic	pheno/trace	(19)
	0.31	basaltic	pheno/trace	(19)
	0.38	basaltic	pheno/matrix	(19)
Zr	0.142	basaltic	pheno/matrix	(22)
	0.45	basaltic	pheno/trace	(19)
	1.15	basaltic	pheno/trace	(19)
	1.24	basaltic	pheno/matrix	(19)
Y	0.42	basaltic	pheno/matrix	(23)
	0.69	alkali bas.	pheno/matrix	(32)
	0.20	basaltic	pheno/matrix	(23)
La	0.02	basaltic	pheno/trace	(23)
	0.064	basaltic	pheno/matrix	(22)
Ce	0.04	basaltic	pheno/trace	(23)
	0.359	basaltic	pheno/matrix	(24)
	0.208	basaltic	pheno/matrix	(11)
	0.043	basaltic	pheno/matrix	(11)
	0.097	basaltic	pheno/matrix	(22)
	0.098	peridotite	compilation	(50)
Nd	0.09	basaltic	pheno/trace	(23)
	0.69	basaltic	pheno/matrix	(24)
	0.427	basaltic	pheno/matrix	(11)
	0.065	basaltic	pheno/matrix	(11)
	0.194	basaltic	pheno/matrix	(22)
	0.21	peridotite	compilation	(50)
Sm	0.26	peridotite	compilation	(50)
Eu	0.31	peridotite	compilation	(50)

[E: Partition Coefficients]

Gd	0.30	peridotite	compilation	(50)
Dy	0.33	peridotite	compilation	(50)
Er	0.30	peridotite	compilation	(50)
Yb	0.28	peridotite	compilation	(50)
K	0.0054	basaltic	pheno/trace	(13)
	0.0013	basaltic	pheno/trace	(13)
	0.002	basaltic	pheno/matrix	(14)
	0.03	basaltic	pheno/matrix	(14)
	0.03	basaltic	pheno/matrix	(15)
	0.026	basaltic	pheno/matrix	(15)
	0.0448	basaltic	pheno/matrix	(16)
	0.0271	basaltic	pheno/matrix	(16)
	0.0084	basaltic	pheno/matrix	(16)
Rb	0.0017	basaltic	pheno/trace	(13)
	0.0326	basaltic	pheno/matrix	(16)
	0.08	basaltic	pheno/matrix	(14)
Ba	0.0016	basaltic	pheno/trace	(13)
	0.0035	basaltic	pheno/matrix	(34)
	0.0137	basaltic	pheno/trace	(13)
	0.047	basaltic	pheno/matrix	(21)
	0.0133	basaltic	pheno/matrix	(16)
	0.0310	basaltic	pheno/matrix	(16)
Sr	0.0719	basaltic	pheno/trace	(13)
	0.098	basaltic	pheno/matrix	(21)
	0.128	basaltic	pheno/matrix	(16)
	0.0934	basaltic	pheno/matrix	(16)
U	0.043	basaltic	pheno/matrix	(15)
	0.031	basaltic	pheno/matrix	(15)
	0.017	basaltic	pheno/matrix	(34)
Th	2.5	basaltic	pheno/trace	(19)
	3.0	basaltic	pheno/trace	(19)
	4.0	basaltic	pheno/matrix	(19)
	0.013	basaltic	pheno/matrix	(34)
	0.0016	synth. bas.	fission tracks	(32)
Pb	0.145	basaltic	pheno/matrix	(22)
	1.0	basaltic	pheno/trace	(19)
Ni	1.67	basaltic	pheno/matrix	(17)
	4.4	basaltic	pheno/matrix	(18)
	2.8	basaltic	pheno/matrix	(20)
Cr	13.0	basaltic	pheno/matrix	(18)
	4.8	basaltic	pheno/matrix	(17)

	2.19	basaltic	pheno/matrix	(19)
	3.4	basaltic	pheno/trace	(19)
Co	0.86	basaltic	pheno/matrix	(17)
	1.04	basaltic	pheno/matrix	(17)
	1.32	basaltic	pheno/matrix	(18)
Sc	2.42	basaltic	pheno/matrix	(17)
	3.23	basaltic	pheno/matrix	(17)
V	0.74	basaltic	pheno/matrix	(18)
	1.27	basaltic	pheno/trace	(19)
	3.8	basaltic	pheno/trace	(19)
	1.33	basaltic	pheno/matrix	(19)
Zn	0.33	basaltic	pheno/trace	(19)
	0.47	alkali bas.	pheno/matrix	(32)
	1.05	basaltic	pheno/matrix	(19)
	1.41	basaltic	pheno/trace	(19)
Cu	0.07	basaltic	pheno/trace	(19)
	0.18	basaltic	pheno/matrix	(18)

Garnet

element	D	composition	method	reference
Ti	0.3	basic	compilation	(32)
Nb	0.10	basic	compilation	(32)
	0.03	basaltic	pheno/trace	(32)
Zr	0.3	basic	compilation	(32)
	0.02	basaltic	pheno/trace	(32)
	2.42	basaltic	pheno/trace	(32)
Y	2.0	basic	compilation	(32)
	3.28	basaltic	pheno/trace	(32)
La	0.0004	kimberlite	pheno/matrix	(38)
Ce	0.007	basaltic	pheno/matrix	(38)
	0.021	peridotite	compilation	(50)
Nd	0.026	basaltic	pheno/matrix	(38)
	0.087	peridotite	compilation	(50)
Sm	0.217	peridotite	compilation	(50)
Eu	0.320	peridotite	compilation	(50)
Gd	0.498	peridotite	compilation	(50)
Dy	1.06	peridotite	compilation	(50)

Er	2.0	peridotite	compilation	(50)
Yb	4.03	peridotite	compilation	(50)
K	0.02	dacitic	pheno/matrix	(16)
Rb	0.009	dacitic	pheno/matrix	(16)
Ba	0.017	dacitic	pheno/matrix	(16)
Sr	0.0154	dacitic	pheno/matrix	(16)
Ni	0.17	basaltic	pheno/trace	(32)
	0.96	basaltic	pheno/trace	(32)
Cr	3.6	kimberlite	pheno/matrix	(38)
	3.29	basaltic	pheno/matrix	(38)
Co	0.40	basaltic	pheno/trace	(32)
	6.0	basaltic	pheno/trace	(32)
	0.53	kimberlite	pheno/matrix	(38)
	0.97	basaltic	pheno/matrix	(38)
Sc	2.61	basaltic	pheno/trace	(32)
	65	basaltic	pheno/trace	(32)
	4.3	kimberlite	pheno/matrix	(38)
	5.4	basaltic	pheno/matrix	(38)
V	0.01			
	2.64			
Zn	0.51	basaltic	pheno/trace	(32)
	0.55			
Cu	0.17			
	0.22			

Ilmenite

element	D	composition	method	reference
Nb	0.81	syn. lunar bas.	% doping	(46)
	7.5	basaltic	pheno/trace	(32)
	22.5	basaltic	pheno/trace	(32)
Zr	0.19	basaltic	pheno/trace	(32)
	1.38	basaltic	pheno/trace	(32)
Y	0.4	basaltic	pheno/trace	(32)
La	0.098	gabbro	pheno/trace	(25)
Ce	0.110	gabbro	pheno/trace	(25)